IONIC CONDUCTIVITIES IN MIXTURES OF N,N–DIMETHYLFORMAMIDE WITH WATER

A thesis presented for the degree of

MASTER OF SCIENCE

of

The University of Adelaide

by

GLEN CHITTLEBOROUGH, B.Sc., Dip.Ed.

Department of Physical and Inorganic Chemistry

January 1976

TABLE OF CONTENTS

SUMMARY

Mixtures at 25°C of N, N-dimethylformamide (DMF) and water have been the solvents for 13 conductance runs involving the solutes CsCl, KCl and KNCS. The table below summarizes the solutions and solvent compositions for which limiting equivalent conductances have been determined.

Limiting equivalent conductances performed in DMF/water solvents at 25°C in this research

	Mole per cent DMF				
Salt	*0*	*9*	*30*	*50*	*75*
CsCl	●	●	●	●	●
KCl			●		●
KNCS	●			●	●

A flaskcell has been designed to facilitate mixing during a run. The limiting equivalent conductances have been evaluated with the full Fuoss-Hsia conductivity equation. The Robinson-Stokes equation, used for the estimation of limiting equivalent conductance, is shown to give very similar values to those given by the Fuoss-Hsia equation. Also presented are the corresponding values of the parameters a (the ion-size parameter) and K_A (the association constant). The values obtained for K_A are small. Plots of log K_A (KCl) against reciprocal of dielectric constant and against the logarithm of water concentration show maxima. In the latter case, some evidence is presented that this indicates the participation of both water and DMF in the formation of ion-pairs in DMF/water mixtures.

The autogenic rising boundary method has been used to determine, in DMF/water solvents at 25°C, the limiting cationic transport numbers of KNCS in mixtures containing 0.5 and 0.75 mole fraction of DMF. Within experimental error, no concentration dependence of transport number has been detected in the former solutions; in 0.75 mole fraction of DMF, slight concentration dependence has been observed. In the latter solvent, corrections for ionic association are within the experimental error. Limiting ionic equivalent conductances derived from the above transport numbers and conductances are presented. The corresponding Stokes radii have been calculated. Plots against $100/D$ of the Stokes radii of K^+, Cl^-, Cs^+ and NCS^- are presented for complete range of DMF/water solvents at 25°C. The data obtained in this research for K^+ and Cl^- confirm the suspected shape, in DMF-rich regions of the existing plots for these ions. The shape of the Stokes radius plot for Cs^+ resembles that of K^+. $R^{\infty}_{Cs^+}$ values calculated from the slope and from the intercept are anomalous. The plot for NCS^-, although limited to four points, exhibits a

similar shape to the plot for Cl^-. Tentative $R^{\infty}_{NCS^-}$ values have been calculated.

A search for correlations between solute and solvent properties in DMF/water mixtures has been conducted. Densities, ionic equivalent conductances, viscosities and excess volumes of mixing have been plotted against solvent composition. Free volumes of the solvent mixtures have been calculated and used as the abscissae for plots of ionic conductances, viscosities and Walden Products. No simple correlations have been observed. However, the plot of viscosity, against solvent composition provides evidence for the existence of at least one DMF-water complex. The 'hard sphere' volume of this complex has been estimated by two methods and a molecular formula has been proposed.

A published theory which attempts to explain variations in Walden Product with solvent composition has been described and tested. Data for Cl^- in DMF/water mixtures at 25°C indicate that the theory does not hold in this system.

Declaration

I hereby certify that this thesis contains no material which has been accepted for the award of any other University, and to the best of my knowledge contains no material previously published or written by any other person, except where due reference is made in the text.

Glen Chittleborough

January 1976

ACKNOWLEDGEMENTS

During the course of this research the guidance and advice of my supervisor, Dr. B.J. Steel has been of great value; to him I extend thanks and appreciation.

To Messrs. Arthur Bowers, Gavin Duthie and Keith Shepherdson and their colleagues in the three workshops in this department I wish to extend my thanks for capable assistance in the construction and modification of apparatus.

Dr. P.J. Carson kindly assisted me in the modification of a non-linear least square program published in his Ph.D thesis.

The photograph of flaskcell H (Figure 2.2) was provided through the co-operation of the Advisory Centre for University Education.

The typing of this thesis has involved the joint labours of Mrs. Ann Dickson and Mrs. Elizabeth Lee whose cheerful co-operation is gratefully acknowledged. Also involved in the preparation of the thesis layout was Mrs. D. Kautsky, who kindly arranged the listings of the computer programs listed in the Appendix.

From my wife Helen have come encouragement and support for which I make grateful acknowledgement.

GLOSSARY OF PRINCIPAL SYMBOLS

The following symbols are applicable throughout this thesis. Other symbols have meanings applicable only to the chapter in which they appear.

a	The distance of closest approach of ions.
B	The coefficient of the ion-size term in Debye-Hückel theory.
B_1	The coefficient of the relaxation term in the Robinson-Stokes conductivity equation.
B_2	The coefficient of the electrophoretic term in the Robinson-Stokes conductivity equation.
C	Concentration of solution in mol dm^{-3}.
D	Dielectric constant.
e	The protonic charge.
exp	The exponent, e.
F	The Faraday constant.
f	The mean rational activity coefficient.
K_A	The association constant in conductance theory.
k	The Boltzmann constant.
log	Logarithms to base 10.
ln	Logarithms to base e.
N	The Avogadro constant.
N	Normality, equivalents per dm^3 of solution.
T	Absolute temperature.
t_+	Cationic transport number.
z_1, z_2	Algebraic valencies of cation and anion respectively.
γ	The fraction of solute existing as non-associated ions.
η	Viscosity of solvent.
κ	In Debye-Hückel theory, the 'reciprocal length' of the ionic atmosphere, proportional to the square root of ionic strength; in Chapter 4, the specific conductance.
Λ	The equivalent conductance of an electrolyte.

λ_+, λ_- The equivalent conductances of the cation and anion respectively.

Σ Summation.

σ The standard error of fit of the data to an empirical or theoretical equation.

σx The standard error of the coefficient x.

Ω Resistance as ohm.

GENERAL INTRODUCTION

In the study of electrolyte solutions, Walden's Rule[1] has long been used as an approximate guide to the inter-relationship between the two important parameters λ^0 and η. The rule is based on the assumption that dissolved ions moving in a solvent are adequately modelled by spheres moving in a continuum for which Stokes Law[2] applies. In 1959, Fuoss[3] proposed that ion-solvent interactions resulted in an increase in the local viscosity of an ion. This led to a new expression for the Stokes radius of an ion, incorporating dependence upon the dielectric constant, D.

$$R_i = R_i^{\infty} + S/D$$

R_i^{∞} is the Stokes radius of the ion in a solvent of infinite dielectric constant and S is a constant related to the magnitude of ion-solvent interactions. Later Boyd[4, 5] and Zwanzig[6, 7] provided theoretical confirmation of Fuoss' arguments and derived an expression S showing that it was related to the dielectric relaxation time of the solvent and also contained a term in R_i^{∞}. Consequently the Fuoss-Boyd-Zwanzig (FBZ) equation above provides for estimates of the quantity R_i^{∞}, both from the slope S, and from the intercept of a plot of R_i against D^{-1}.

Fuoss and co-workers[8] have used the intercept method extensively for 1–1 electrolytes in dioxane/water mixtures. In many of these cases R_i shows linear or near-linear plots against D^{-1} and the values of R_i^{∞} obtained from the intercept have been realistic although generally smaller than the respective crystal radii. However with some of the alkali halides such as LiCl and NaCl , minima occur in the plots of R_i at fairly high values of dielectric constant, indicating deviations from FBZ theory. An important assumption of the Fuoss School was that transport numbers are independent of solvent composition. James[12] on the other hand, working with KCl and KBr in mixtures with water of N, N-dimethylformamide (DMF), showed that transport numbers were solvent-dependent.

DMF is a polar liquid with a moderately high dielectric constant compared to dioxane. Its mixtures with water therefore produce only a comparatively narrow range of dielectric constants but offer fairly extensive opportunities for solvent-solvent and ion-solvent interactions. As such, DMF/water mixtures constitute solvents whose properties contrast markedly with those of dioxane/water, thereby providing a suitable different medium in which to test the FBZ theory.

James[12] also determined limiting ionic equivalent conductances for KCl and KBr and thus calculated the respective Stokes radii. His plot of R_{K^+} against D^{-1} was linear for most of the range of D, but showed a minimum (as in the cases of LiCl and NaCl in dioxane/

water) at a fairly high value of dielectric constant. A more serious challenge to FBZ theory comes from the contradictory and anomalous values of R_i^{∞} obtained from the slopes and the intercepts of the R_i *vs.* D^{-1} plots. A not unrealistic value of R_i^{∞} is given by the slope, but the intercept gives a substantially negative value.

This research extends James' work with alkali halides in DMF/water solvents.

In the first instance the range of solvent composition has been extended from a DMF mole fraction of 0.496 to 0.75. The determination of the limiting equivalent conductance of KCl and the limiting cationic transport number of KNCS in 0.75 mole fraction DMF fills a gap between the data of James at 0.496 mole fraction of DMF and the data of Ames and Sears[13] and Prue and Sherrington[14] in pure DMF. This work confirms the shapes of the Stokes radius plots for K^+ and Cl^- in this region.

A major portion of this research has been directed towards ascertaining whether the Stokes radius plot for Cs^+, like that of K^+, gives results which conflict with the predictions of the FBZ theory. Presented in Chapter 5 are results which indicate this to be so, leading to the view that the sphere-in-continuum model, upon which the FBZ theory is based, is too simple to explain the observed changes in conductance with solvent composition. Recent papers by members of the Fuoss School[9-11] working in isodielectric mixtures subscribe to this view also.

Chapter 1 of this thesis presents an account of the modern theory of conductance as embodied in the Fuoss-Hsia conductivity equation.[15] This three-parameter equation has been used in this research to calculate the limiting equivalent conductance, the ion-size parameter a and the association constant K_A. Chapter 2 describes experimental methodology for the measurement of equivalent conductance. Results of these measurements for KCl, CsCl and KNCS in DMF/water mixtures at 25°C are presented in Chapter 3 together with the respective values of a and K_A. The presented value of the limiting equivalent conductance of KNCS in water appears to be the first such value presented in the last 45 years. The reported limiting equivalent conductance of CsCl leads to a limiting equivalent conductance for Cs^+ which is near the top of a puzzlingly wide range of values for this ion, as provided by nine literature reports. Although not of major concern in this thesis, the change with solvent composition of K_A for KCl and for CsCl has been discussed in Chapter 3. Some evidence is presented for the participation of both water and DMF molecules in the process of ion-pair formation of KCl.

In Chapter 4 are described practical aspects of the determination of limiting cationic transport numbers using the autogenic rising boundary method. Values of this parameter for KNCS in DMF/water mixtures containing 0.5 and 0.75 mole fraction of DMF are

reported, together with limiting equivalent conductances of K^+, NCS^-, Cs^+ and Cl^- derived therefrom. This chapter also discusses interpolation procedures which have been used to obtain limiting equivalent conductances of Cl^- at the chosen solvent compositions.

In addition to a discussion of the FBZ theory and tests of it, Chapter 5 contains a report of a search for correlations between solute and solvent parameters in DMF/water mixtures. Plots of density, ionic equivalent conductance, viscosity and excess volume of mixing against solvent composition are presented. Following a suggestion by James and Fuoss[10], free volumes of the solvents were calculated and correlations were sought with conductance, viscosity and Walden Product. No simple correlations were apparent but results of the investigations of changes in viscosity led to evidence for the existence of one or more DMF-water complexes whose likely formulae have been proposed.

The chapter and the thesis concludes with the discussion and testing of a theoretical paper by Hemmes.[16] This paper indicates the complexities in the variation of the Walden Product likely to arise as a result of solvation of dissolved species by each of the components of a mixed solvent.

References

1. Walden, P., Ulich, H. and Busch, G., *Z. Phys. Chem.*, **123**, 429, (1926); Walden, P. and Birr, E.J., *ibid.*, **153A**, 1, (1931).
2. Stokes, G.G., *Trans. Camb. Phil. Soc.*, VIII, 287, (1845).
3. Fuoss, R.M., *Proc. Natl. Acad. Sci., U.S.A.*, **45**, 807, (1959).
4. Boyd, R.H., *J. Chem. Phys.*, **35**, 1281, (1961).
5. Boyd, R.H., *J. Chem. Phys.*, **39**, 2376, (1963).
6. Zwanzig, *J. Chem. Phys.*, **38**, 1603, (1963).
7. Zwanzig, *J. Chem. Phys.*, **52**, 3625, (1970).
8. a. NaCl; Kunze, R.W. and Fuoss, R.M., *J. Phys. Chem.*, **67**, 911, (1963).
   b. KCl; Lind, J.E., Jr., and Fuoss, R.M., *ibid.*, **65**, 999, (1961).
   c. RbCl; Kunze, R.W. and Fuoss, R.M., *ibid.*, **67**, 914, (1963).
   d. CsCl; Justice, J.-C. and Fuoss, R.M., *ibid.*, **67**, 1707, (1963).
   e. LiCl, RbI; Fabry, T.L. and Fuoss, R.M., *ibid.*, **68**, 971, 974, (1964).
   f. CsI; Lind, J;E., Jr., and Fuoss, R.M., *ibid.*, **65**, 1414, (1961).
   g. RbBr; Lind, J.E., Jr., and Fuoss, R.M., *ibid*, **66**, 1727, (1962).
9. D'Aprano, A. and Fuoss, R.M., *J. Soln. Chem.*, **3**, 45, (1974).
10. James, C.J. and Fuoss, R.M., *ibid*, **4**, 91, (1975).
11. D'Aprano, A. and Fuoss, R.M., *ibid*, **4**, 175, (1975).

12. James, C.J., Ph.D. thesis, University of Adelaide, South Australia, 1972.
13. Ames, D.P. and Sears, P.G., *J. Phys. Chem.*, **59**, 16, (1955).
14. Prue, J.E. and Sherrington, P.J., *Trans. Faraday,Soc.*, **57**, 1795, (1961).
15. Fuoss, R.M. and Hsia, K-L., *Proc. Natl. Acad. Sci., U.S.A.*, **57**, 1550; *ibid*, **58**, 1818, (1967).
16. Hemmes, P., *J. Phys. Chem.*, **78**, 907, (1974).

Chapter 1
CONDUCTANCE–THEORY

Chapter 1
CONDUCTANCE – THEORY

1.1 Introduction–The importance of the Debye-Hückel theory

Since the earliest days of electrochemical research, it has been known that the equivalent conductance of electrolyte solutions decreases with increasing concentration. Clearly interactions between charges on the ions in solution must be a primary cause of these observations. In 1923 Debye and Hückel provided a means of explaining these interactions with a theory which described the distribution of charges around an ion in solution.

The model used to develop this theory involves treating an electrolyte solution as a single reference ion *j*, standing alone in an ionic 'atmosphere' of opposite sign. This atmosphere comprises a continuum dielectric (representing the solvent molecules) which possesses a net charge density contributed by all ions in the solution except the reference ion.[1] Debye and Hückel used this model to develop an expression for the electrical potential ψ_j, at a point in the solution in terms of concentration, ionic charges and solvent properties. The expression obtained for ψ_j is

$$\psi_j = \frac{z_j e}{D} \cdot \frac{exp(\kappa a)}{(1+\kappa a)} \cdot \frac{exp(-\kappa r)}{r} \qquad (1.1)$$

where a is the distance of closest approach of the ions, assumed the same for all pairs of ions. κ, formally known as the Debye-Hückel reciprocal length, is given by

$$\kappa^2 = \frac{4\pi e^2 \Sigma n_i z_i^2}{DkT} \qquad (1.2)$$

Equation 1.2, defining κ, can be rewritten in terms of concentration of ions,

$$\kappa^2 = \frac{4\pi e^2 \mathrm{N}}{1000\, DkT} \cdot \Sigma c_i z_i^2 \qquad (1.3)$$

or in terms of ionic strength

$$\kappa = \left[\frac{8\pi e^2 \mathrm{N}}{1000\, DkT}\right]^{1/2} \sqrt{I} \qquad (1.4)$$

Thus
$$\kappa = B\sqrt{I} \qquad (1.5)$$

where
$$B = \left[\frac{8\pi e^2 \mathrm{N}}{1000\, DkT}\right]^{1/2} \qquad (1.6)$$

The κ function is a useful parameter of the ionic atmosphere. It can be shown[2] that at a distance $r = \kappa^{-1}$ from the surface of the reference ion, the charge contained in a spherical shell of thickness dr reaches a maximum. κ^{-1}, having dimensions of length is thus known as the 'thickness' of the ionic atmosphere.

Ever since the publication of the Debye-Hückel theory, workers in the field have leaned heavily on it in developing an understanding of the interactions of ionic charges in solution. Two major effects of this interaction are the *electrophoretic effect* and the *time of relaxation effect*. In each case, development of satisfactory theoretical expressions for these effects depended upon the use or adaptation of the Debye-Hückel expression for the potential.

1.2 The electrophoretic effect

An externally applied electric field acts both on a given *j* ion in solution and on its ionic atmosphere. These two entities, the *j* ion and its atmosphere, are of opposite charge and tend to move in opposite directions in the field. The moving *j* ion therefore experiences an increased viscous retardation arising from the contrary motion or 'counterflow'[3] of the solvent molecules of the ionic atmosphere.

The term *electrophoresis* applies to the migration of fairly large entities (10–10000Å) in an electric field; the ionic atmosphere can be considered such an entity—it has a 'thickness' (κ^{-1}) of about 100Å for a 1-1 electrolyte of concentration 10^{-3} mol dm^{-3}.[4] The motion of the ionic atmosphere contrary to that of the *j* ion is therefore known as the *electrophoretic effect* and the viscous retarding force it causes is the *electrophoretic force.* Clearly the effect is concentration dependent.

A thorough mathematical treatment of electrophoresis has been made by Onsager and Fuoss[5] and adapted by Robinson and Stokes.[6] The approach to the treatment was to assume spherical symmetry in the ionic atmosphere and to apply the Debye-Hückel expression for the potential ψ_j, and the classical Stokes equation relating the velocity of a particle moving in a viscous medium to the viscous retarding frictional force given by equation 1.7.

$$v = F/6\pi\eta r \tag{1.7}$$

The resulting expression for the electrophoretic effect $\Delta\Lambda_e$, on the equivalent conductance is

$$\Delta\Lambda_e = -\frac{F^2}{6\pi\eta N} \cdot (|z_1| + |z_2|) \cdot \frac{\kappa}{1+\kappa a} \qquad (1.8)$$

1.3 The relaxation effect

In the absence of an external force the ionic atmosphere of a reference ion *j* is symmetrical and the centre of charge of the atmosphere coincides with that of the *j* ion. When an external electric field of intensity X is applied to the solution the *j* ion moves, but, because of frictional resistance, the ionic atmosphere takes a finite time to relax and reform in response to this movement. During this time the ion *j* has moved on and further relaxation and reformation of the atmosphere must occur. The overall result is that the moving ion possesses a lagging asymmetric ionic atmosphere which can be viewed as egg-shaped.[7] Consequently the two centres of charge are permanently non-coincident and the resulting electrostatic force (taken as the relaxation field, ΔX, opposite to the applied field X) causes a retardation of the ion. This retardation is known as the *relaxation effect*, given by $\Delta X/X$. Like the electrophoretic effect, it is concentration dependent.

Debye and Hückel[8] made the first theoretical approach to explaining this phenomenon but a more successful result[9] was obtained by Onsager.[10] The latter simplified the Debye-Hückel expression for the potential by assuming, for very dilute solutions, that $1+\kappa a = 1$. In essence this assumes ions to be point charges and converts equation 1.1 to

$$\psi_j = \frac{z_j e}{D} \cdot \frac{exp(-\kappa r)}{r} \qquad (1.9)$$

Using this expression Onsager obtained

$$\frac{\Delta X}{X} = \frac{z_1 z_2 e^2}{3DkT} \cdot \frac{q\kappa}{1+\sqrt{q}} \qquad (1.10)$$

where q is a function of ionic charges and conductances which simplifies to ½ for 1-1 electrolytes. Thus

$$\frac{\Delta X}{X} = \frac{z_1 z_2 e^2}{6DkT} \cdot \frac{\kappa}{1+\sqrt{0.5}} \qquad (1.11)$$

1.4 The combined influence of electrophoresis and relaxation

The combined influence of the electrophoretic and relaxation effects upon the conductance can be expressed in the equation

$$\Lambda = (\Lambda^0 - \Delta\Lambda_e)\left(1+\frac{\Delta X}{X}\right) \tag{1.12}$$

The above expression for $\Delta X/X$ (equation 1.11) and an expression for $\Delta\Lambda_e$ (equation 1.8, simplified by taking $1+\kappa a = 1$) can be substituted in equation 1.12. If the cross-term $\frac{\Delta X}{X}\cdot\Delta\Lambda_e$ is neglected we obtain

$$\Lambda = \Lambda^0 - \underbrace{\frac{|z_1 z_2|e^2}{6DkT}\cdot\frac{\Lambda^0\kappa}{(1+\sqrt{0.5})}}_{\text{relaxation term}} - \underbrace{\frac{F^2(|z_1|+|z_2|)\kappa}{6\pi\eta N}}_{\text{electrophoretic term}} \tag{1.13}$$

It can be seen that this equation takes the form

$$\Lambda = \Lambda^0 - (B_1\Lambda^0 + B_2)\sqrt{C} \tag{1.14}$$

where B_1 and B_2 are related to properties of the solvent. For a given solvent

$$\Lambda = \Lambda^0 - \text{constant}.\sqrt{C} \tag{1.15}$$

which is a statement of the *Onsager limiting law*. It provides theoretical justification for the empirically derived Kohlrausch relationship

$$\Lambda = \Lambda^0 - S\sqrt{C} \tag{1.16}$$

published about a century ago.[11]

It should be noted that the Onsager equation (1.15) is the tangent to the conductance curve at zero concentration rather than an equation for the conductance curve itself.

Falkenhagen and co-workers[12] retained the $(1+\kappa a)$ term in the denominator of the expression for ψ_j and hence in the denominator of the relaxation effect expression (equation 1.11). In this way they accounted for the effects of finite ion size which the Onsager approach did not, and this modification made possible an increase in the range of validity of the theory. The analogous equation to 1.13 (which applies to 1-1 electrolytes) then becomes

$$\Lambda = \Lambda^0 - \frac{|z_1 z_2|e^2}{6DkT}\cdot\frac{\Lambda^0}{(1+\sqrt{0.5})} - \frac{F^2(|z_1|+|z_2|)}{6\pi\eta N}\cdot\frac{\kappa}{1+\kappa a} \tag{1.17}$$

Robinson and Stokes[13] have rearranged this equation in the form

$$\Lambda^0 = \Lambda + \frac{(B_1\Lambda+B_2)\sqrt{C}}{1+(Ba-B_1)\sqrt{C}} \qquad (1.18)$$

B_1 and B_2 are quoted in equation 1.14 in relation to 1.13. B is given by equation 1.5.

Equation 1.18, known familiarly as the Robinson–Stokes equation, has been used in this research to obtain approximate values of Λ^0 from Λ and concentration data.

1.5 The Fuoss-Onsager Equations

For 25 years after the Onsager paper on the relaxation effect[10] there was no major progress in developing the theory of this effect. This fact is an indication, perhaps, of the mathematical difficulty in the computation of ΔX.[14] Contributions from a number of workers in the early 1950's were capped by a most comprehensive treatment of conductance by Fuoss and Onsager.[15] Using a model of rigid charged spheres in a hydrodynamic and electrostatic continuum and retaining higher terms in the equations of continuity and motion[16] they obtained a conductance function for unassociated electrolytes. This function was[17] a cumbersome combination of algebraic and transcendental terms for which calculations (without the electronic computers of later years) would be unduly lengthy. Simplification was achieved[18] by selective retention of terms arising from the integration of the differential equations which describe the relaxation field. Only linear or lower terms in concentration were retained; all terms of order $C^{3/2}$ were dropped. The resulting linearized equation had the form

$$\Lambda = \Lambda^0 - SC^{1/2} + E'ClnC + J(a)C \qquad (1.19)$$

The coefficient S, corresponding to the S of the Onsager limiting law, is a function of Λ^0. Likewise E' depends on Λ^0 and is determined by theory. J explicitly depends on the centre to centre distance at contact of spheres representing the ions. The Fuoss-Onsager equation is thus a two parameter equation, embracing the arbitrary constants Λ^0 and a.

Because of the simplification procedure, the range of application of the linearized equation was restricted to concentrations where $\kappa a \leqslant 0.1$ or about 0.01N for 1–1 salts in water.

A little later Fuoss extended this equation to the case of associated electrolytes.[19] Making the *ad hoc*[20] hypothesis that ion pairs in contact would not contribute to (dc) transport of charge, Fuoss obtained

$$\Lambda = \Lambda^0 - SC^{1/2}\gamma^{1/2} + E'C\gamma lnC\gamma + JC\gamma - K_A c\gamma f^2\Lambda \qquad (1.20)$$

where $1-\gamma$ is the fraction of salt associated as ion-pairs and is related to the association constant by the mass action equation

$$1-\gamma = K_A C\gamma^2 f^2 \tag{1.21}$$

Equation 1.20 is a 3 parameter equation (Λ_0, a_0, K_A) which satisfactorily reproduced $\Lambda - C$ data for dielectric constants greater than 10, provided still that concentrations were chosen such that $\kappa a \leqslant 0.1$.

1.6 The '1965' Fuoss-Onsager Equation

A series of five papers by Fuoss and Onsager re-investigated the equations which led to equation 1.19. The *ad hoc* character of the generalization of equation 1.19 to 1.20 needed examination. Fuoss and Onsager felt that if ion association were a consequence of Coulomb forces only, then the corresponding decrease in Λ with increasing C should be predictable from the equations of continuity, equations of motion and the Poisson equation. A second motive for the re-investigation was the observation that a values calculated from $J(a)$ systematically increased for a given electrolyte as D decreased. There were two possible explanations for this relationship. Either it occurred as a result of mathematical approximations made in deriving equation 1.19, or the model of the system was inadequate. The two mathematical approximations made were the dropping of all terms in $C^{3/2}$ and the approximation of the Boltzmann expression in the equation of continuity to the first three terms of the series.

When the higher terms of the Boltzmann expression were retained explicitly, terms emerged in the expression for the relaxation field[21] which possessed the form of the K_A parameter which had appeared in the 1957 equation (equation 1.19). This meant that association of ions arose from the fundamental equations rather than in the arbitrary manner adopted earlier by Fuoss and Onsager. Combining the new expression for the relaxation field with an electrophoretic term which had also been re-investigated[22] incorporating higher terms, Fuoss, Onsager and Skinner[21] published the equation

$$\Lambda = \Lambda^0 - SC^{1/2} + E' C ln\tau^2 + LC - A\Lambda^0 Cf^2 \tag{1.22}$$

where $\tau^2 = 6E_1' C$ and E_1' is a function of solvent properties and A and L are constants. In the same paper the equation was generalized, incorporating ionic association. The coefficient A closely approximated to K_A and the generalized form became

$$\Lambda = \Lambda^0 - SC^{1/2}\gamma^{1/2} + E' C\gamma ln(6E_1' C\gamma) + LC\gamma - K_A C\gamma f^2 \Lambda \tag{1.23}$$

This became known as the '1965' equation. Equation 1.22 reproduces conductance data for 1–1 electrolytes in solvents of higher dielectric constant. Equation 1.23 is required for conductance data of 1–1 electrolytes when D is small enough to stablilize ion-pairs in contact. The two equations confirmed the 1957 conductance equation and established that the ion association term arose directly from application of the equations of continuity, equations of motion and the Poisson equation, i.e. from first principles.

Contact distances calculated from the application of precise data to these equations still showed an increase with decreasing D. It therefore was proposed by Fuoss and Onsager that the source of this variation lay not in the original mathematical approximations involved in solving the differential equations—rather it lay in the inadequacy of the sphere-in-continuum model upon which the theory was based.

Fuoss, Onsager and Skinner noted that a $C^{3/2}$ term arising from the 'explicit product' gave only marginal improvement to their equations. They decided to neglect this term and allow A and L to absorb any errors arising and therefore to restrict the range of application of the equations to concentrations where the $C^{3/2}$ contribution was negligible. In summary, the Fuoss-Onsager equations may be presented together.

$$\Lambda = \Lambda^0 - SC^{1/2} + E'C \log C + JC \tag{1.19}$$

$$\Lambda = \Lambda^0 - SC^{1/2}\gamma^{1/2} + E'C\gamma \log C\gamma + JC\gamma - K_A C\gamma f^2 \Lambda \tag{1.20}$$

$$\Lambda = \Lambda^0 - SC^{1/2} + E'C\ln\tau^2 + LC - A\Lambda^0 Cf^2 \tag{1.22}$$

$$\Lambda = \Lambda^0 - SC^{1/2}\gamma^{1/2} + E'C\gamma \ln(6E_1'C\gamma) + LC\gamma - K_A C\gamma f^2 \Lambda \tag{1.23}$$

Equations 1.20 and 1.23 are identical as equations of concentration. 1.20 and 1.23 both have 1.22 as a limit for γ near unity. For $f^2 \doteqdot 1$ (or $K_A = 0$) 1.22 approaches 1.19. When D is large and/or the salt has large ions, equations 1.19 and 1.23 are indistinguishable.

1.7 The Fuoss-Hsia Equation

The linearized Fuoss-Onsager equation (1.19) for unassociated salts, which becomes

$$\Lambda = \Lambda^0 - SC^{1/2} + E'C\ln C + JC - K_A \Lambda^0 C \tag{1.24}$$

for slightly associated salts was tested by Fuoss and Hsia[23] with data in which the concentration of salt exceeded the limit of applicability (about 0·01N for 1–1 electrolytes in water) set previously by Fuoss and Onsager as a result of the mathematical approximations referred to earlier. They found that Λ^0 and J values depend

upon concentration and diagnosed, not unexpectedly, that the functional form of equation 1.19 was incorrect for $C>0.01N$ in water. They showed that data of high precision[24, 25] and involving concentrations up to about $0.10N$ could be reproduced within experimental error by a semi-empirical equation of the form

$$\Lambda = \Lambda^0 - SC^{1/2} + EC\log C + AC + BC^{3/2} \qquad (1.25)$$

They were thus encouraged to repeat the integrations which led to equation 1.19, retaining all $C^{3/2}$ terms. This led to a complicated function too complex for desk calculators but which could be handled by an electronic computer.[23] Their theoretical conductance function had a range of applicability such that $\kappa a<0.5$ (which corresponds to concentrations less than about 0.25mol dm^{-3} for a 1-1 electrolyte in water).

Fuoss and Hsia pointed out that the symbolic expression for the conductance function is

$$\Lambda = \gamma(\Lambda^0 - \Delta\Lambda_e)\,(1+\frac{\Delta X}{X})\quad(1+{}^{3\phi}/_{2}) \qquad (1.26)$$

where ϕ is the volume fraction of one species of ion. The term $(1+{}^{3\phi}/_{2})$ is incorporated to account for the reduction in mobility of ions caused by the *obstruction effect*.[26] This effect becomes apparent in the more concentrated solutions of the ranges to which the Fuoss-Hsia equation may be applied. In such solutions the volume of solute is no longer a negligible fraction of the total volume and the necessity for migrating cations and anions to detour around each other contributes to a net retardation of each ion. For the lower range of concentrations (0.001N to 0.01N) used in this research the obstruction effect is negligible.

Fuoss and Hsia[23] have written a computer program designed to analyse a set of data points (C_j, Λ_j) according to their conductance equation in order to evaluate the parameters Λ^0, K_A and a. A similar program based on this equation and devised by Kay[27] and used in adapted form[28] in the determination of these three parameters in the present research. The adapted program does not modify the Fuoss-Hsia equation, it retains a $C^{3/2}$ term.

1.8 A new conductance equation

Recently conductance data have been processed by Renard and Justice[29] using a new conductance equation. This equation, developed by Fuoss, incorporates the Chen electrophoretic effect[30] but details of this effect and the related equation have not yet

been published. The new equation gives values of Λ^0 virtually identical with those obtained from the Fuoss-Hsia equation.

1.9 The concentration dependence of transport numbers

Transport (or transference) numbers are essentially ratios of conductances. The limiting transport number t_i^0, of an ion is simply related to the limiting ionic conductance, λ_i^0 and the limiting equivalent conductance, Λ_0 by the relation

$$t_i^0 = \frac{\lambda_i}{\Lambda^0} \tag{1.27}$$

Because of this, transport numbers usually exhibit a smaller concentration dependence than do conductances themselves. The extent of concentration dependence is related to the difference between the transport number and the value 0.5. For example, Robinson and Stokes[31] have observed that for non-associated 1-1 electrolytes the form of concentration dependence of the cationic transport number is as follows.

* If the transport number is near 0.5, scarcely any concentration depence applies.

** If the transport number is less than 0.5, it decreases further with increasing concentration.

*** When the transport number is greater than 0.5, it increases further with increasing concentration.

Such observations are readily explained by the theory of conductance already outlined in this chapter. Equation 1.12 can be restated for a particular ion in the form

$$\lambda_i = (\lambda^0 - \Delta\lambda_e)(1 + \Delta X/X) \tag{1.12a}$$

where $\Delta\lambda_e$ and $\Delta X/X$ are the expressions for the electrophoretic and relaxation effects applied to *i* ions only.

For symmetrical electrolytes the respective values of $\Delta\lambda_e$ and $\Delta X/X$ are the same for both cation and anion. Application of equation 1.12a to equation 1.27 thus leads, with cancellation of relaxation terms, to

$$t_i = \frac{\lambda_i^0 + \Delta\lambda_e}{\Lambda^0 + 2\Delta\lambda_e} \tag{1.28}$$

$\Delta\lambda_e$ is obtained from the single ion form of equation 1.8.

$$\Delta\lambda_e = -\frac{F^2}{6\pi\eta N} \cdot |z_i| \cdot \frac{\kappa}{1+\kappa a} \tag{1.8a}$$

Substition for $\Delta\lambda_e$ in equation 1.28 and application to 1-1 electrolytes[32] leads to

$$t_i = \frac{\lambda_i^0 + \frac{1}{2} B_2 \sqrt{C}/(1+\kappa a)}{\Lambda^0 - B_2 \sqrt{C}/(1+\kappa a)} \qquad (1.29)$$

This equation has been rearranged[33, 34] in the useful form

$$t_i^{0\prime} = t_i + \frac{(0.5 - t_i) B_2 \sqrt{C}}{(1+Ba\sqrt{C})\Lambda^0} \qquad (1.30)$$

This form of equation 1.29 provides a precise statement for the concentration dependence of transport numbers which theoretically justifies observations (a), (b), (c) outlined above. Tests of equation 1.29[35] give a high degree of agreement between observed and calculated values. Accordingly, equation 1.30 has been used in this research to evaluate limiting transport numbers from transport numbers determined at a range of finite concentrations.

References

1. Bockris, J.O'M. and Reddy, A.K.N., *Modern Electrochemistry*, Volume 1, Macdonald and Co., London, 1970, page 183.
2. Reference 1, pages 196-197.
3. Spiro, M., in Weissberger, A., (Ed.) *Techniques of Chemistry*, Volume 1, Part IIA, John Wiley and Sons, 1971, page 214.
4. Reference 1, page 425.
5. Onsager, L. and Fuoss, R.M., *J. Phys. Chem.*, **36**, 2689, (1932).
6. Robinson, R.A. and Stokes, R.H., *Electrolyte Solutions*, Butterworths, London, Second Edition, Revised 1965, page 134.
7. Reference 1, page 424.
8. Debye, P. and Hückel, E., *Phys. Z.*, **24**, 305, (1923).
9. Reference 6, page 137.
10. Onsager, L., *Phys. Z.*, **28**, 277, (1927).
11. Fuoss, R.M. and Accascina, F., *Electrolytic Conductance*, Interscience Publishers, New York and London, 1959, Chapter 1.
12. Reference 6, pages 138-139.
13. Reference 6, page 145.
14. Reference 6, page 136-137.
15. Fuoss, R.M. and Onsager, L., *Proc. Nat. Acad. Sci. U.S.A.*, **41**, 274, 1010, (1955).
16. Fuoss, R.M. and Onsager, L., *J. Phys. Chem.*, **36**, 2689, (1932).

17. Fuoss, R.M., *Second Australian Conference on Electrochemistry,* Butterworths, 1968, page 9.
18. Fuoss, R.M. and Onsager, L., *J. Phys. Chem.*, **61**, 668, (1957).
19. Fuoss, R.M., *J. Amer. Chem. Soc.*, **79**, 3301, (1957).
20. Fuoss, R.M., *J. Amer. Chem. Soc.*, **80**, 5059, (1958).
21. Fuoss, R.M., Onsager, L. and Skinner, J.F., *J. Phys. Chem.*, **69**, 2581, (1965).
22. Fuoss, R.M. and Onsager, L., *J. Phys. Chem.*, **67**, 628, (1963).
23. Fuoss, R.M. and Hsia, K.-L., *Proc. Nat. Acad. Sci. U.S.A.*, **57**, 1550, (1967); **58**, 1818, (1967).
24. Chiu, Y.-C. and Fuoss, R.M., *J. Phys. Chem.*, **72**, 4123, (1968).
25. Hsia, K.-L. and Fuoss, R.M., *J. Amer. Chem. Soc.*, **90**, 3055, (1968).
26. Reference 6, pages 310-313.
27. Kay, R.L., *J. Amer. Chem. Soc.*, **82**, 2099, (1960).
28. James, C.J., Ph.D. thesis, The University of Adelaide, 1972, page A48.
29. Renard, E. and Justice, J.-C., *J. Soln. Chem.*, **3**, 633, (1974).
30. Chen, M.S., Ph.D. thesis, Yale University, U.S.A. (1969).
31. Reference 6, page 156.
32. Reference 6, page 157.
33. Steel, B.J., *J. Phys. Chem.*, **69**, 3208, (1965).
34. Steel, B.J., Stokes, J.M. and Stokes, R.H., *J. Phys. Chem.*, **62**, 1514, (1958).
35. Reference 6, page 158.

Chapter 2
CONDUCTANCE–EXPERIMENTAL

Chapter 2
CONDUCTANCE--EXPERIMENTAL

2.1 Introduction

The conductance of electrolyte solutions may be very precisely determined. In this research, a precision as good as, or better than 0.01% has been sought. Accordingly steps were taken in this research to ensure that the chemicals, apparatus, equipment and associated techniques were capable of yielding such a precision. As will be seen in detail during this chapter, attention has been given to all factors likely to influence the precision of the measurements. Such factors include the purity of chemicals, cleanliness of glassware, accuracy of temperature control and the adequacy of technique.

2.2 Materials

Conductance water

Deionized water obtained from the bulk laboratory supply was distilled into, and stored in, a plastic container. Distillate collected in the early stages of the distillation was discarded – only water which had a specific conductance equivalent to the range $1.1 - 1.5 \times 10^{-6}$ ohm^{-1} cm^{-1} at 25°C was collected for use. Only freshly distilled conductance water was used.

Potassium chloride

Samples of this salt were originally purified by James.[1] Analytical reagent grade salt had been twice recrystallized from conductance water and dried successively in an air oven and a vacuum oven. It was then fused in a platinum crucible. The solid, broken into small lumps, was stored over silica gel in a desiccator. The salt was considered by James to be of high purity. Cell constants determined using aqueous solutions of his sample were in very close agreement with values obtained for the same cells used by other workers in this department, using different samples of purified potassium chloride.

Caesium chloride

Mulcahy[2] had purified this salt by recrystallizing it three times from doubly distilled water then drying in a vacuum oven. A sample submitted to AMDL* (now AMDEL) for analysis by flame photometry had shown impurities as Na(18 ppm), K(1 ppm), Rb(40 ppm) and Li(less than 1 ppm).

---

*Australian Mineral Development Laboratories, Glenunga, South Australia.

Potassium thiocyanate

Analar grade BDH* potassium thiocyanate was crystallized from conductance water, washed with a small quantity of chilled conductance water then dried in a vacuum oven at 60 - 80°C for about 12 hours. The crystals were stored in a vacuum desiccator.

Molecular sieves

BDH molecular sieves, type 3A, were used in pellet form to dehydrate dimethylformamide (DMF) prior to the final distillation of this liquid.

The sieves were washed several times with demineralized water prior to use, then dried in a stream of dry nitrogen in an oven at 250 - 300°C. Regeneration of the sieves after use was achieved by a similar procedure.

DMF

The following procedures for purification was recommended by James after investigation and trial of a variety of procedures.[3] He reported that the method adopted produced DMF with a water content between 0.0003 mol dm^{-3} and 0.001 mol dm^{-3} as measured by the Karl Fischer technique.

DMF from the store was treated with anhydrous copper sulphate. This removed much of the water present (originally about 0.01 mol dm^{-3}) and also complexed amines formed by the hydrolysis of DMF. After standing with intermittent shaking for not less than a week, the DMF mixture was fractionally distilled at a pressure of between 5 and 10mm mercury, discarding the first 50 cm^3 and the last 100 cm^3 of distillate for each initial cubic decimetre. The middle cut was dried further by storage over pre-dried type 3A molecular sieves for at least 2 days. Immediately prior to use, the DMF was again fractionally distilled. The physical conditions and the rejection of fractions of distillate were the same as in the first distillation.

DMF purified by this procedure had a specific conductance in the range $1.0 - 3.0 \times 10^{-7}$ ohm^{-1} cm^{-1}.

2.3 The cleaning of glassware

Flasks, flaskcells and beakers which were used to contain samples of purified DMF, conductance water or DMF/water solvents were cleaned by a routine procedure. Initially the internal walls of the vessel were treated with chromic acid to remove grease. Then followed at least six rinses and an overnight 'soaking' with demineralized water. Having been steamed for at least 30 minutes, the vessel was rinsed with conductance

---

*BDH Chemicals Ltd., Poole, England.

water and dried in an air oven. Subsequent to initial usage, the chromic acid and steaming steps were normally omitted from the cleaning procedure. Weight burettes could not be steamed but underwent the remainder of the cleaning procedure.

2.4 Weighing procedures

Preliminaries

Prior to weighing, the outer surfaces of all vessels were wiped with a clean cloth followed by clean chamois leather. Any adhering material was thus removed. The handling of vessels was carried out either by using stainless steel forceps tipped with polythene (normally for empty flasks or for weighing bottles), or by clean chamois leather fingerstalls. Flasks and weighing bottles were always weighed with a small watch-glass covering the mouth of the vessel.

In all cases except where otherwise noted, masses were always determined by first allowing thermal equilibration to occur.

Potassium chloride and caesium chloride

A Mettler B6C200 balance was used to weigh a sample of the salt in a weighing bottle. This balance permitted estimation of mass to 10^{-5} gram. At the same time the mass of an empty flask was obtained on a Mettler B5C1000 balance; this balance gave estimations of mass to 10^{-4} gram.

The salt was quantitatively transferred from the bottle to the flask and each vessel was then reweighed. The weight of solid transferred was taken as the change in the weight of the weighing bottle (plus contents) following transference of the salt. As a check the change in weight exhibited by the flask was also noted.

Potassium thiocyanate

Because of its hygroscopic/deliquescent nature, this salt was weighed under conditions designed to minimize absorption of atmospheric water vapour.

The weighing bottle containing a weighed sample of the salt was transferred (with watchglass) to a vacuum oven set at 80°C and left for approximately one hour. The vessel was then transferred to a vacuum desiccator to cool over silica gel. Thereafter the bottle was quickly reweighed on the Mettler B6C200 and the solid transferred to a weighed flask without delay. As soon as possible the bottle was again weighed to obtain the mass of potassium thiocyanate transferred to the flask. After the weight of the flask and its contents had been noted, solvent was quickly added to the flask. Dissolution of salt was ensured by thorough, careful swirling of the flask's contents.

Liquids, mixed solvents and solutions

Pure liquids were weighed in a flask on the Mettler B5C1000 if the total mass to be measured was less than 1 kg (the capacity of this balance). When the mass exceeded this value the Stanton H.D.2 beam balance was used, employing the method of swings.[4] The balance masses were calibrated on the Mettler B5C1000. Beam errors, were evaluated for 500g and 1000g by Gauss' method of double weighing[4] and were found to be - 0.0203% of the mass of the tare for 1000g mass. Brass masses were handled either with brass forceps or chamois leather fingerstalls.

The preparation of mixed solvents from DMF and water is characterized by the evolution of heat of mixing. In such preparations it was essential to allow the mixture to thermally equilibrate with the balance room before reweighing.

While potassium thiocyanate dissolved readily in all solvents used, the chlorides of potassium and caesium dissolved only with difficulty in solvents containing 0.5 mole fraction of DMF or more. In such cases a magnetic stirrer-bar coated with teflon was carefully inserted into the mixture after all weighing was completed. The flask, sealed with a teflon-sleeved ground-glass stopper, was placed on a magnetic stirrer for overnight mixing. Stirring was continued next day if necessary.

Buoyancy corrections

All solutions and solvents were prepared by weight and air buoyancy corrections were applied as indicated by Vogel.[5]

Solution densities

The density of moderately dilute solutions can be approximated by the relation

$$d_{solution} = d_0 + W_p \Delta d$$

where d_0 is the density of pure solvent, W_p is the weight percentage of solute in the solution and Δd is the charge in density of solution per unit weight per cent. For aqueous KCl and CsCl, $d_{solution}$ could be calculated since all variables in the above equation were known. However, for solutions of these salts in DMF/water solvents Δd is not known. In such cases Δd was taken as that pertaining to an aqueous solution of the salt. Errors incorporated in this assumption are extrapolated out when extrapolations to infinite dilution are made in the calculation of Λ^0.

2.5 Conductance measurements

2.5.1 Temperature control and measurement

The oil thermostat was regulated by a mercury-toluene regulator linked to a heating coil activated by a thyratron control unit. Temperature control to ±0.003°C or better, was achieved. Temperature was measured by a bomb calorimeter type thermometer which was graduated in 0.01 degree. Estimations to 0.001 degree were achieved with a magnifier. The thermometer had been calibrated against a platinum resistance thermometer by various members of this department.

2.5.2 Measurement of resistance – apparatus

Resistances were measured with a Leeds-Northrup model of a Jones-Dike bridge according to procedures outlined by Dike.[6]

Incorporated into the circuit were an oscillator, tunable amplifier and a cathode-ray oscilloscope as detector, all linked by shielded cables connected to a common earth. The bridge was isolated from the oscillator and the detector by transformers, thus permitting proper functioning of the Wagner earth. The oscillator output was held at 0.4 volt to avoid heating the solution between the electrodes of the flaskcell. The sensitivity of the combined apparatus varied from about 1 part in 10^5 at resistances above 5kΩ to about 1 part in 10^6 (or better) below 3kΩ and down to 400Ω.

2.5.3 Frequency dependence of resistance

The resistance of the flaskcells varied linearly with the reciprocal of frequency over the range 1.5kHz to 5kHz. Above the latter frequently the resistance behaviour of the flaskcells varied according to the magnitude of the resistance being measured. In the case of cell resistances lower than about 8kΩ, resistance tended to increase with increasing frequency beyond 5kHz and this tendency became less marked as the cell resistance became smaller. With fairly dilute solutions (or with solvents) whose cell resistance exceeded about 8kΩ, the resistance behaviour at frequencies greater than 5kHz was to decrease markedly as frequency increased. Plots of resistance against reciprocal of frequency typical of a conductance run in cell H are shown in Figure 2.1.

Solvent resistances were measured in the flaskcells using two 10kΩ resistances tapped from the bridge and connected as 20kΩ parallel with the flaskcell as recommended by Dike.[6] The same two resistors were always used for solvent resistance measurements since their frequency dependence had been measured and this knowledge was used to apply corrections to the bridge readings. Similarly, frequency dependence corrections were applied to the single 10kΩ resistor used for measuring resistances exceeding 10kΩ.

Corrections were also applied for the resistance of the cell leads.

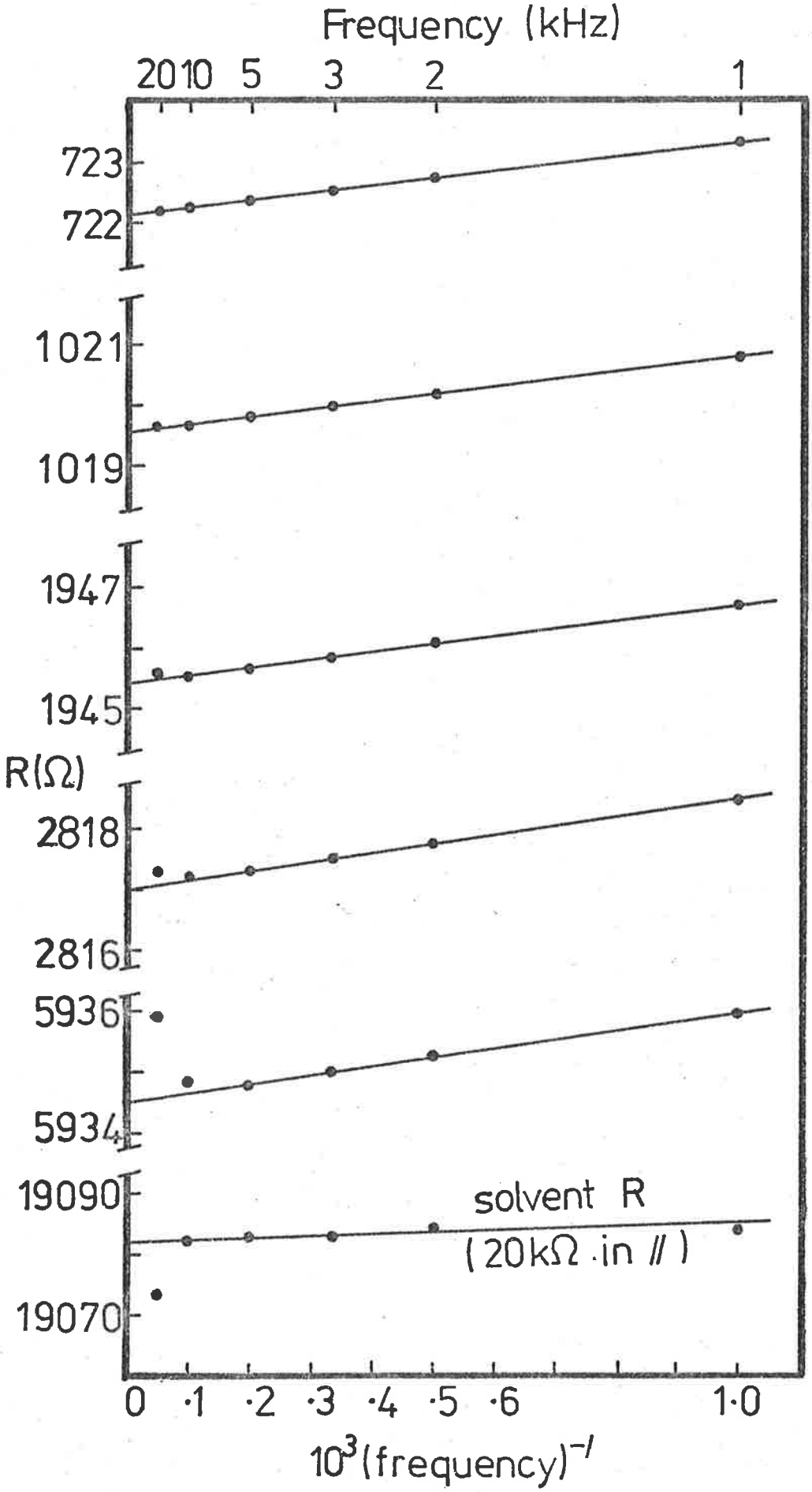

FIGURE 2.1 Frequency dependence of flaskcell H at various resistances.

The procedure adopted for the determination of each cell resistance was to plot measured resistance against reciprocal frequency and to extrapolate the linear portion of the plot to infinite frequency. The intercept at this frequency was taken to be the frequency independent resistance, that is the true ohmic resistance. The application of such procedures which ignore deviations from linearity has been justified by James[7] and Robinson and Stokes[8] and used by Hawes and Kaye[9] between 0.5 and 6kHz.

The value of the frequency independent resistance was subsequently used in the calculation of the equivalent conductance of the solution as indicated in section 2.5.5, a solvent correction being applied in each case.

2.5.4 Conductance flaskcells

Flaskcells G2 (cell constant 5.745_5) and H (cell constant 0.6748_5) were designed by the author to facilitate the mixing and agitating of flaskcell contents during a conductance run. Efficient mixing is achieved by physical manipulation of the flask – no electrical stirring is required.

The construction of flaskcell H is illustrated in Figure 2.2. The main feature of the construction is the connection of the cell to the flask by two glass tubes. With two possible avenues of exit or entry by liquid or air, the cell can be readily flushed. Further, by appropriate tilting of the flask a large air bubble may be trapped in the cell then allowed to escape into the flask, causing vigorous mixing as it passes through the liquid. Excessive tilting of the flask is to be avoided, otherwise wetting of the teflon stopper may occur, possibly incorporating errors into subsequent measurements. This precaution is to be followed especially when the volume of liquid contained in the flask cell approaches 420 cm^3, the upper limit of effective mixing.

Platinum plate electrodes sealed into cell chamber were very lightly platinized to reduce the frequency dependence of the resistance of the cell. Excessive platinizing was avoided in order to prevent both adsorption of ionic or organic species from solution and the possible catalytic decomposition of the organic component of the solvent

Flaskcell G2 was used to determine only one limiting equivalent conductance, cell H being used for all other such determinations.

The cell constants of the flaskcells were each determined by at least one conductance run with aqueous potassium chloride in the manner outlined in section 2.5.5. It was observed that the cell constant exhibited a 'level effect', probably due to the nature of the construction of the flaskcell. Two pathways for the passage of current are available in this flaskcell. Of these, the less direct pathway (via the solution in the flask proper) appears to exhibit a decrease in resistance, up to a limit, with increasing depth of liquid.

FIGURE 2.2 Flaskcell H

Conductance runs were performed with a minimum of 320 cm^3 of solution in the flaskcell, thus avoiding any possible variation of the cell constant. Data for the cell constant determinations are given in Table 2.1.

Table 2.1 Cell constant determinations

Flaskcell H	
Cumulative Volume (cm^3)	*Cell Constant*
286	0.675157
296	0.674971
306	0.674930
316	0.674916
337	0.674833
358	0.674851
371	0.674815
Cell constant taken as	0.67485

Flaskcell G2	
Cumulative Volume (cm^3)	*Cell Constant*
320	5.74560
341	5.74620
350	5.74596
363	5.74556
376	5.74515
Cell constant taken as	5.7456

2.5.5 *Procedure for a conductance run at 25° C*

The flaskcell, containing a known weight of solvent, was placed in the oil thermostat to thermally equilibrate. The flaskcell was stoppered with a tapered teflon stopper to minimize adherence of solvent condensate. When a steady resistance value at a particular frequency was noted, the flaskcell was removed and thoroughly agitated, then replaced in the thermostat to re-equilibrate. A single repetition of this agitation procedure was generally sufficient to remove the Soret effect.[10] The resistance of the cell was measured with 20kΩ resistors in parallel at the frequencies 1.5,2,3,5, 10kHz. These data together with appropriate corrections mentioned earlier, were used to determine the specific conductance of the solvent, a parameter both indicative of the quality of the solvent and necessary as a correction to be applied to conductances of the electrolyte solutions studied.

A stock solution, containing a known concentration of salt in the above solvent, was carefully added to the flaskcell from a tared weight burette handled with chamois leather fingerstalls. Usually the volume added was between 10 and 20 cm^3. The weight of added stock was obtained by difference on the Mettler B6200 balance. The flaskcell was now removed from the thermostat, its contents thoroughly mixed and then allowed to equilibrate with the thermostat. The Soret effect was removed, as above, by two more agitations of the equilibrated flask and the checking of resistance until successive readings were equal. The resistance of the cell was then measured at the same frequencies as indicated above for the solvent. The conductance run was continued by adding more

stock solution and repeating the above procedure.

Resistance data was plotted against reciprocal of frequency, as previously outlined, to obtain the resistance at infinite frequency for each concentration of the salt. A set of raw data, involving weights of added stock solution together with the corresponding resistance of flaskcell solution at infinite frequency, was thus generated. This raw data together with information including data for corrections for buoyancy, solution density, solvent and leads resistance, was used as input data for a computer program *'C and* Λ *from raw data'* constructed[11] for use on a Hewlett-Packard 9820A Model 20 calculator. Output from this program provided the respective concentrations and equivalent conductances following each addition of stock. This information was in turn used as input data (together with appropriate values of the coefficients B, B_1 and B_2 (equations 1.6, 1.14) and an estimate of a) in a program[11] entitled *'Robinson and Stokes calculation of Lambda 0'*. This program employs the Robinson-Stokes equation (1.18) to give estimations of the limiting equivalent conductance from each set of concentration/Λ data supplied to it. From this output a plot of 'Robinson-Stokes Λ^0' against concentration was made and extrapolated to zero concentration. This gave a good estimate of 'true' Λ^0 which is one of the input data for the program UNASS and LOAOKA which compute Λ^0 and a, (LOAOKA also computes K_A) using the Fuoss-Hsia conductance equation. Table 2.2 compares some values of Λ^0 obtained by the Robinson-Stokes procedure and the Fuoss-Hsia equation. The difference in Λ^0 obtained by the two methods is given by $\Delta\Lambda^0 = \Lambda^0(F\text{-}H) - \Lambda^0(R\text{-}S)$.

Table 2.2 Comparison of estimates of Λ^0

Salt	*DMF mole %*	$\Lambda^0(F\text{-}H)$	$\Lambda^0(R\text{-}S)$	$\Delta\Lambda^0$
CsCl	0	153.670	153.65	+0.02
CsCl	9	81.906	81.86	+0.04
CsCl	30	44.364	44.30	+0.064
CsCl	50	45.689	45.55	+0.139
CsCl	75	62.176	62.10	+0.076
KNCS	0	139.987	139.95	+0.037
KNCS	50	48.295	48.25	+0.045
KNCS	75	66.786	66.65	+0.131

This remarkably good agreement suggests that workers interested only in the Λ^0 values of solutions of moderately high dielectric constant may save computing time and lose little in accuracy were they to restrict their calculations to those of the comparatively simple Robinson-Stokes procedure.

References

1. James, C.J., Ph.D. thesis, The University of Adelaide, 1972, page 36.
2. Mulcahy, D.E., Ph.D. thesis, The University of Adelaide, 1967, pages 42–43.
3. Reference 1, Chapter 5.
4. Vogel, A.I., *A Text-Book of Quantitative Inorganic Analysis,* Longmans Green and Co., London, Third Edition, 1961, pages 148–151.
5. Reference 4, pages 152–155.
6. Dike, P.H., *Rev. Sci. Inst.,* **2**, 379, (1931).
7. Reference 1, page 49.
8. Robinson, R.A. and Stokes, R.H., *Electrolyte Solutions,* Butterworths, London, Second Edition, Revised 1965, page 95.
9. Hawes, J.L. and Kaye, R.L., *J. Phys. Chem.,* **69**, 2420, (1965).
10. Stokes, R.H., *J. Phys. Chem.,* **65**, 1277, 1242, (1961).
11. Steel, B.J., Department of Physical and Inorganic Chemistry, University of Adelaide.

Chapter 3
CONDUCTANCE – RESULTS AND DISCUSSION

Chapter 3
CONDUCTANCE – RESULTS AND DISCUSSION

3.1 Introduction

The conductances of solutions of CsCl, KNCS and KCl in various DMF/water solvent mixtures have been measured at 25°C. The maximum proportion of DMF was 0.75 mole fraction and the upper limit of concentrations used was 0.016 mol dm^{-3}.

This upper limit of concentration resulted from the design of the flaskcell (Chapter 2). The design was aimed at ease and effectiveness of mixing. However, the level effect, inherent in the design and operative up to a total solution volume of about 320cm^3, reduced the maximum possible added volume of stock to about 100cm^3. This limitation resulted in most runs covering the range 0.001–0.01 mol dm^{-3}.

In applying the Fuoss-Hsia equation to a set of data, the computer program LOAOKA evaluated the three parameters Λ^0, a and K_A simultaneously, using a method of successive approximations. These were aimed at minimising the quantity σ^2 in the expression

$$(n-3)\sigma^2 = \Sigma(\Lambda_{calc} - \Lambda_{obs})^2 \qquad (3.1)$$

where n is the number of data points. (In the program UNASS, used for the non-associated case, K_A is assumed to be zero and the program computes only Λ^0 and a). In the evaluation of the activity coefficient $f_{\pm}$, needed for the calculation of K_A, the extended form of the Debye-Hückel theory, given by

$$\ln f_{\pm} = - \frac{|z_1 z_2| e^2}{2DkT} \cdot \frac{\kappa}{1+\kappa a} \qquad (3.2)$$

has been used rather than the limiting law used by Fuoss.[1] The value of a used in this expression was allowed to converge during the successive approximation procedure to the value required by other terms in the conductance equation.

Values obtained in this research for Λ^0, a and K_A are displayed in Table 3.1. Raw data for each run are to be found in Appendix 3.1.

3.2 Results for Λ^0

It can be seen that the standard error of fit of the data to the conductance equation is generally about 0.01%. Uncertainties in Λ^0 are mainly in the range 0.01–0.02% giving a satisfactory degree of precision. In Chapters 4 and 5 the Λ^0 values will be used to obtain

Table 3.1 Λ^0, a and K_A for KCl, KNCS and CsCl in DMF/water mixtures at 25°C

Salt	*DMF mole fraction*	C_{max}	Λ^0	$\pm\sigma\Lambda^0$	a	$\pm\sigma a$	K_A	$\pm\sigma K_A$	σ
CsCl	0	0.010	153.68_2	0.022	3.208	0.022	0.0	0.0	0.008
	0	0.010	153.629	0.015	2.852	0.015	0.0	0.0	0.006
	9	0.012	81.906	0.015	6.479	0.746	1.581	0.180	0.006
	30	0.011	44.391	0.025	7.42	2.4_3	4.9	1.0	0.013
	50	0.012	45.689	0.012	9.506	0.454	11.471	0.174	0.007
	75	0.010	62.176	0.005	2.650	0.035	12.757	0.137	0.002
KNCS	0	0.010	139.987	0.023	3.786	0.023	0.0	0.0	0.008
	50	0.011	48.295	0.004	8.410	0.166	2.804	0.086	0.003
	50	0.012	48.284	0.004	8.508	0.137	2.840	0.066	0.002
	75	0.010	66.786	0.005	9.374	0.110	6.554	0.082	0.002
KCl	30	0.012	44.600	0.036	6.779	1.796	3.214	0.802	0.005
	75	0.016	59.615	0.003	2.231	0.013	3.366	0.061	0.002

values of λ^0 and Stokes radius with a view to discussing the variation of these parameters with solvent properties. However, two particular Λ^0 values may be discussed here.

There appear to be no recent reports in the literature of the value of Λ^0(KNCS) in water at 25°C. Washburn[2] presents conductances first published in 1912. In 1930 Garb and Hlasko[3] published values of the 'coefficient of conductance' at three concentrations in the range 0.002 - 0.05N. Their value of Λ^0, apparently based on an estimate of the degree of dissociation of KNCS in water,was 142.98. Surprisingly no Λ^0 determinations for this system using a modern conductance equation appear to have been made, although values for Λ^0(KNCS) in a number of organic solvents have been published. No valid comparison with the result presented on Table 3.1 can therefore be made.

In the case of Λ^0(CsCl) in water at 25°C, application of $\lambda^0_{Cl^-} = 76.35$[4] to the mean of the values presented gives $\lambda^0_{Cs^+} = 77.31$. This provides an interesting comparison with a number of literature values, displayed on Table 3.2.

Table 3.2 $\lambda^0_{Cs^+}$ values in water at 25°C

Salt	$\lambda^0_{Cs^+}$†	*Author*	*Reference*
CsCl	77.26	Voisinet	5
	76.46	Justice and Fuoss	6
	76.92	Accascina and Goffredi	7
	76.70	Treiner, Justice and Fuoss	8
	76.91*	Renard and Justice	9
	77.31*	this research	
CsBr	76.77	Treiner, Justice and Fuoss	8
	77.23*	Hsia and Fuoss	10
CsI	77.20	Lind and Fuoss	11
	77.33*	Hsia and Fuoss	10

*Calculated from the difference between values of the published Λ^0 and λ^0 found in reference 4.

† Units $ohm^{-1}\ cm^{-2}\ eq^{-1}$ used throughout this thesis.

Even allowing for slight differences due to both experimental error and calculation procedures for Λ^0, the substantial variations in the tabulated values of $\lambda^0_{Cs^+}$ are perplexing in a field of research acknowledged for its precision.

3.3 Results for a and K_A

Although Λ^0 is the quantity of main interest, some comment is necessary on the values obtained for the interdependent parameters a and K_A. On Table 3.1 the uncertainties presented for a and K_A are typically 1 - 3% and 1 - 5% respectively, but reaching 20% for K_A and even higher for a. In view of the satisfactory precision of the

Λ^0 values, these uncertainties reflect the lack of sensitivity of the σ function (equation 3.1) to the effect of only slight degrees of ionic association $(1-\gamma)$ arising from the combination of fairly low concentrations and small values of K_A prevailing in these systems.

It is clear from Table 3.1 that a, the distance of closest approach of ions in solution, varies with solvent composition. Since the model upon which the conductance equation is based assumes that a is constant for a given salt, these results cast some doubt on the model and upon the significance of these association constants, K_A, to which a is related.

The tabulated values of K_A for KCl may be discussed in relation to the results of James[12] for KCl and KBr in DMF/water solvents containing up to 0.496 mole fraction of DMF. Although the variation in K_A with solvent composition is small (a range similar to that for CsCl) it is of interest to note that for both KCl and KBr James' data gave linear plots of log K_A against $100/D$, supporting the Denison-Ramsey-Fuoss theory[13, 14] of ion-pair formation. Further, the James data also indicated that log K_A is a linear function of log C_{H_2O} where C_{H_2O} is the concentration of water (mol dm^{-3}) in a mixed solvent. According to Quist and Marshall[15, 16], such a result occurs when water alone is involved in solvation changes during ion-pair formation. However when James' data is combined with the data obtained in this research for KCl in DMF/water solvent containing 0.75 mole fraction, the resulting plots suggest that log K_A is linear in neither $100/D$ nor log C_{H_2O} rather, a maximum appears in each plot (Table 3.3 and figures 3.1 and 3.2). The limited data for CsCl (Table 3.4) similarly suggests non-linear plots (figures 3.1 and 3.2) and the likelihood of a maximum therein.

In an attempt to rationalize these observations, the proposals of Quist and Marshall[16] concerning selective solvation in non-aqueous solvents has been applied to the KCl/DMF/water system.

If it is assumed that both H_2O and DMF are involved in solvation changes during ion-pair formation it is possible to write

$$K^+_{(solv)} + Cl^-_{(solv)} \rightleftharpoons KCl_{(solv)} + pH_2O + q\text{DMF} \qquad (3.3)$$

for which the 'complete' constant K_A^0 is given by

$$K_A^0 = \frac{a_{KCl(solv)} \cdot (a_{H_2O})^p \cdot (a_{DMF})^q}{a_{K^+_{(solv)}} \cdot a_{Cl^-_{(solv)}}} \qquad (3.4)$$

Table 3.3 Properties of DMF/water solvents and values of log K_A for KCl at 25°C

Mole % DMF	K_A	*log* K_A	*100/D*	*log* C_{H_2O}
0.0	0.79_2	-0.101	1.273	1.74
6.005	1.00	0.0048	1.339	1.64
13.49	1.70	0.229	1.443	1.53
26.94	3.75	0.574	1.650	1.34
30.00	3.25[a]	0.512	1.706	1.30
35.06	5.00	0.699	1.783	1.24
49.63	9.58	0.988	2.008	0.60_6
75.00	3.37[a]	0.527	2.388	1.04

a. presented on Table 3.1

Table 3.4 Properties of DMF/water solvents and values of log K_A for CsCl at 25°C

Mole % DMF	K_A[a]	*log* K_A	*100/D*	*log* C_{H_2O}
9	1.58	0.199	1.37	1.60
30	4.78	0.679	1.70	1.30
50	11.47	1.06	2.01	1.03
75	12.76	1.11	2.39	0.60_6

a. presented on Table 3.1

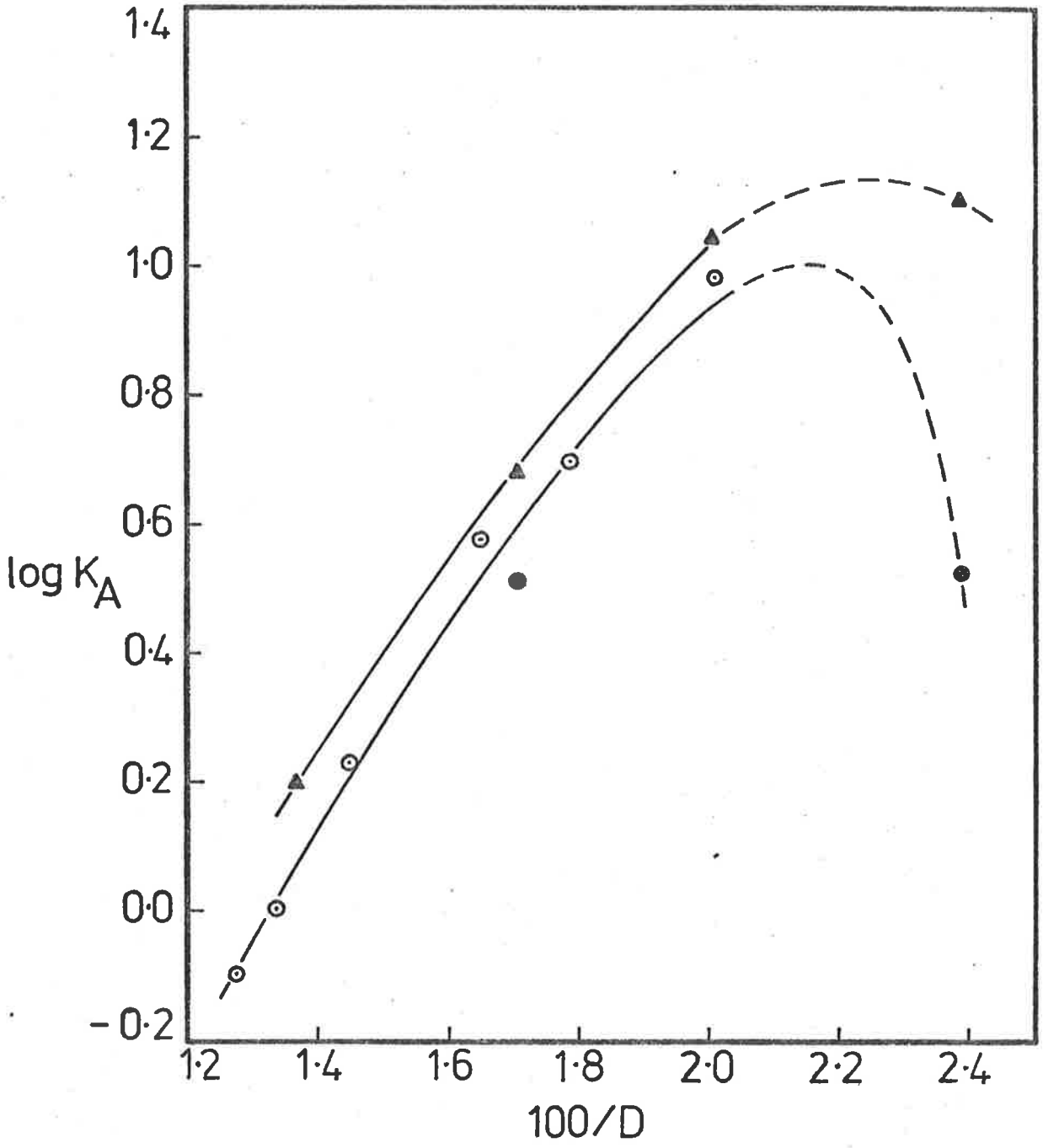

FIGURE 3.1 The dependence of log K_A upon the reciprocal of the dielectric constant of DMF/water mixtures at 25°C

- ⊙ KCl, data of James
- ● KCl, this research
- ▲ CsCl, this research

Note: Typical errors for the K_A values used are discussed in section 3.3.

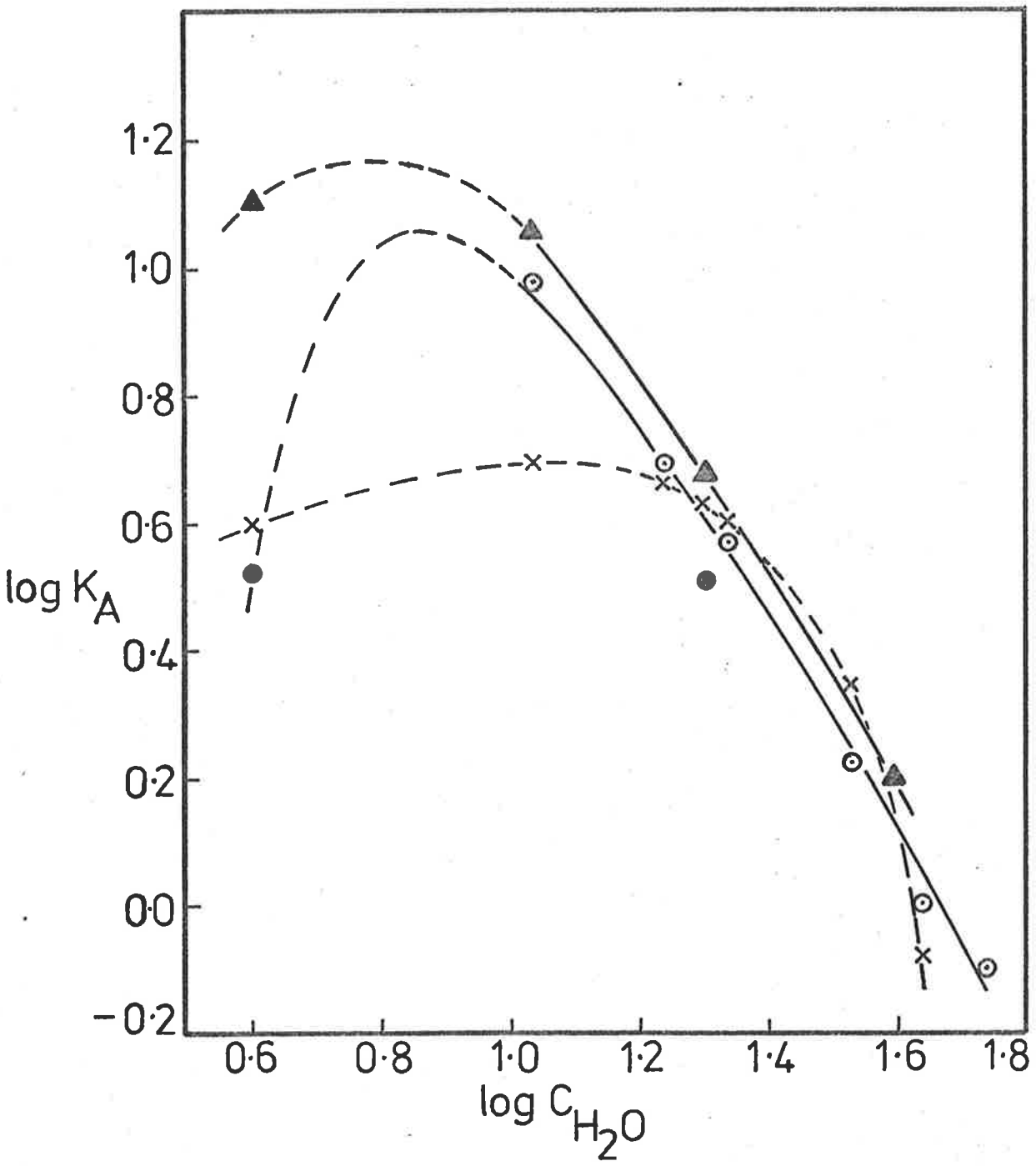

FIGURE 3.2 The dependence of log K_A upon log C_{H_2O} in DMF/water mixtures at 25°C.

⊙ KCl, data of James
● KCl, this research
▲ CsCl, this research
× KCl, derived equation

Note: Typical errors for the K_A values used are discussed in section 3.3.

or $$K_A^0 = K_A \cdot (a_{H_2O})^p \cdot (a_{DMF})^q \qquad (3.5)$$

where K_A is the conventional association constant and K_A^0 is independent of solvent composition. Applying logarithms to equation 3.5 and assuming that activities of solvent components of the mixture are given by concentrations, we obtain

$$\log K_A = \log K_A^0 - p \log C_{H_2O} - q \log C_{DMF} \qquad (3.6)$$

The shape of a plot of $\log K_A$ *vs.* $\log C_{H_2O}$ will depend upon the sign and magnitude of both p and q.

In order to test equation 3.5 the logarithmic data on Table 3.3 was analysed with a multiple linear regression program whose output included values of K_A^0, p and q which fitted the data. The results were $\log K_A^0 = -1.42$, $p = -0.352$, $q = -1.70$, values whose order of magnitude appears reasonable. However, the negative sign of p and q implies that the ion-pair is more solvated than the separate ions. From a qualitative or intuitive viewpoint such a situation seems improbable. As a check on the computer result, values of $\log K_A$ given by equation 3.6a were calculated for the values of $\log C_{H_2O}$ and $\log C_{DMF}$ given on Table 3.3.

$$\log K_A = -1.42 + 0.352 \log C_{H_2O} + 1.70 \log C_{DMF} \qquad (3.6a)$$

The results of these calculations are plotted on Figure 3.2, showing that the general form of the original plot is retained by the derived data. However the lack of data at lower C_{H_2O} values has tended to bias the values of p and q and hence the shape of the derived plot in this region. Clearly if firmer inferences are to be drawn concerning the application of the proposals of Quist and Marshall to this system, more data points are needed especially in the DMF-rich solvent mixtures. In any case, caution would be needed in the making of such inferences because of the uncertainties inherent in a system whose K_A values are small and the precision of which is lower than might be desirable.

References

1. Fuoss, R.M., in *Second Australian Conference on Electrochemistry,* Butterworth and Co. (Australia) Ltd., 1968, page 9.
2. Washburn, E.W., (ed.), *International Critical Tables of Numerical Data, Physics, Chemistry and Technology,* Volume 5, National Research Council, New York, 1929, page 252.

3. Garb, B. and Hlasko, M., *Roczniki Chem.*, **10**, 248, (1930).
4. Robinson, R.A. and Stokes, R.H., *Electrolyte Solutions*, Butterworths, London, Second Edition, revised 1965, page 463.
5. Voisinet, W.E., Thesis, Yale University, U.S.A., 1951.
6. Justice, J.-C. and Fuoss, R.M., *J. Phys. Chem.*, **67**, 1707, (1963).
7. Accascina, F. and Goffredi, M., reference 6 in reference 8 (below).
8. Treiner, C., Justice, J.-C. and Fuoss, R.M., *J. Phys. Chem.*, **68**, 3886, (1964).
9. Renard, E. and Justice, J.-C., *J. Soln. Chem.*, **3**, 633, (1974).
10. Hsia, K.-L. and Fuoss, R.M., *J. Amer. Chem. Soc.*, **90**, 3055, (1968).
11. Lind, J.E., Jr., and Fuoss, R.M., *J. Phys. Chem.*, **65**, 1414, (1961).
12. James, C.J., Ph.D. thesis, University of Adelaide, South Australia, 1972.
13. Denison, J.T. and Ramsay, J.B., *J. Amer. Chem. Soc.*, **77**, 2615, (1955).
14. Fuoss, R.M., *J. Am. Chem. Soc.*, **80**, 5059, (1958).
15. Marshall, W.L. and Quist, A.S., *Proc. Natl. Acad. Sci., U.S.A.*, **58**, 901, (1967).
16. Quist, A.S. and Marshall, W.L., *J. Phys. Chem.*, **72**, 1536, (1968).

Chapter 4
TRANSPORT NUMBER DETERMINATIONS

Chapter 4
TRANSPORT NUMBERS

4.1 Introduction

The theory of the concentration dependence of transport (or transference) numbers has been discussed in Chapter 1. For other matters relating to the theory and determination of transport numbers the reader is referred to the literature[1,2,3], Spiro[3] having published a very comprehensive coverage of the topic.

In the present research attention has been given to the determination of the cationic transport number of potassium thiocyanate in DMF-rich compositions (0.5 and 0.75 mole fraction) of the mixed solvent DMF/water. The ultimate objective of these determinations was to obtain the limiting equivalent conductances of the ions K^+, Cl^- and Cs^+ in these solvents. This follows the work of James[4] who determined the cationic transport number of potassium chloride in DMF/water solvents containing up to about 0.5 mole fraction of DMF. James used the modified Hittorf method of Steel and Stokes.[5,6]

Difficulties arise when this method is applied to potassium halides in DMF-rich compositions of such solvents. The silver halides used on the reversible silver/silver halide electrodes dissolve readily, forming silver halide complex ions. Such complexes contribute to the transport of electric current. Thus what is measured is the transfer of ion-constituents[7] rather than the transfer of simple individual ions. Potassium thiocyanate was the only readily available alternative salt which was sufficiently soluble in the above solvents. However silver thiocyanate, like the silver halides, is also unsuitable for use on an electrode since it dissolves in the solutions of potassium thiocyanate forming soluble silver complex anions. The use of another alternative, silver electrodes and silver nitrate solutions, was unfavourably reviewed by James[4] who found that such solutions were unstable even when stored in the dark, precipitating solid material (probably silver oxide) after 24 hours. Consequently the modified Hittorf method was judged unsuitable for the determinations envisaged and the autogenic rising boundary method,[8] using a cadmium anode, was adopted.

In this procedure Cd^{2+} ions from the anode enter the solution (in this research, of 1-1 electrolyte) to form a sharp boundary with the faster moving univalent cations M^+. The cathode used was silver gauze. Cathodic reduction in the systems studied involved formation of gaseous and alkaline products. However, the design of the cell in the vicinity of the cathode (compartment F) precluded mixing of these products with solution in the tube M. This was shown to be so in a dummy run in which phenolphthalein was added to the solution in compartments F and G prior to switching on the current.

During this run the solution in compartment F gradually acquired the characteristic red colour of phenolphthalein in alkaline solution but at no stage did this colour appear in compartment G. This result indicated that the cathode reactions could not affect the transport number measurements.

KNCS was selected as solute in the chosen solvents because of its ready solubility and ability to form fairly sharp boundaries. KCl and CsCl, of much lower solubility, appeared not to form detectable boundaries.

In principle the procedure of the moving boundary method is to measure the volume traversed by the boundary when a known quantity of electricity has passed through the cell. In practice the procedure is to measure the time taken by the boundary to traverse a fixed known volume of tubing under the influence of a measured amount of current. The transport number is then given[8] by

$$t^{+}_{obs} = \frac{VCF}{iT} \qquad (4.1)$$

where V is the measured volume (cm^3), i is the average current (mA), T is the time taken (second), and C is concentration of solution (mol dm^{-3}).

A correction for the solvent conductance may be applied as indicated by equation 4.2.[8]

$$t_{+} = t^{+}_{obs}(1 + \kappa_{solvent}/\kappa_{solute}) \qquad (4.2)$$

A correction for the volume changes associated with the dissolution of the cadmium anode may be applied[8] by use of the equation

$$t_{+} = t^{+}_{obs} - C\Delta V \qquad (4.3)$$

where, for KNCS solutions, ΔV in litres per Faraday is given[8] by

$$\Delta V = \tfrac{1}{2}\overline{V}_{Cd(NCS)_2} - t_{+}\overline{V}_{KNCS} - \tfrac{1}{2}V_{Cd(s)} \qquad (4.4)$$

V and $\overline{V}$ are molar and partial molar volumes respectively. However, data for $Cd(NCS)_2$ are not available and the volume correction for KNCS cannot be calculated. An estimate of the likely magnitude of this correction at 0.04 mol dm^{-3} KNCS was made by calculating ΔV for KCl[9] at this concentration and assuming that the corrections for these two salts were similar. The calculation gave $C\Delta V = -0.0002_9$. Since the uncertainty of the

cationic transport number of KNCS in 0.75 mole fraction DMF/water solution is about ±0.0010 in this research (section 4.5.2) the assumption that the volume corrections for KNCS solutions are within experimental error and can be omitted, appears to be justified.

4.2 Materials

Solutes, solvents and solutions used in the transport number measurements were purified and/or prepared as indicated in Chapter 2.

4.3 Apparatus and equipment

4.3.1 Thermostat bath

The thermostat bath had glass viewing panels at front and back. The thermostatic fluid was demineralized water whose temperature was held at 25°C ± 0.005 by a mercury-toluene regulator connected to a heating element activated by a thyratron control unit. The control so achieved far exceeded that necessary for transport work where transport numbers exhibit changes of the order of 0.1% per C. degrees.

The stirrer motor was positioned so that the blades at the end of the drive shaft created maximum turbulence near the heater. The temperature of the thermostat was measured by a bomb calorimeter type thermometer similar to that described in Chapter 2.

4.3.2 The autogenic moving boundary cell

The simple cell design chosen resembles a design recommended by Spiro.[10] This is illustrated in figure 4.1.

M is a 30cm length of precision-bore pyrex capillary tubing of internal diameter 3 mm. Calibration marks 1,2,3,4, approximately 5 cm apart are ceramic decals (transfers) delineating calibrated sections 1,2,3 as shown. Ground glass socket C is size B7 into which the carefully turned and lapped cadmium anode E1 fits snugly. A light smearing of stopcock grease produced a leak-free fit when E1 is firmly placed in position. Sockets A and B are size B14. A is used for access to the tube M for filling and emptying and is stoppered when the tube is in use. E2 is the cathode assembly comprising a roll of silver gauze (the cathode proper) welded to medium gauge platinum wire which is itself sealed into the glass tubing. The B14 groundglass cone of E2 is slotted to permit the escape of gas generated at the cathode when the cell is functioning with E2 in position in compartment F.

With E1 in position, polythene gas tubing covers the lead from the positive terminal of the constant current supply; the end of the tubing is forced over the ridge of socket C thus ensuring a tight fit and providing complete electrical insulation of both the lead and the

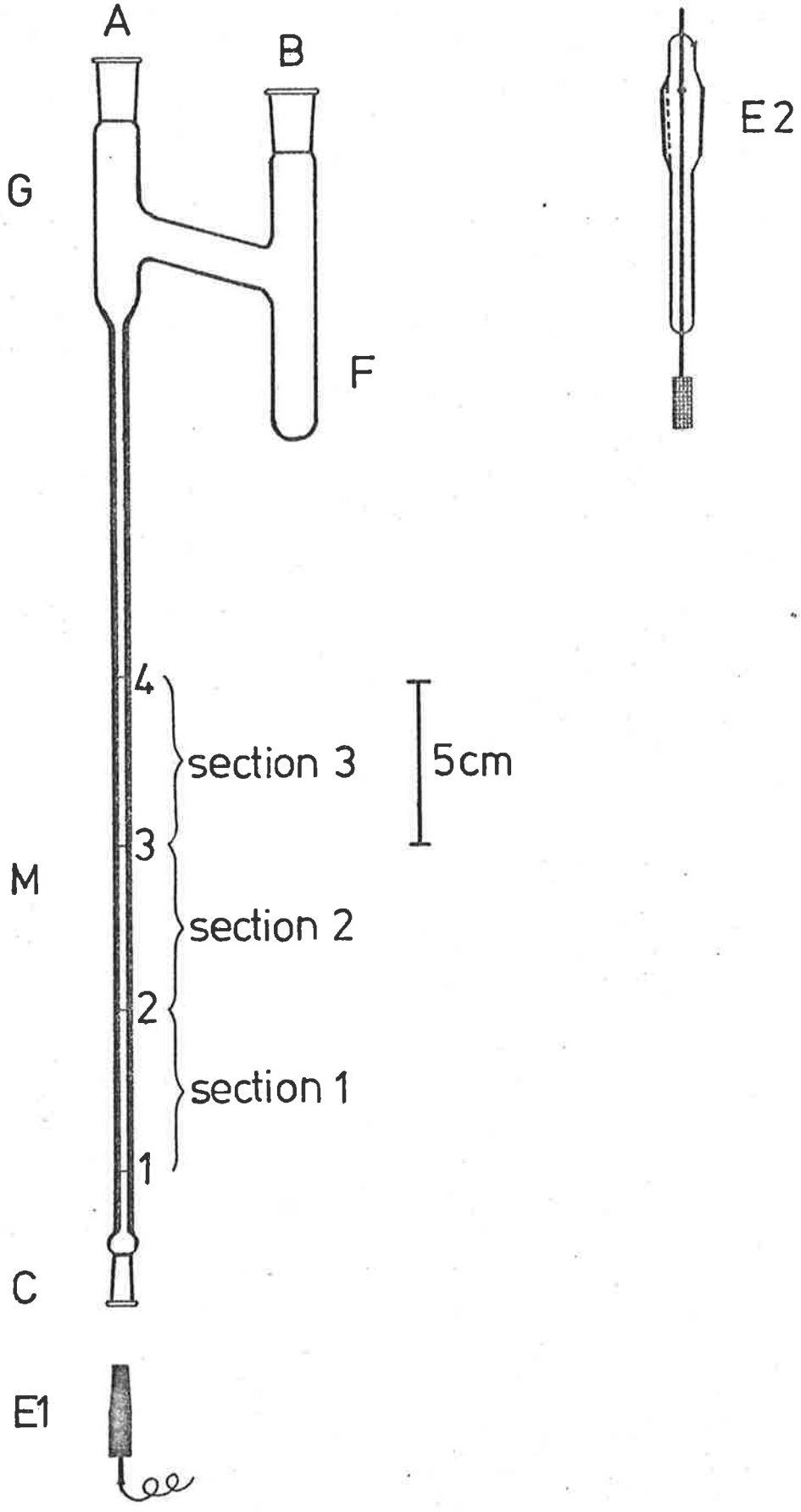

FIGURE 4.1 The autogenic moving boundary cell.

anode from the thermostat water.

The cell is firmly fixed on a vertical cradle mounted centrally on a metal box-frame. This frame in turn is clamped to a horizontal frame resting on a three point mounting on top of the thermostat bath. The position of the cell was checked, adjusted and rechecked for verticality using an accurate engineer's level. The metal box-frame was always returned to the same position on the horizontal frame if removal was necessary.

4.3.3 The supply and measurement of current

A 'constant' current supply unit, manufactured in the Electronics Workshop of this department, was used to provide currents up to 0.5 milliamp. Such currents were supplied at a potential of about 550 volts. Consequently a safety rule was laid down that adjustments to apparatus in the vicinity of the cell or the power supply would only be made when the mains supply was disconnected.

The amount of current passing through the cell was determined by measuring the potential difference across one of a set of calibrated resistors of between 1k Ω and 100kΩ. The resistors were incorporated into the circuit between the earthed positive terminal of the supply and the anode. This arrangement avoided errors caused by any leakage of current from cathode to earth via the thermostat bath. The potential across the resistors was measured with a Doran* dc potentiometer which was capable of a precision of better than 0.01%. This instrument had previously been calibrated by James[11] against a certified Cambridge potentiometer type 44248.

During a run this potential was measured and recorded at intervals usually of about 5 minutes. The performance of the constant current supply can be gauged from a typical plot shown in figure 4.2.

An estimation of the mean potential difference for each section of the run was made either from a plot of the potential or by an integrating program for the Hewlett-Packard 9820A Model 20 calculator. Corresponding currents were obtained by the application of Ohm's law.

4.3.4 Cathetometer

The cathetometer, used for viewing the boundary, stood on a rigid steel table which was bolted to the floor in front of the thermostat in such a position that the telescope objective lens was approximately 30 cm from the front window of the thermostat or about 45 cm from the m.b. tube. This permitted the telescope to focus on the tube. The depth of

---

*Doran Instrument Co. Ltd. Stroud. Glos. England.

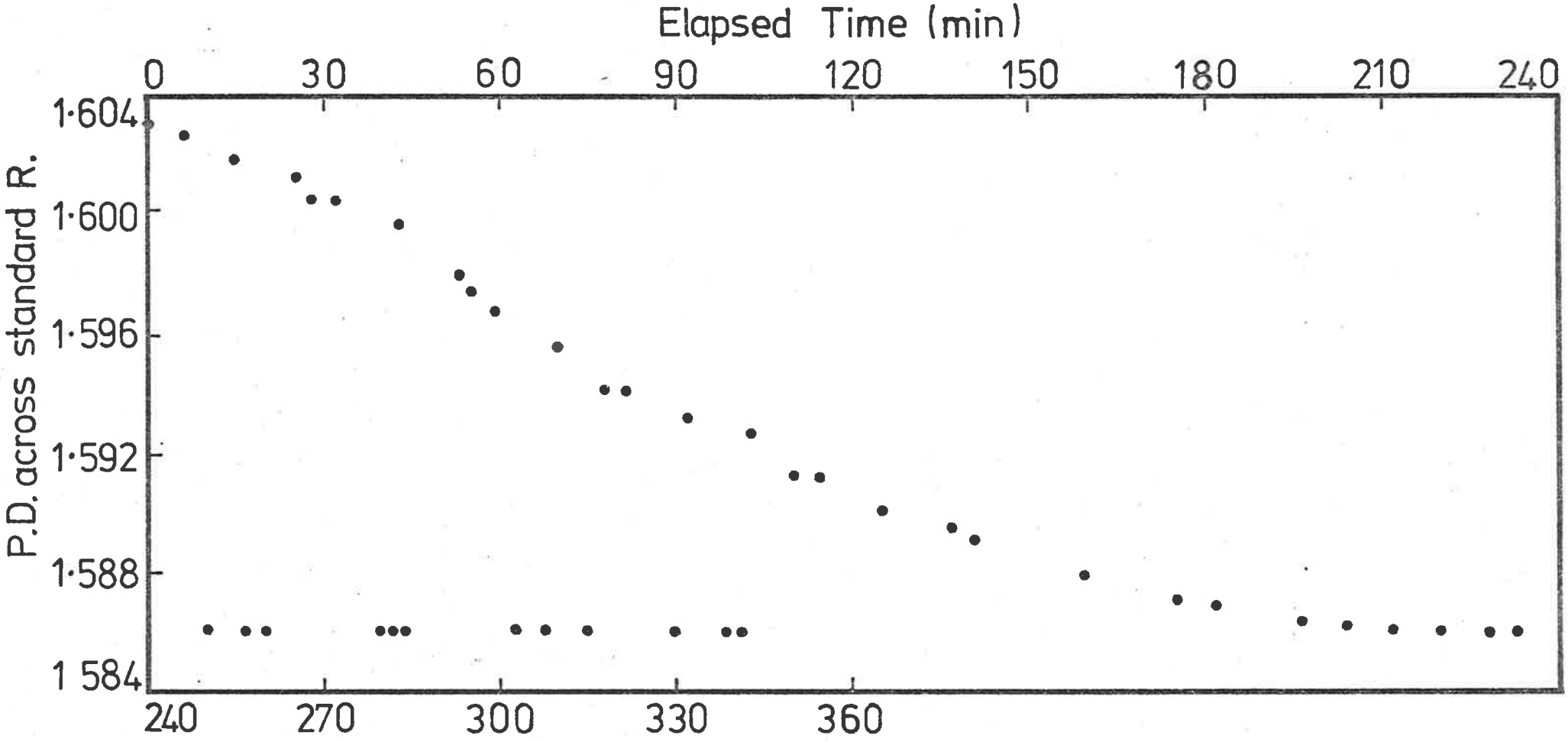

FIGURE 4.2 Typical performance of constant current supply during a transport number run—potential across a standard resistance.

field of this optical system was such that, once a clear focus on a calibration mark had been achieved, the image of the boundary could also be clearly seen without further adjustment.

Care was taken to ensure that the optical axis of the telescope was horizontal. This was accomplished with the aid of an engineer's level, guaranteed true.

The verticality of the cathetometer pillar was then established using the horizontality of the telescope as a criterion. This involved applying the principle that rotation about a truly vertical pillar would not affect the levelling bubble mounted on a truly horizontal telescope.

Once the pillar had been established in a vertical position the verticality of the m.b. tube could be checked by viewing the tube while the telescope was racked up or down on the pillar. Verticality of the tube in a vertical plane at right angles to the optical axis of the telescope could not be checked in this manner.

4.3.5 Timers

Two timers were used during a run, one being started simultaneously with the stopping of the other as the moving boundary passed a calibration mark on the tube. In a normal run four such marks were passed. Both timers were built in the Electronics Workshop of this department. One timer, had E1T counting tubes incorporated into its design. The second timer, using integrated circuitry with semiconductors for counting and display, was used in conjunction with a 60 watt 250mA filter to reduce its susceptibility to 'spikes' from the mains supply.

Each timer was calibrated against a Schlumberger Model FH2524 Universal Counter.

4.3.6 Apparatus for enhancing the visibility of the boundary

Moving boundaries may often be detected optically by virtue of a difference in the refractive index of the solutions in the vicinity of the boundary. Detection of a boundary is therefore enhanced by light passing through the boundary region towards the viewer. In this research light was shone on the m.b. tube through the rear window of the thermostat bath using a lamp mounted on a carriage which ran smoothly over a pair of vertical runners fixed firmly to the bench behind the bath. The arrangement described has been suggested by Spiro.[8] The vertical position of the lamp could be adjusted by means of a pulley system controlled at the bench front by a thread-and-screw assembly. The lamp itself was mounted inside a blackened lampcover which was horizontally slotted to produce a rectangular opening about 10 cm long and 5 mm high. Filter paper fitted inside and behind the opening produced uniform band of diffused light. A vertical cylindrical glass tube 10 cm wide and 36 cm high and filled with demineralized water was placed between the lamp and the rear window of the thermostat. This acted as a cylindrical lens which improved the visibility of the boundary and reduced the dark appearance of the inside walls of the

m.b. tube.

Viewed through the telescope, the boundary tube could be seen outlined against the narrow horizontal band of light produced by the lamp. The boundary itself only becomes visible when its image is seen as being close to either of the horizontal edges of the band of light. When viewed near the lower edge, the boundary is seen as a bright line; by suitable adjustment of the vertical position of the lamp the boundary can be seen as a dark line near the upper edge of the band of light. The dark line image of the boundary was preferred as being more easily detectable and more suitable for the timing technique outlined later in section 4.4.2.

4.4 Practical aspects of the transport number determinations

4.4.1 Some procedures in preparing for a run

The m.b. apparatus was cleaned in the first instance by treatment with chromic acid followed by rinsing and soaking with demineralized water in a manner similar to that used for conductance glassware. Thereafter chromic acid was not used. The normal preparation of the tube involved filling, flushing and emptying it at least six times using the test solution. This was achieved with the aid of syringes fitted with long stainless steel capillaries.

To avoid the formation of air bubbles the test solution was de-gassed just prior to the final filling of the m.b. tube. The apparatus, stoppered at A and with electrode E2 in place, was allowed to equilibrate with the thermostat bath. A visual check for bubbles was then made using the telescope of the cathetometer. A check on the verticality of the cathetometer pillar and the m.b. tube could be made at the same time.

The telescope was adjusted so that sharp images both of the cross-hairs and a selected calibration mark exhibited a minimum of parallalax. This was to ensure that a minimum of parallalax error would occur when the image of the moving boundary appeared to coincide with that of the cross-hairs. That such a minimum was achieved was checked when the boundary appeared. Thereafter the focus of the telescope was retained in this position for the duration of the run.

4.4.2 Timing technique

The timing of the passage of the boundary from one calibration mark to the next involved two important techniques. These were

* *Positioning the cross-hairs of the telescope accurately in relation to each calibration mark.*

This was achieved by ensuring that the top edge of the image of the calibration mark coincided with the point of intersection of the bottom edges of the image of the cross-hairs.

** *Judging consistently the instant of commencement or completion of a time measurement.*

As the moving boundary approached one of these points in time, the triangle of light formed by the intersection of images of the boundary and cross-hairs gradually dwindled to a single tiny spot of light.

At the instant of disappearance of this spot the timer switch was pressed.

Judgement of this moment was enhanced by adjusting the position of the lamp to produce maximum darkness in the image of the boundary.

4.4.3 Specific conductance of solvent and solution

During the transport run the resistance of the solvent was monitored in a solvent cell or a flask cell thermostatted in an oil bath at 25°C. In most cases slight hydrolysis of the DMF caused a increase in the specific conductance of the solvent for the duration of the run. A typical example of this change was from 3.3×10^{-7} ohm^{-1} cm^{-1} to 3.6×10^{-7} ohm^{-1} cm^{-1}.

The resistance of the solution was measured in a thermostatted dip-cell to give the specific conductance of the solution under study.

The ratio of the two specific conductances was then available for the calculation of the solvent correction (equation 4.2). This factor had typical values in the range 1.0002 to 1.0016.

4.4.4 Calibration of the cell

The literature contains accurate values of the cationic transport number of KCl in water over the range 0.001 – 1.0 mol dm^{-3}. Accordingly the three volumes delineated by calibration marks 1, 2, 3 and 4 on the tube M were calibrated using the convenient concentration 0.1 mol dm^{-3} of KCl in water, for which $t_+ = 0.4899$.[12] This data can be used in equation 4.1 to evaluate the volume of the relevant section of the tube, subject to the correction applied by equation 4.2. In one of the four runs a higher current gave the same results within experimental error, thus indicating an absence of current dependence in the system. The results of these calibrations are shown on Table 4.1.

A useful check was afforded by the measurement of physical dimensions of the cylindrical volumes between adjacent marks. The internal radius of the tube was evaluated

Table 4.1 Calibrations of moving boundary tube

(a) Electrical method (at 25°C) (using aqueous KCl, 0.10089_5 mol dm^{-3})

	Section 1			*Section 2*			*Section 3*		
Run No.	*ave. current (mA)*	*time (sec)*	*volume (cm^3)*	*ave. current (mA)*	*time (sec)*	*volume (cm^3)*	*ave. current (mA)*	*time (sec)*	*volume (cm^3)*
1	3.0488	2297.9	0.3525_6	3.0480	2293.9	0.3518_5	3.0475	2248.3	0.3448_0
2	3.0454	2294.7	0.3516_7	3.0450	2295.9	0.3518_0	3.0445	2245.5	0.3440_4
3	3.0452	2300.8	0.3525_9	3.0452	2298.0	0.3521_6	3.0452	2250.3	0.3448_4
4	4.0473	1731.5	0.3526_7	4.0473	1730.7	0.3525_0	4.0473	1690.2	0.3442_5
		mean	0.3523_7		*mean*	0.3520_7		*mean*	0.3444_8

(b) Physical method : dimensions of cylindrical volume

	Section 1	*Section 2*	*Section 3*
Internal radius (mm)	1.5006	1.5006	1.5024
Length (cm)	4.982	4.969	4.863
Volume (cm^3)	0.3524	0.3516	0.3449

by using a travelling microscope to measure the length of a column of mercury of known volume, applying a correction for assumed hemispherical ends of the column. The distance between adjacent calibration marks was measured with the cathetometer. Volumes calculated from this data are shown on Table 4.1. The values obtained give fairly good agreement with the electrical calibrations but because the physical measurements are of lower precision, the volumes obtained are not included in the final calibration values.

4.4.5 *Concentration dependence*

In chapter 1 reference was made to the concentration dependence of transport numbers. This dependence was summarized by the equation

$$t_i^{0\prime} = t_i + \frac{(0.5-t_i)B_2\sqrt{C}}{(1+Ba\sqrt{C})\Lambda^0} \qquad (1.30)$$

Because of imperfections in the theory, values of the apparent limiting transport number $t_i^{0\prime}$ show a small concentration dependence rather than a constant value. Consequently the 'true' limiting transport number t_i^0 must be obtained by evaluating $t_i^{0\prime}$ over a range of concentrations and then extrapolating to infinite dilution. (This procedure is analogous to the Robinson-Stokes procedure for the evaluation of Λ^0, outlined in Chapter 2). In the current research t_+^0 has been so obtained.

4.4.6 *Allowing for ionic association*

During the computation of Λ^0 values for KNCS in the DMF-rich solvents, out-put from PROGRAM LOAOKA showed that, at the concentrations used, 2–10% ionic association occurred. (This was expected in view of the lower dielectric constants involved). Allowance for the effects of inter-ionic attractions were therefore necessary and were accomplished by application of the mass action law to the equilibrium

$$K^+NCS^- \underset{K_A}{\overset{1/K_A}{\rightleftharpoons}} K^+ + NCS^-$$

This gives

$$\frac{1}{K_A} = \frac{\gamma^2 C}{1-\gamma} \cdot \frac{f_\pm{}^2}{f_{KNCS}} \qquad (4.5)$$

where γ is the percentage of salt existing as discrete ions, $f_\pm$ is the mean ionic activity coefficient and f_{KNCS} is the activity coefficient of the ion pair. Taking $f_{KNCS} = 1$ we have

$$\frac{1}{K_A} = \frac{\gamma^2 C}{1-\gamma} \cdot f_\pm{}^2 \qquad (4.6)$$

The value of K_A was available in the output data of PROGRAM LOAOKA. $f_\pm$ can be obtained from the Debye-Hückel expression

$$\log f_\pm = - \frac{A\sqrt{C}}{1+Ba\sqrt{C}} \qquad (4.7)$$

where $A = \frac{1.8246 \times 10^6}{(DT)^{3/2}}$ and $B = \frac{50.29 \times 10^8}{(DT)^{1/2}}$

The value of a was obtained from the output of PROGRAM LOAOKA.

Substitution for $f_\pm$, K_A, a and C in equation 4.6 leads to a quadratic equation in γ. Solving for γ permits the calculation of the value of γC, the fraction of the concentration actually present as discrete ions. The value of γC was then substituted in equation 1.30 in place of the analystical concentration C, and a new value of $t_i^{0\prime}$ was determined.

4.4.7 Current dependence

Spiro[13] has warned against assuming independence of current in transport work. This warning has been heeded in the present research. For example, calibration of the cell with KCl at a concentration of 0.1 mol dm^{-3} was performed with two different currents.

In the DMF/water solvents studied, the choice of current magnitude was limited by the observation that, for a given concentration, a solution tended to exhibit a characteristic optimum current for the formation of a sharp boundary. Currents in excess of the optimum gave curved, less dark boundaries; currents less than the optimum gave more diffuse boundaries. In either case precision suffered. As a result, variation of the current at a given concentration was not studied. However since the 'optimum' current changed with concentration, a range of currents has been used in the determination of t_+^0 for a given solvent. This can be observed in Tables 4.2 and 4.3.

4.5 Results and discussion

4.5.1 t_+^0(KNCS) in 0.5 mole fraction DMF/water

Table 4.2 displays results for two concentrations of the salt.

Table 4.2 Cationic transport numbers of KNCS in 0.5 mole fraction DMF/water solvent at 25°C

$C \times 10^2$ (mol dm^{-3})	Solution volume (cm^3)	Average current (mA)	Time (second)	t_+	$t_+^{0\prime}$
1.9741	1.0489	0.30464	14042.9	0.4689	0.4712
3.9157	1.0489	0.44340	19141.4	0.4681	0.4709 [a]

a. For the more concentrated solution γ was found to be 94.3%. Substitution of the value of γC for that of C in equation 1.30 had no effect on the calculated value of $t_i^{0\prime}$.

The solution volume indicated represents the passage of the boundary from mark 1 to mark 4 on the tube. Times at which the boundary passed marks 2 and 3 were also noted so that three separate estimations of t_+ could be made (see Appendix 4.1). These estimations showed a precision of about 0.1%, suggesting that such a precision also applies to the overall run. (The main source of error in the determination appears to occur in the timing technique where the uncertainty was about ±4 seconds, arising from a difficulty in ascertaining the disappearance of the spot of light, a technique discussed in section 4.4.2). Since the two values of $t_+^{0\prime}$ are within this experimental error, no concentration dependence can be inferred. Accordingly the value of t_+^0 is taken as the mean of the $t_+^{0\prime}$ values. This means that the most precise value which can be taken is $t_+^0 = 0.4710 \pm 0.0005$.

The determination of t_+^0(KNCS) in this solvent provided a check on technique through $\lambda^0_{K^+}$. The mean value of Λ^0(KNCS) (Chapter 3) was determined as 48.289 ±0.005 which leads to $\lambda^0_{K^+} = 22.7_4$. James[4] used a modified Hittorf method to obtain t_+^0(KCl) in a range of DMF/water solvents including one containing 20% water (0.496 mole fraction DMF). He subsequently obtained $\lambda^0_{K^+} = 22.6_9$ for this solvent. Interpolation, at 0.5 mole fraction, of the $\lambda^0_{K^+}$ values presented by James gave $\lambda^0_{K^+} = 22.7_4$. Since the evaluation of the two λ^0_+ values involved determinations of a total of four fundamental parameters (two each of t_+^0 and Λ^0), each with its own indeterminate errors, the agreement can be regarded as very satisfactory.

4.5.2 t_+^0 in 0.75 mole fraction DMF/water

The work of James with KCl and KBr[14] in DMF/water solvents was confined to the range 0-0.496 mole fraction of DMF. Prue and Sherrington[15] found t_+^0 for KNCS in pure DMF, but no other data appears to be available between 0.5 and 1.0 mole fraction of DMF in the aqueous mixtures. The value of t_+^0 in 0.75 mole fraction DMF has therefore been determined. This permits calculation of λ^0 for K^+, Cs^+, Cl^- and NCS^- from

conductance data obtained in this research, and also provides an additional point in the plots of Stokes radius *vs.* $100/D$ for these ions.

Table 4.3 summarizes the results of five runs at four concentrations of KNCS in 0.75 mole fraction DMF. Precision obtaining in these determinations of t_+ is inferior to that obtained in 0.5 mole fraction DMF, about 0.25% or better, being achieved.

Table 4.4 presents three sets of values of $t_+^{0\prime}$ obtained from the t_+ data using either the analytical concentration C, or γC for the concentration terms in equation 1.30. The effect of the choice of a value on $t_+^{0\prime}$ can be seen. The value $a = 9.37$ was obtained during the computation of Λ^0 for KNCS by PROGRAM LOAOKA. Values of $t_+^{0\prime}$ obtained using this value of a produced a positive slope when plotted against concentration (Figure 4.3). The use of $a = 12.0$ reduced the slope without changing its sign.

Extrapolation of these data to infinite dilution to give t_+^0 was achieved by the use of a least square program. Results appear on Table 4.5. It is clear that the choice of a has at least a 0.1% effect in this instance, upon the result of the extrapolation, but the use of γC or C in the concentration terms of equation 1.30 makes little difference to the value of t_+^0 obtained. Such differences are within experimental error.

The value $t_+^0 = 0.3973 \pm 0.0010$ is taken as the limiting cationic transport number of KNCS in 0.75 mole fraction DMF/water at 25°C.

4.6 Transport numbers and ionic conductances

One of the principal practical applications of a limiting transport number is its use in splitting limiting equivalent conductances of strong electrolytes into their respective limiting ionic conductances, assuming that the transport number used (always that of the ion-contituent) is numerically equal to ionic transport number. Once a transport number for a given ion is known, the limiting ionic conductances of any number of ions in the same solvent can be calculated from the appropriate limiting conductances of electrolytes. Table 4.6 illustrates this point for three salts used in this research.

Table 4.6 Limiting ionic equivalent conductances in 0.75 mole fraction DMF/water solvent at 25°C derived from limiting equivalent conductances and $t_+^0(\text{KNCS}) = 0.397_3$

Salt	Λ^0	λ_+^0	λ_-^0
KNCS	66.78_6	26.5_3	40.2_6
KCl	59.61_5		33.0_9
CsCl	62.17_6	29.0_9	

Table 4.3 Cationic Transport Numbers of KNCS in 0.75 mole fraction DMF/water solvent at 25°C

$C \times 10^2$ (mol dm^{-3})	Solution volume (cm^3)	Average current (mA)	Time (sec)	t_+
0.9989	1.0489	0.19671	13151.9	0.3908
1.0754	0.3523_7	0.20164	4650.6	0.3906
2.1790	1.0489	0.29714	19032.6	0.3903
3.1484	1.0489	0.39933	20482.8	0.3897
3.9318	0.6965_5	0.49324	13760.6	0.3893

Table 4.4 Apparent Limiting Cationic Transport Numbers of KNCS in 0.75 mole fraction DMF/water at 25°C according to the values of a and the nature of the concentration term used in the calculation

			Apparent Limiting Cationic Transport Numbers		
			concentration = C	concentration = γC	
$C \times 10^2$ (mol dm^{-3})	γ	t_+	$a = 9.37$	$a = 9.37$	$a = 12.0$
0.9989	0.960	0.3908	0.3982	0.3981	0.3976
1.0754	0.958	0.3906	0.3982	0.3980	0.3975
2.1790	0.930	0.3903	0.3999	0.3997	0.3988
3.1484	0.908	0.3897	0.4005	0.4001	0.3991
3.9318	0.893	0.3893	0.4009	0.4005	0.3993

Table 4.5 Limiting Cationic Transport Numbers of KNCS in 0.75 mole fraction DMF/water at 25°C. Comparison of values obtained by a least square program

concentration term used	a	S. Error ($\times 10^4$)	S. Error for t_+^0 ($\times 10^4$)	t_+^0
C	9.37	3.48	3.44	0.3974
γC	9.37	3.58	3.54	0.3973
γC	12.0	3.05	3.02	0.3970

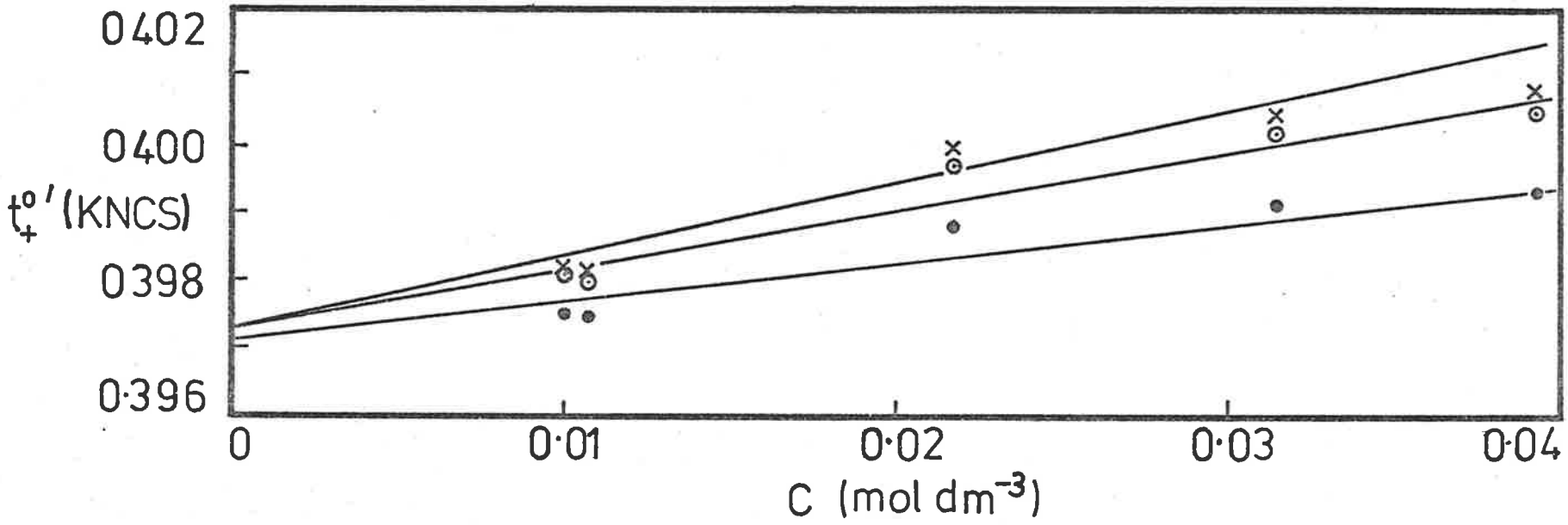

FIGURE 4.3 Values of $t_+^{0\prime}$ for KNCS in 0.75 mole fraction DMF/water mixtures at 25°C.

× a = 9.37; no correction for ionic association

⊙ a = 9.37; corrected for ionic association

● a = 12.0; corrected for ionic association

Table 4.7 indicates the two λ^0 values derived from t_+^0 obtained in 0.5 mole fraction DMF/water solvent for KNCS solutions.

Table 4.7 Limiting ionic equivalent conductances in 0.5 mole fraction DMF/water solvent at 25°C derived from Λ^0(KNCS) = 48.289 and t_+^0(KNCS) = 0.4715

$\lambda^0_{K^+}$	$\lambda^0_{NCS^-}$
22.7_7	25.5_2

The values of $\lambda^0_{Cl^-}$ in 0.09, 0.3, and 0.5 mole fraction DMF/water solvents have been obtained by interpolations of the available data, thus permitting the calculation of $\lambda^0_{Cs^+}$ from the Λ^0 values obtained for CsCl. The interpolations were performed in several ways. The simplest method used was to interpolate on a direct plot of $\lambda^0_{Cl^-}$ against either weight percent of water or mole fraction of DMF. Another approach involved the evaluation of a deviation function of the form

$$f(\lambda) = \lambda^0_{Cl^-} - b\,(\text{mole fraction} - 0.35)^2$$

where b is a convenient arbitrary constant chosen so that the range of values of $f(\lambda)$ was no more than two λ units. Such a narrow range of values increased the precision with which $f(\lambda)$, and hence $\lambda^0_{Cl^-}$, could be interpolated, either by computer or by graphical methods. The results of all interpolations were averaged. Table 4.8 displays the values of λ^0 for Cl^- and Cs^+ over the range of DMF/water solvents from 0–1.0 mole fraction DMF.

Table 4.8 Limiting ionic equivalent conductances of Cl^- and Cs^+ in DMF/water mixed solvents at 25°C

mole fraction DMF	Λ^0	$\lambda^0_{Cl^-}$	$\lambda^0_{Cs^+}$
0.0	153.65_7	76.35 [a]	77.3_1
0.09	81.90_6	39.2_9 [b]	42.6_2
0.30	44.39_1	21.3_1 [b]	23.0_8
0.50	45.68_9	22.1_7 [b]	23.5_2
0.75	62.17_6	33.0_9 [c]	29.0_9
1.00	–	55.1 [d]	34.5 [d]

a. Robinson and Stokes, reference 16.
b. Interpolated value, data from a, c, d and reference 14.
c. this research, via $\lambda^0_{K^+}$ and Λ^0(KCl).
d. Prue and Sherrington, reference 15.

The interpolated value for $\lambda^0_{Cl^-}$ in 0.3 mole fraction DMF leads to $\lambda^0_{K^+} = 23.2_9$, obtained

from the determined value of Λ^0 for KCl in this solvent, thus providing an additional data point to the range of $\lambda^0_{K^+}$ values determined by James.[14] Application of the literature value[16] of 73.5_0 for $\lambda^0_{K^+}$ in pure water led to the value $\lambda^0_{NCS^-} = 66.49$ when applied to the determined value of Λ^0 (KNCS) for that solvent.

The values of λ^0 presented on Table 4.8 clearly indicate a substantial dependence upon solvent composition. It is clear also that such a dependence must be due to ion-solvent interactions rather than ion-ion interactions since, at infinite dilution (a condition pertaining to the definition of λ^0) interactions between ions cease to exist.

In the next chapter the λ^0 values presented above will provide key data both for the calculation of Stokes radii and for a discussion of ion-solvent interactions.

References

1. Robinson, R.A. and Stokes, R.H., *Electrolyte Solutions,* 2nd ed., Butterworths, London, 1959.
2. Spiro, M., *Determination of Transference Numbers,* in *Physical Methods of Organic Chemistry,* Weissberger, A., (ed.) 3rd edition, *Interscience,* New York, 1959, chapter 46.
3. Spiro, M., *Transference Numbers,* in *Techniques of Chemistry,* Volume 1, Part IIA, Weissberger, A., (ed.), 1st edition, John Wiley and Sons, 1971, Chapter 4.
4. James, C.J., Ph.D. thesis, University of Adelaide, South Australia, 1972.
5. Steel, B.J. and Stokes, R.H., *J. Phys. Chem.*, **62**, 450, 1958.
6. Steel, B.J., Ph.D. thesis, University of New England, New South Wales, Australia, 1960.
7. Reference 3, page 209.
8. Reference 3, page 235 – 240.
9. MacInnes, D.A. and Longsworth L.G., *Chem. Rev.*, **11**, 171, (1932).
10. Reference 3, page 255, figure 4.21b.
11. Reference 4, page 143.
12. Reference 3, page 281.
13. Reference 3, page 258.
14. Reference 4, page 175.
15. Prue, J.E. and Sherrington, P.J., *Trans. Faraday Soc.*, **57**, 1795, (1961).
16. Reference 1, page 463.

Chapter 5
IONIC CONDUCTANCE AND SOLVENT PROPERTIES IN DMF/WATER MIXTURES

Chapter 5

IONIC CONDUCTANCE AND SOLVENT PROPERTIES IN DMF/WATER MIXTURES

5.1 The development of the Fuoss-Boyd-Zwanzig theory

The velocity of a rigid spherical particle moving in an ideal hydrodynamic continuum was shown by G.G. Stokes[1] to obey the relation

$$v = F/6\pi\eta r \tag{1.7}$$

where r is the radius of the sphere and F the force acting on it. This relation has long been the basis for the construction or discussion of models for the behaviour of ions in real solutions.

When an ion is treated as a rigid charged sphere moving in a continuum solvent, the application of Stokes' Law leads to an expression relating the limiting ionic conductance and the viscosity of the solvent.

$$\lambda_i^0 = |z_i|F^2/6\pi\eta R_i N \tag{5.1}$$

When R_i, the Stokes radius of the ion, is expressed in Angstrom units, equation 5.1 becomes, for a univalent ion,

$$R_i = 0.8194/\lambda_i^0\eta \tag{5.2}$$

Since in this model R_i is constant, the product λ_i^0, known as the Walden Product, is also constant. Hence, according to the model, any observed differences in λ_i^0 for a given ion in different solvents must be attributable to differences in the viscosity of the respective solvents.

In practice only a few solutions obey Walden's Rule. Examples[2] include large ions such as those of tetraethyl ammonium picrate in a variety of solvents. The failure of most other electrolyte solutions to obey this rule has been attributed to a number of possible causes including the solvation of ions[3, 4, 5] leading to a variation in the size of a given cation from solvent to solvent. Another suggested cause of the failure of Walden's Rule has been the non-constancy of the magnitude of the viscous frictional coefficient. Thus Robinson and Stokes[6] have suggested that, although the Stokes equation may be of the correct form, the numerical coefficient may not be 6π. They have proposed a correction procedure based upon a knowledge of the mobilities of the tetra-substituted ammonium ions. Another suggestion[7] for refinement of the rule centred on the viscosity term itself, proposing that the Walden relationship is better represented as

$$\lambda_i^0\eta^p = constant \tag{5.3}$$

where p is an arbitrary constant, devoid of theoretical meaning. However, for aqueous-nonelectrolyte solutions the index p has been shown[7] to vary both with the nature of the ion and with the nonelectrolyte component.

Fuoss,[8] in observing the dependence of the Walden product upon the dielectric constant of the solvent, proposed that electrostatic forces between ions and dipolar solvent molecules contributed to an increase in the solvent viscosity in the vicinity of each ion. The ions were thus subject to a greater retardation than that due to the bulk viscosity alone. This proposal led to a modified form of equation 5.1

$$\lambda_i^0 = \frac{|z_i|F^2}{6\pi N\eta (R_i^\infty + S/D)} \tag{5.4}$$

where S is an empirical constant. The dependence of the Stokes radius upon dielectric constant could thus be written as

$$R_i = R_i^\infty + S/D \tag{5.5}$$

where R_i^∞ is the hydrodynamic radius of an ion in a hypothetical solvent of infinite dielectric constant, a solvent in which all electrostatic forces are zero.[8] A plot of Stokes radius against $1/D$ should be a straight line of slope S and intercept R_i^∞. The plots presented by Fuoss in support of this proposal were indeed mostly linear; non-linear sections of plots for polar-polar mixed solvent systems were explained in terms of the rate of hydrogen bonding in the hydrodynamics near an ion.

Later Boyd[9, 10] and Zwanzig[11, 12] evaluated the coefficient S theoretically and found that it was related both to the dielectric relaxation time, Γ, of the solvent, and to the viscosity.

$$S = \frac{\Gamma e^2}{6\pi\eta(R_i^\infty)^3} \cdot \frac{D - D_\infty}{2D + 1} \tag{5.6}$$

D_∞ is the high frequency dielectric constant. If D_∞ is assumed to be much less than D and D much greater than unity[12], S is given by

$$S = \frac{\Gamma e^2}{32\pi\eta(R_i^\infty)^3} \tag{5.7}$$

Since R_i^∞ for a given ion is constant by definition, S should be proportional to the ratio Γ/η

$$S = constant.\ \Gamma/\eta \tag{5.8}$$

A theoretical equation by Debye[13] showed that Γ was proportional to η and to the cube of r, the radius of an orientable particle. Dannhauser and Johari[14] observed direct proportionality between Γ and η even in associated liquids such as water for which Debye's equation should be inapplicable. The theory of Fuoss, Boyd and Zwanzig (FBZ) thus developed gives

$$R_i = R_i^{\infty} + \frac{constant.\ \Gamma}{(R_i^{\infty})^3\,\eta} \cdot \frac{1}{D} \qquad (5.9)$$

where the coefficient of the $\frac{1}{D}$ term is S, a measure of ion-solvent-dipole interaction.

If Γ/η is independent of D

$$R_i = R_i^{\infty} + \frac{constant'}{(R_i^{\infty})^3} \cdot \frac{1}{D} \qquad (5.10)$$

Thus the predicted linear plot of Stokes radius against $1/D$ should provide a value of R_i^{∞} either from the intercept or from the slope of the line.

5.2 Tests of the FBZ theory

Early tests[8] of the FBZ theory proved to be encouraging without being completely satisfactory. More recent work, including some by the author and another[20] in this department, has shown that the theory has serious inadequacies, these residing largely in the dependence of the theory upon too simple a model for an electrolyte solution. Outlined below is an examination of the results of a number of workers.

Fuoss and co-workers[15-19] have evaluated R_i for alkali halides in dioxane/water solvents. In a number of cases, notably LiCl, NaCl and KCl, a plot of R_+ against $100/D$ shows a small minimum at fairly high values of D. For lower values of D (less than about 30) the plots tend to be linear. By extrapolating these linear sections of the plots, values of R_i^{∞} were obtained which, almost without exception, were smaller than the respective lattice radii.

James[20] extended these studies by examining the Stokes radius of K^+, Cl^- and Br^- in DMF/water mixtures over the range 0–100% DMF. As indicated in Chapter 4, part of this research complements James' work, providing λ^0 values and hence R_i for K^+ and Cl^- in 0.75 mole fraction DMF/water solvent. All the conductance data in DMF/water, unlike that of the Fuoss school mentioned above, are based on the determination of transport numbers in each solvent, thus avoiding the assumption that transport numbers are independent of solvent composition. Data for K^+ and Cl^- is presented on Table 5.1. Plots of the corresponding Stokes radii are to be found on Figure 5.1.

Table 5.1 Ionic equivalent conductances and Stokes radii of K^+ and Cl^- in DMF/water mixtures at 25°C

DMF mole %	*D*	*100/D*	η *(cP)*[d]	$\lambda^0_{K^+}$	R_+*(Å)*	$\lambda^0_{Cl^-}$	R_{Cl^-}*(Å)*
0	78.54	1.273	0.8903	73.5_0	1.25_2	76.35	1.20_5
5.80	74.8	1.337	1.40_2	49.6_8	1.176	-	-
6.01	74.7	1.339	1.42_0	-	-	47.3_3	1.21_9
13.52	69.3	1.443	2.01_5	34.2_7	1.187	31.6_7	1.28_4
26.99	60.6	1.650	2.50_2	24.3_0	1.34_8	21.9_6	1.49_1
30.00	58.8	1.700	2.48_9	23.2_9[a]	1.41_3	21.3_1[b]	1.41_3
35.11	56.1	1.783	2.39_4	22.0	1.56	20.9	1.63_8
49.62	49.8	2.008	1.87_4	22.6_9	1.92_7	22.0_3	1.98_4
75.00	41.8	2.388	1.14_5	26.5_3[a]	2.69_5	33.0_9	2.16
100.00	36.7	2.724	0.801_2	30.8[c]	3.3_5	55.1[c]	1.87

a. This research, presented in Chapter 4.

b. Interpolated value, presented in Chapter 4.

c. Data of Prue and Sherrington, Trans. Faraday Soc., 57, 1795, (1961).

d. Obtained or interpolated from data on page 131 of reference 20, presented in Appendix 2.1.

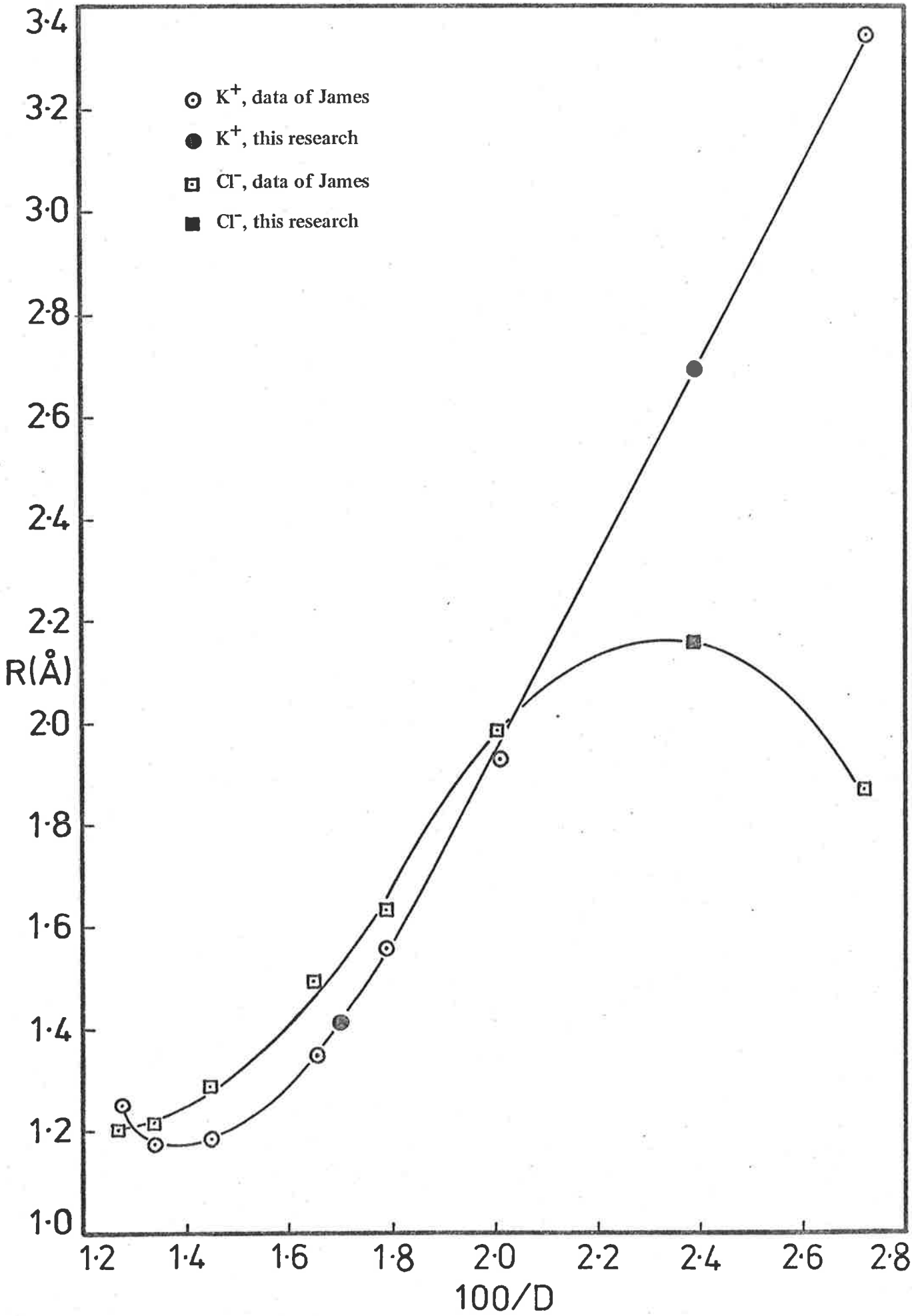

FIGURE 5.1 The dependence of the Stokes radius of K^+ and Cl^- upon reciprocal of dielectric constant of DMF/water mixtures at 25°C.

A comparison of the R_+ plot with those for alkali halides in dioxane/water mentioned above provides both similarities and marked differences. Similarities occur in that a small minimum occurs at fairly high D (in DMF/water $100/D \doteqdot 1.4$) while the remainder of the plot ($100/D$ values from 1.6 to 2.7) is nearly linear. However the significant divergence from FBZ theory (evident in the appearance of the minimum in the R_+ plot) becomes even more serious when values of R_+^∞ are determined from the curve. The slope of the near-linear section gives R_+^∞ = 1.3 Å (approximately the crystal radius) but the intercept gives the unreal value of −1.8 Å. The FBZ theory is further challenged by the existence of a well-defined maximum in the plot for Cl^-, occurring at $100/D$ = 2.4 or thereabouts. Further, the intercept of the linear section of the plot gives a slightly negative value of Stokes radius although from the slope R_-^∞ = 1.4 Å.

A considerable part of this research was devoted to obtaining a Stokes radius plot (*vs* $100/D$) for Cs^+ in order to make a comparison with that for K^+ outlined above. Results are presented on Table 5.2; also included are results for NCS^- at four solvent compositions. The Stokes radius plots are displayed on Figure 5.2.

A number of similarities to the respective plots on Figure 5.1 can be observed. The cation plots both have a minimum near $100/D$ = 1.4 as well as near-linear sections for $100/D > 1.65$. These plots both give anomalous values for R_+^∞ obtained from the intercept—Cs^+ giving −1.18 Å. From the slope of the linear section, the plot for Cs^+ yields R_+^∞ = 1.42 Å, a size somewhat less than the crystal radius.

The anion plots are also similar in that maxima occur near $100/D$ = 2.4, although the curve for NCS^- is flatter. The available points for this ion suggest a near-linear section for $100/D < 2.0$ and a tentative extrapolation of this section indicates R_-^∞ near 0.8 Å. Tentatively, the slope indicates a value for R_-^∞ of about 4.6 Å.

In other mixed solvents such as methanol/water and ethanol/water, anomalous results for $R_+^\infty(K^+)$ are also found[20] – negative values are yielded by the intercepts but the slopes give positive values.

Such inconsistent and anomalous results as have been described constitute a serious challenge to the assumptions of the FBZ theory and to the sphere-in-continuum model upon which the theory is based. One source of inconsistency may lie in the assumption that Γ/η is constant. Values of Γ and corresponding values of η for a series of dioxane/water solvents, as cited by Atkinson and Mori[21], indicate a two-fold variation in Γ/η over the range 0–95.15% dioxane. Few values of Γ are available for other mixed solvents.

A general conclusion to be drawn from the evidence presented is that a model based on the sphere-in-continuum is too simple to represent the conductance behaviour of electrolyte solutions. This conclusion is supported by a number of workers[5, 22] including

Table 5.2 Ionic equivalent conductances[a] and Stokes radii of Cs^+ and NCS^- in DMF/water mixtures at 25°C

DMF mole %	*D*	*100/D*	*η(cP)*[d]	$\lambda^0_{Cs^+}$	R_{Cs^+}(Å)	$\lambda^0_{NCS^-}$	R_{NCS^-}(Å)
0	78.54	1.273	0.8903	77.31	1.19_1	66.49	1.38_4
9	72.7_7	1.374	1.67_7	42.6_2	1.14_6	-	-
30	58.6	1.70_6	2.48_9	23.0_8	1.42_6	-	-
50	49.6_6	2.01_4	1.85_7	23.5_2	1.87_6	25.5_2	1.72_9
75	41.8_7	2.38_8	1.14_6	29.0_9	2.45_9	40.2_6	1.77_7
100	36.71	2.72_4	0.801_2	34.5[b]	2.96	60.5[c]	1.69

a. λ^0 values, except those for pure DMF were presented in Chapter 4.

b. Data from reference 24.

c. Derived from data from reference 23 and reference 24.

d. Values obtained or interpolated from data on page 131 of reference 20, presented in Appendix 2.1.

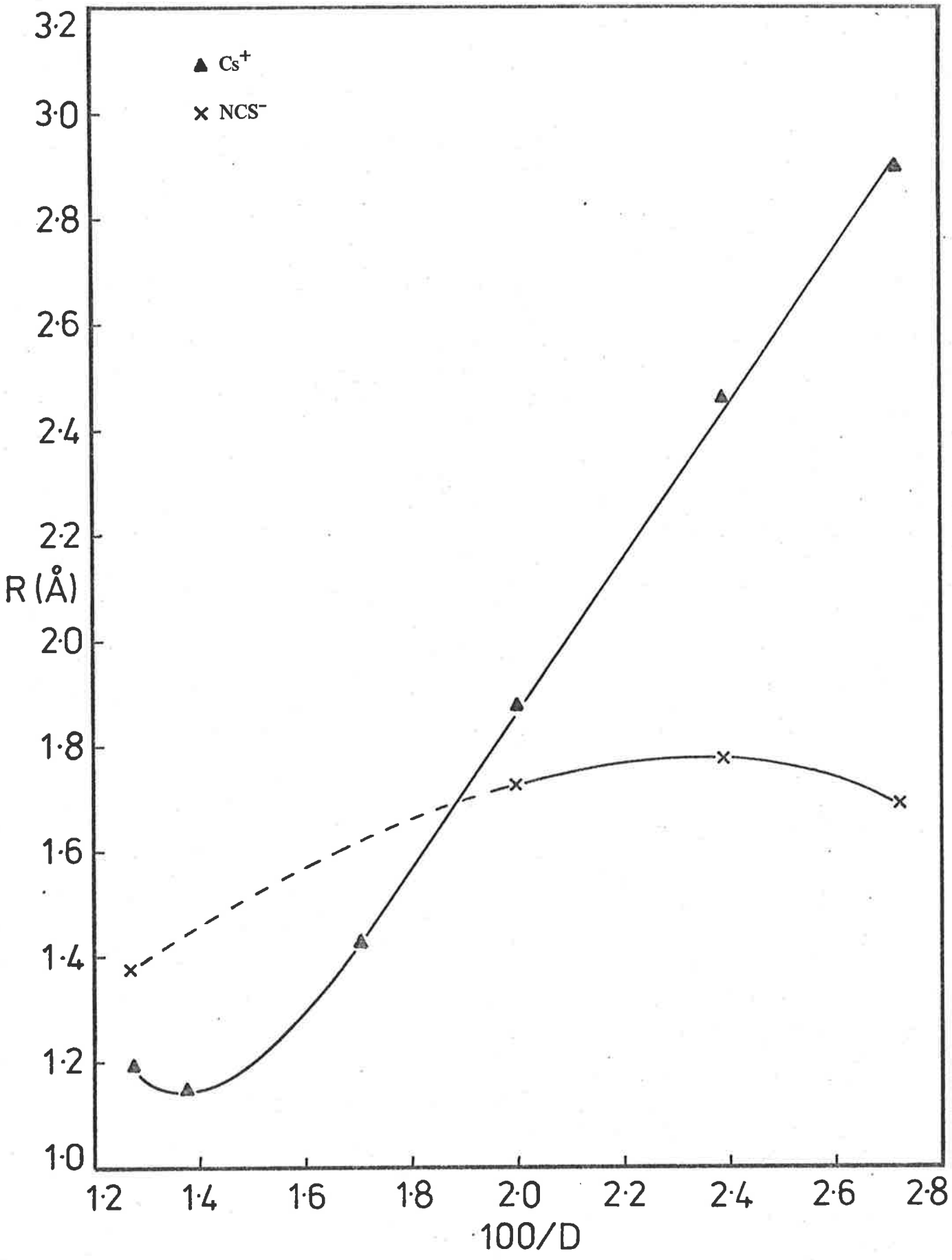

FIGURE 5.2 The dependence of the Stokes radius of Cs^+ and NCS^- upon reciprocal of dielectric constant of DMF/water mixtures at 25°C.

Fuoss himself. It seems very likely that the relation between conductance and solvent composition is a function of a number of parameters, especially those related to individual properties of the ions and molecules themselves.[5] An examination of the variation of a number of such parameters in DMF/water mixtures comprises the main thrust of the next section.

5.3 Solute and solvent properties in DMF/water solutions—a search for correlations

5.3.1 Densities and solvent composition

Densities of DMF/water mixtures have been measured by James[20] (Appendix 2.1). A plot of these data appears on Figure 5.3. It is interesting to note that the density remains nearly constant over the range 0–*ca*0.2 mole fraction of DMF (the top of this range being one in which four water molecules are present for each molecule of DMF). If, for the sake of discussion, the density is assumed to be constant in this range, the volume occupied in the liquid structure by unit mass of DMF is the same as that occupied by unit mass of water. Given that the respective molar masses of DMF and water are 73g and 18g respectively it follows that 1/73 mole of DMF occupies the same volume as 1/18 mole of water in this region of interest. This means that one molecule of DMF occupies the same volume in the liquid structure as four molecules of water.

Given that liquid water has a more open structure than DMF, this simple calculation provides qualitative evidence for the observed decrease in conductance with increasing proportions of DMF in DMF/water mixtures and foreshadows discussion of solvent free volumes in section 5.3.4.

5.3.2 Ionic conductance, viscosity and solvent composition

James[20], seeking a correlation between conductance and solvent properties, plotted $\lambda^0_{K^+}$, η and the excess volume of mixing $\Delta V_E'$ against solvent composition. His data for $\lambda^0_{Cl^-}$, $\lambda^0_{Br^-}$ and the data of this research for $\lambda^0_{Cs^+}$ have been similarly plotted. The λ^0 plots for the anions are similar, but differ somewhat in shape from those if the cations in the DMF-rich region. However each λ^0 plot has a minimum at a mole fraction of about 0.35. Plots typified by $\lambda^0_{Cs^+}$ and $\lambda^0_{Cl^-}$ appear on Figure 5.4 together with that of solvent viscosity. The latter plot has a maximum at a DMF mole fraction of about 0.27. A significant correlation between λ^0 and η does not therefore appear to occur. (It is interesting, however, to note that η is linear up to about 0.15 mole fraction of DMF in water. This will be discussed in section 5.4).

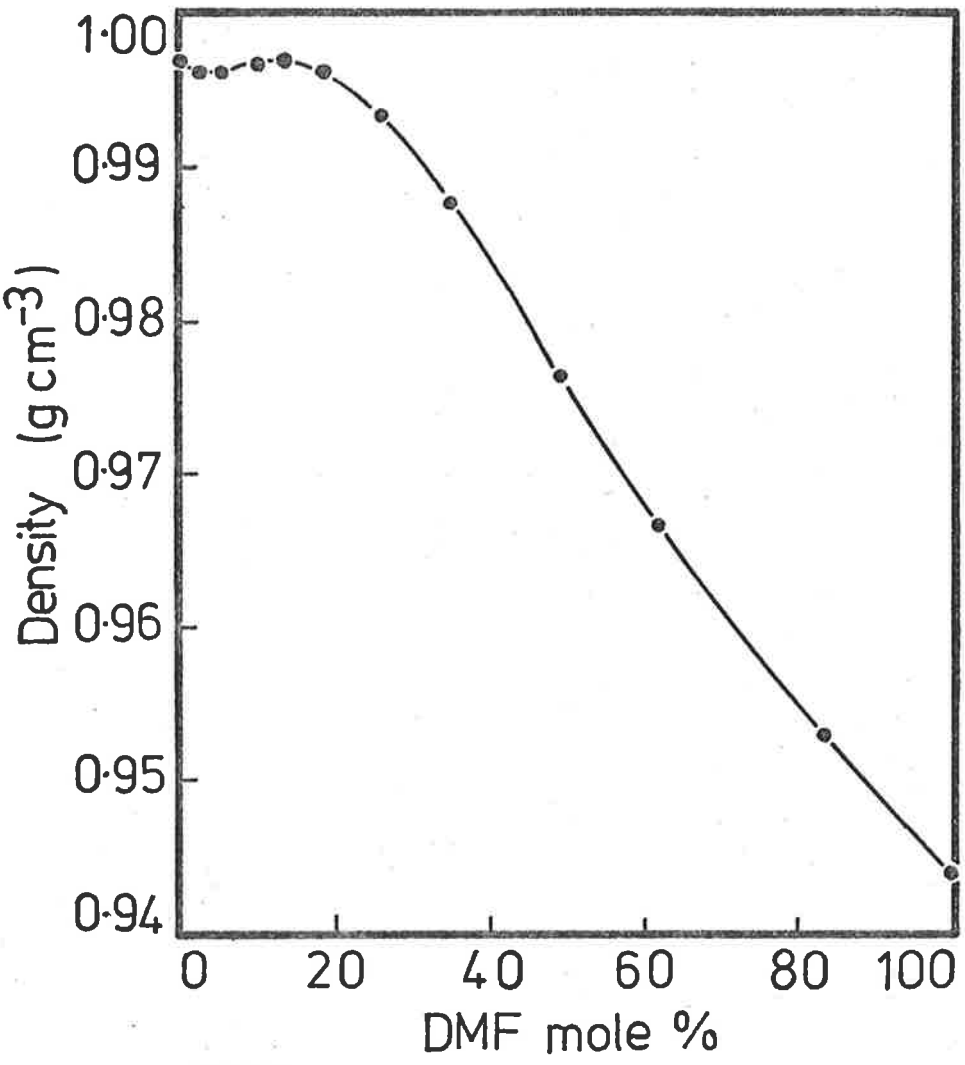

FIGURE 5.3 Densities of DMF/water mixtures at 25°C.

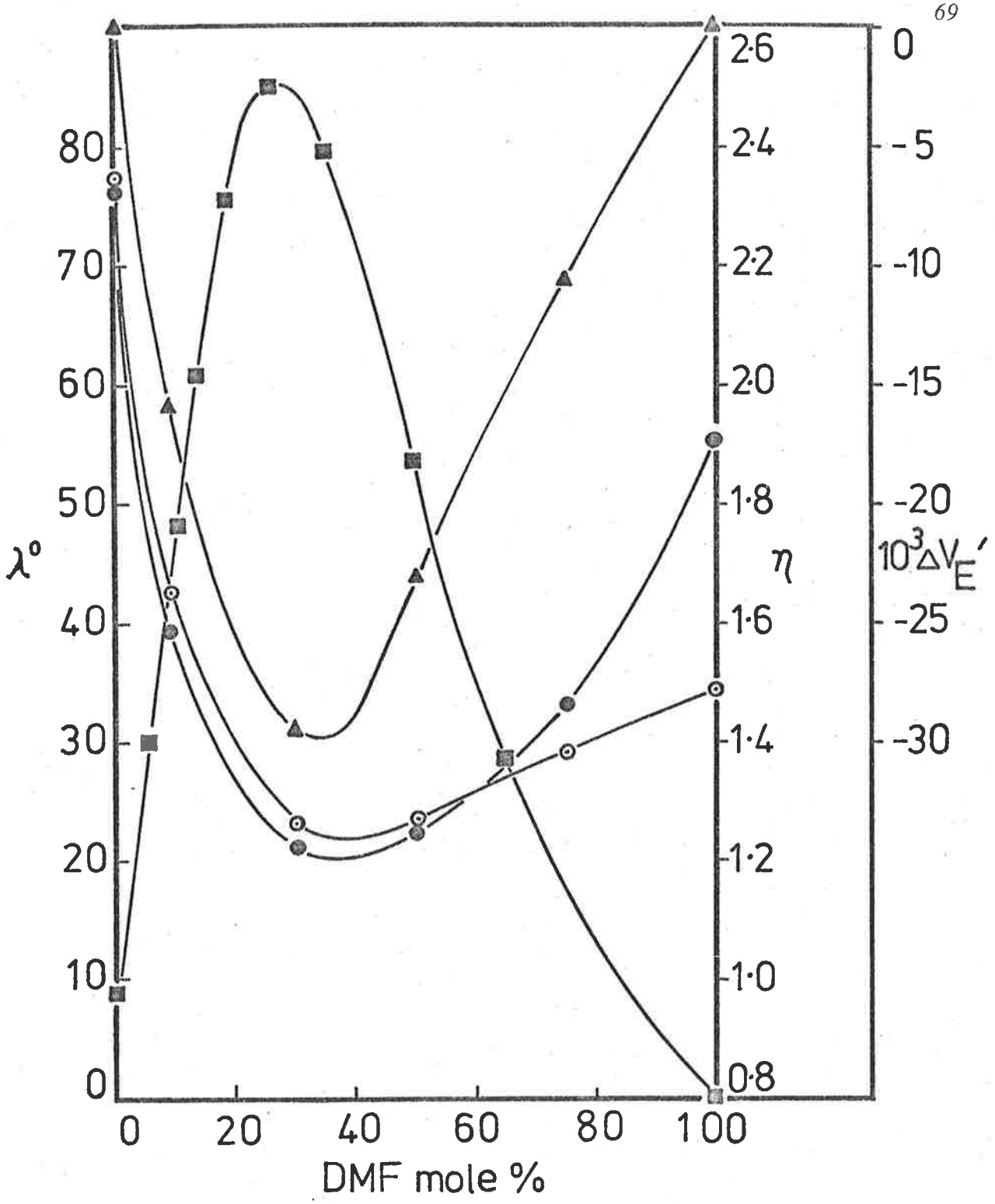

FIGURE 5.4 Limiting ionic equivalent conductances, viscosities and excess volumes of mixing at 25°C as functions of solvent composition.

- ⊙ $\lambda^0_{Cs^+}$
- ● $\lambda^0_{Cl^-}$
- ■ η(cP)
- ▲ $10^3 \Delta V_E'$

5.3.3 Ionic conductance and excess volume of mixing

A correlation does appear to exist between λ^0 values and those of the excess volume of mixing ($\Delta V_E'$) of the solvent. The plot of $\Delta V_E'$ *vs.* mole fraction of DMF (Figure 5.4) shows a minimum at the same solvent composition as each of the λ^0 plots, but the shape of the $\Delta V_E'$ plot more closely resembles that of the λ^0 plot for the anions. Values of ΔV_E (units $cm^3\ mol^{-1}$) were calculated [25] from interpolations of density data[22] (Appendix 2.1) for the mixed solvents. Since, in attempting to find correlations between conductances and excess volumes of mixing, interest centres upon distances travelled by an ion rather than upon the molecules it meets, excess volumes of mixing were recalculated as $\Delta V_E'$, the fractional change in the volume considered. Equation 5.11 indicates the relationship between $\Delta V_E'$ and ΔV_E:

$$\Delta V_E' = \Delta V_E \cdot d_{12} / (x_1 M_1 + x_2 M_2) \qquad (5.11)$$

x_1, x_2 are mole fractions, M_1, M_2 are molar masses (as gram) and d_{12} the density of the mixed solvent as g cm^{-3}. The values obtained for $\Delta V_E'$ are shown on Table 5.3.

Table 5.3 Excess volume of mixing for DMF/water mixtures at 25°C

DMF mole %	*Density*[a]	*1000* $\Delta V_E'$
0	0.99704	0
9	0.99679	-15.863
30	0.99113	-29.607
50	0.97603	-23.149
75	0.95795	-10.785
100	0.94389	0

a. Densities of mixed solvents are interpolated values

The apparent correlation between λ^0 and $\Delta V_E'$ was investigated by preparing plots of λ^0 *vs.* $\Delta V_E'$ and $\lambda^0 \eta$ *vs.* $\Delta V_E'$. These revealed no apparent correlations–in the former plot the curve was a loop, in the latter the plot was horizontally paraboloid.

5.3.4 Free volumes of the solvents

The proposals of Samoilov[26, 27], relating to the process of conductance in water involve the temporary occupancy of suitable interstitial sites in the water structure by the ions during their progress through the liquid. Since the electrical conductivity of electrolytes in DMF/water solvents falls off markedly in the water-rich region, it appears that Samoilov's proposals could be used to explain the conductance behaviour in DMF/water

in terms of a reduction in the number of suitable sites in the water structure resulting from the presence of DMF molecules. Further, it may be possible to use the same kind of approach when attempting to explain the conductance behaviour of electrolytes in the DMF-rich mixtures by proposing that the ions travel via interstitial sites in the DMF structure. Since the availability of interstitial sites suitable for ionic migration could be related to the free volume of the liquid, the free volumes of the DMF/water mixtures were calculated with a view to seeking correlations with conductance and other properties of the system.

The free volume, Θ, of a liquid is taken to be that fraction of the bulk volume represented by the sum of the volumes of the voids between the molecules of the liquid. In the case of closest packing of hard spheres, 74% of the bulk volume is occupied by the spheres. The interstitial or 'free' volume in this case is 26% of the bulk volume. For a pure liquid, Θ can thus be defined as

$$\Theta = (V^0 - N v_m) / V^0 \qquad (5.12)$$

where V^0 is molar volume and v_m is the volume of a discrete molecule. The quantity v_m can be thought of as the 'hard sphere' volume of a single molecule. In the example of closest packing above, Θ = 0.26.

Assarsson and Eirich[28] claim that for dimethylacetamide, the free volume is about 30%, that is, Θ = 0.30. Calculations made in this research (and discussed later in this section) indicate that Θ for DMF is of similar magnitude, but for water this value is nearly doubled.

Free volumes of pure water and pure DMF calculated from volumes of discrete molecules

The volume of a single water molecule was calculated from the *b*-factor in the van der Waals equation of state for gases. This factor represents a volume equal to four times the volume of the molecules themselves (the 'hard-sphere' volume).

For water[29] b = 30.49 $cm^3\ mol^{-1}$ and hence the volume of the water molecule, *per se*, is 7.62 $cm^3\ mol^{-1}$. The molar volume of water at 25°C is 18.07 $cm^3\ mol^{-1}$ and the free volume Θ is thus 0.58.

A satisfactory check on this figure is available through the reasoning of Bernal and Fowler.[30] From estimations of the intermolecular separation of water molecules and hence the 'molecular radius' in ice I, they reasoned that close-packing of water molecules would yield a density of 1.84g cm^{-3}. Allowing 26% of the volume as void space, 1.84g of close-packed water have a 'hard-sphere' volume of 0.74 cm^3. Since 1.84g of real water at 25°C

occupies close to 1.84 cm^3, the free volume calculation gives $\Theta = 0.60$.

Since a search of the literature did not yield any data from which the volume of an individual DMF molecule might be calculated, an estimation of its volume was made using a scale molecular model.* One particular conformation of the model was approximately discoid in shape, having a fairly uniform thickness measured as 3.25Å. The 'profile' of the discoid had an area measured as 28.3$Å^2$, leading to a volume calculated as very close to 92$Å^3$. This volume corresponds to $55._4$ cm^3 mol^{-1}. The molar volume of liquid DMF at 25°C is 77.4 cm^3, hence $\Theta = 0.28_4$.

This result compares satisfactorily with Θ values of 0.29_1 for trimethylamine–obtained from the van der Waals *b*-factor[29] –and about 0.33 for dimethylacetamide.[28]

Free volumes of DMF/water mixtures

When a mixed solvent such as DMF/water is formed, the change in volume, ΔV_E, results from a loss of free volume by each of the liquids. This loss arises from the occupancy of some of the free volume of one liquid by molecules of the other liquid, and *vice versa*. V_f, the free volume *per mole* of mixture is given by

$$V_f = \Theta_1 V_1 + \Theta_2 V_2 + \Delta V_E \qquad (5.13)$$

where $V = xM/d^0$, d^0 being the density of a pure liquid. The free volume Θ_{12} of the mixture is thus given by

$$\Theta_{12} = (\Theta_1 V_1 + \Theta_2 V_2 + \Delta V_E) d_{12} / (x_1 M_1 + x_2 M_2) \qquad (5.14)$$

or

$$\Theta_{12} = \left[(\Theta_1 V_1 + \Theta_2 V_2) d_{12} / (x_1 M_1 + x_2 M_2)\right] + \Delta V_E' \qquad (5.15)$$

The results of calculations of the free volumes of the DMF/water solvents prepared in this research are presented on Table 5.4 and are plotted on Figure 5.5.

The simple shape of this plot does not suggest correlations with known plots of solvent and solute properties *vs.* mole fraction.

*Framework Molecular Model Kit, Prentice-Hall, Inc., Englewood Cliffs, New Jersey, U.S.A.

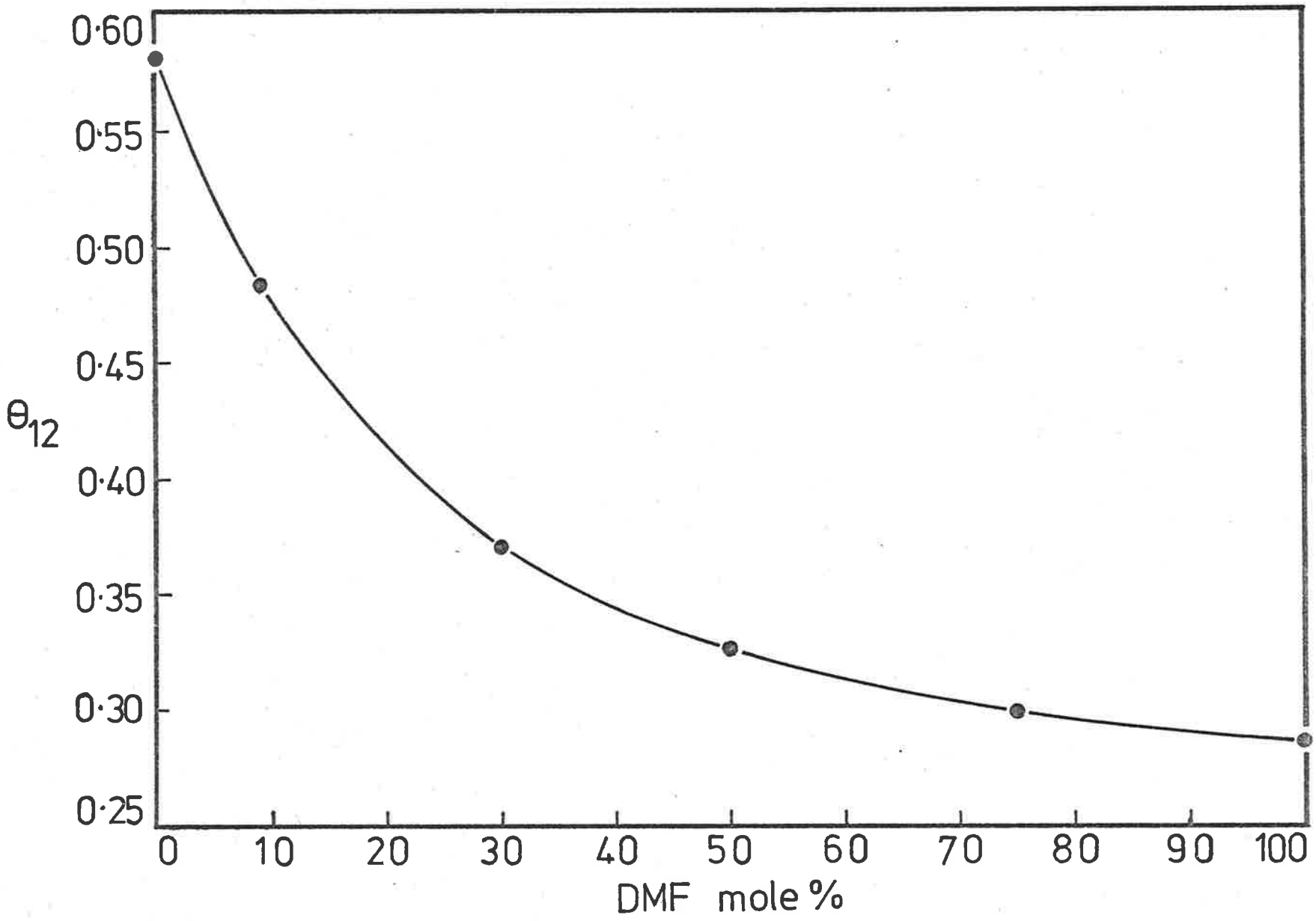

FIGURE 5.5 Free volumes of DMF/water mixtures at 25°C

Table 5.4 Free volumes of DMF/water mixtures at 25°C

DMF mole %	$10^3\Theta_{12}$
0	578.0
9	482.7
30	369.9
50	325.2
75	298.7
100	285.0

5.3.5 Variation of solute and solvent properties with free volume of solvent

Figure 5.6 depicts typical plots of λ^0, η and Walden Product against free volume. The data is summarized on Table 5.5.

Table 5.5 Properties of solute and solvent in DMF/water mixtures at 25°C

DMF mole %	$10^3\Theta_{12}$	$10^2\eta$	$\lambda^0_{Cl^-}$	$10^2\eta\lambda^0_{Cl^-}$	$\lambda^0_{Cs^+}$	$10^2\eta\lambda^0_{Cs^+}$
0	578	0.8903	76.35	0.679_9	77.3_1	0.688_3
9	483	1.677_2	39.2_9	0.659_5	42.6_2	0.714_3
30	370	2.489_2	21.3_1	0.530_4	23.0_8	0.574_5
50	325	1.856_8	22.1_7	0.411_6	23.5_2	0.436_1
75	299	1.145_7	33.0_9	0.379_1	29.0_9	0.333_2
100	285	0.801_2	55.1	0.441_4	34.5	0.276_4

No simple correlation of the plotted parameters with free volume is evident although a portion of each of the $\lambda^0_{Cs^+}\eta$ and η plots is linear between Θ_{12} values of 0.285 and about 0.335 (equivalent to the considerable DMF mole fraction range 1.0 – *ca* 0.45). The linearity of the viscosity plot was checked by calculating additional data points using interpolated data for densities and viscosities from the data of James (Appendix 2.1).

The failure of the limiting ionic equivalent conductances to exhibit a linear relationship with Θ_{12} indicates that, if Samoilov's model for the conductance process is accepted, the number of suitable interstitial sites in the structure of the liquid is not related to the free volume in a simple way. Conversely, it may be that Samoilov's model is too simple to explain such a complex process as ionic conductance in a mixed solvent.

5.4 Solvent-solvent interactions in DMF/water mixtures

The change in viscosity of DMF/water mixtures with solvent properties remains of interest. This research has shown that over different but not insignificant ranges of composition, the viscosity has varied linearly with mole fraction of DMF (0 – *ca* 0.15 mole

FIGURE 5.6 Dependence of λ^0, viscosity and Walden Product upon free volumes of DMF/water mixtures at 25°C

Figure 5.6(a)

- ● $\lambda^0_{Cl^-}$
- ▲ $10^2 \lambda^0_{Cl^-} \eta$
- ■ $10^2 \eta$

Figure 5.6(b)

- ○ $\lambda^0_{Cs^+}$
- △ $10^2 \lambda^0_{Cs^+} \eta$

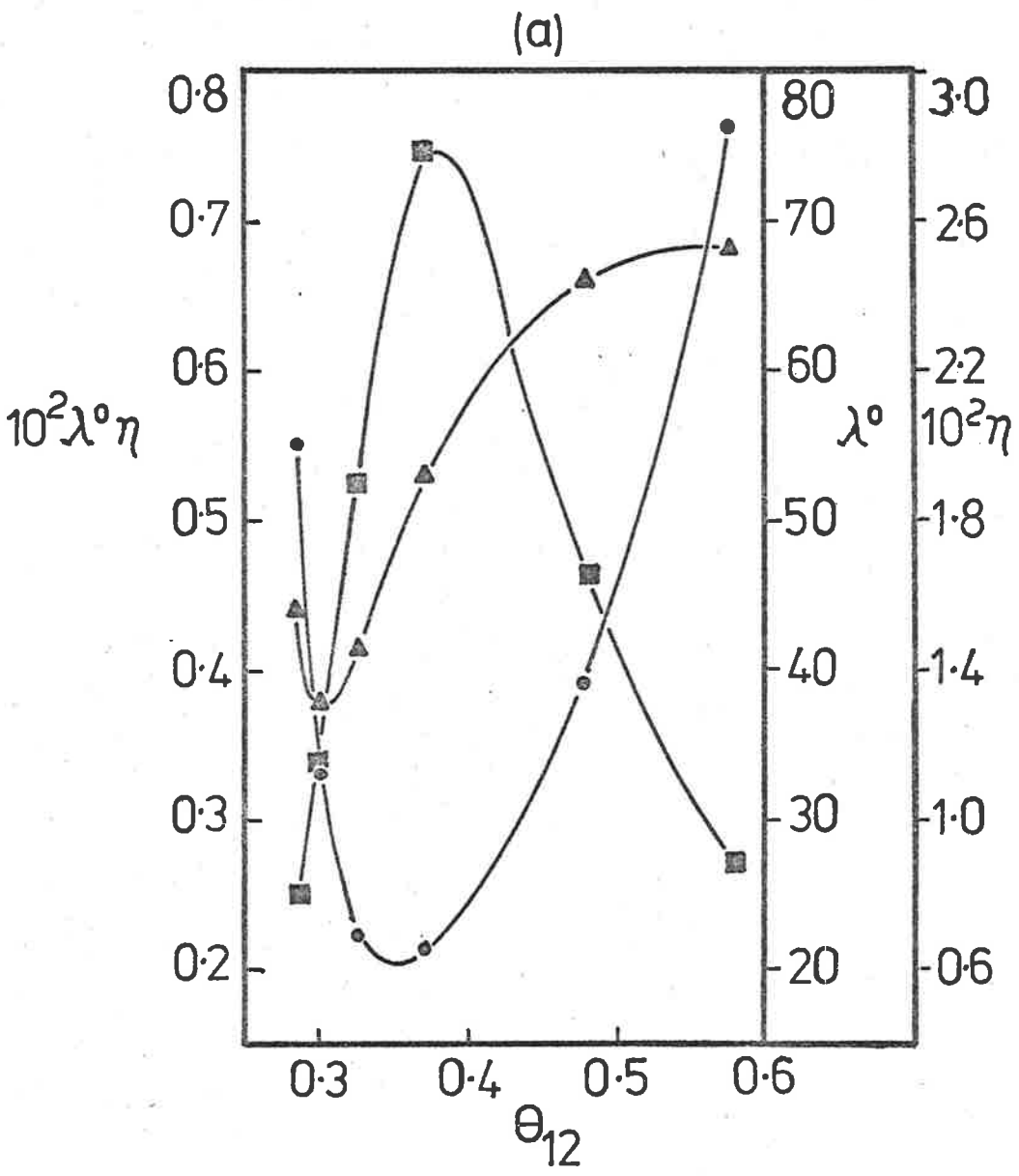
(a)
0·8
0·7
0·6
0·5
0·4
0·3
0·2
80
70
60
50
40
30
20
3·0
2·6
2·2
1·8
1·4
1·0
0·6
$10^2\lambda^\circ\eta$
λ°
$10^2\eta$
0·3
0·4
0·5
0·6
θ_{12}

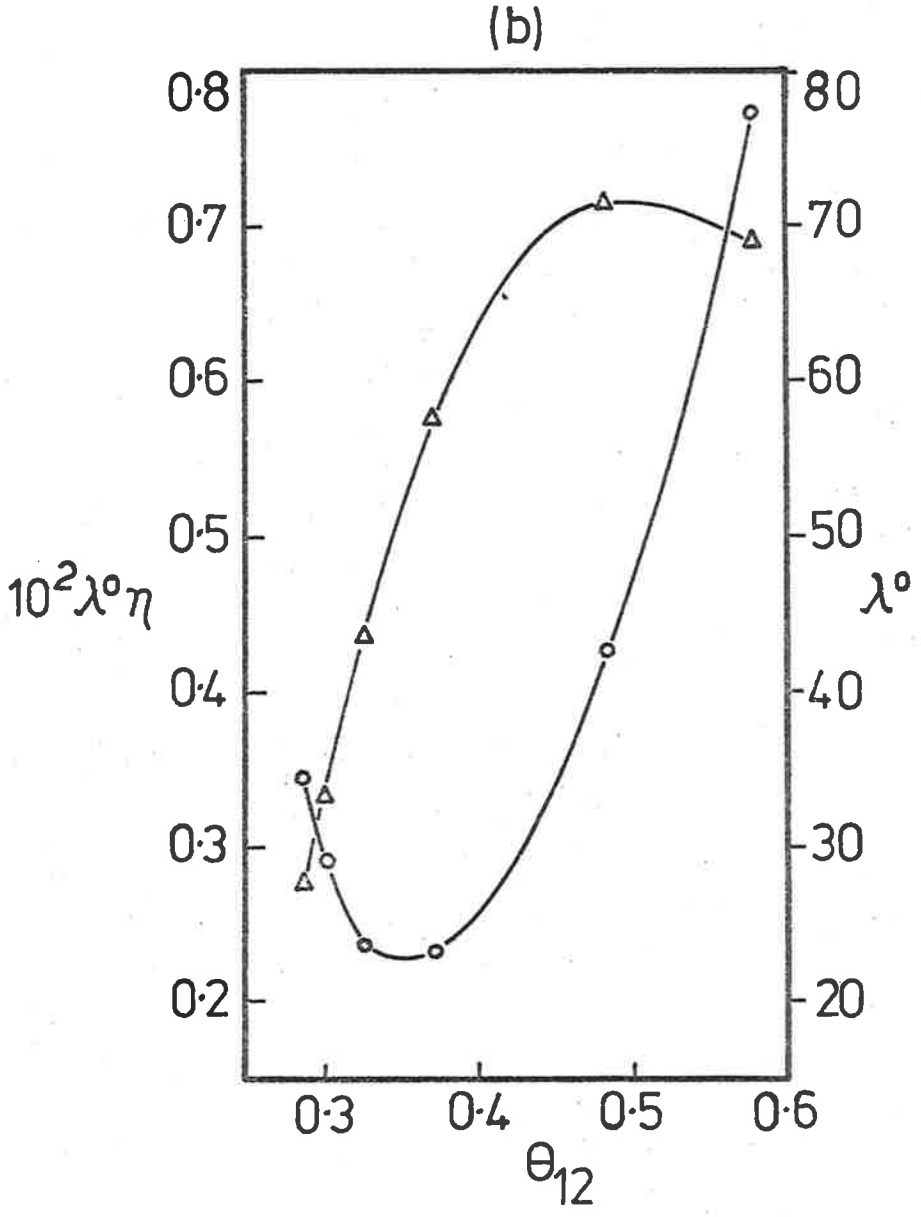
(b)
0·8
0·7
0·6
0·5
0·4
0·3
0·2
80
70
60
50
40
30
20
$10^2\lambda^\circ\eta$
λ°
0·3
0·4
0·5
0·6
θ_{12}

fraction DMF) and linearly with free volume in DMF-rich solvents in a range equivalent to 1.0 – *ca* 0.45 mole fraction. The latter relationship may arise because water added to DMF may enhance both the structure and hence the volume of the liquid through hydrogen bonding thus increasing the frictional resistance exerted by the solvent particles upon each other.

The change of viscosity of DMF/water mixtures with solvent composition has been investigated more fully in this research.

Assarsson and Eirich[28] have examined the viscosity of a number of amide/water mixtures. They have remarked on the occurrence of viscosity maxima at definite integral mole fractions of the amides, suggesting complex formation by bonding between the peptide dipole and water. In the case of DMF/water, the maximum occurs at a DMF mole fraction of about 0.27 (Figure 5.4) suggesting a complex with the formula $DMF(H_2O)_3$ rather than $DMF(H_2O)_2$, as implied by Assarsson and Eirich.

The possibility of the existence of DMF/water complexes was investigated in this research by applying the Einstein relation (equation 5.17) which holds for large solute particles at low concentrations.

$$\eta_{rel} = 1 + 2.5\phi \qquad (5.16)$$

η_{rel} is $\eta_{solvent}/\eta_{water}$ and ϕ is the volume fraction occupied by the solute particles. When ϕ is expressed in terms of the molar volume $\overline{V}$ and concentration C of complex, equation 5.16 becomes

$$\eta_{rel} = 1 + 2.5\overline{V}C \qquad (5.17)$$

The slope of the plot of η_{rel} against C gives a value for $\overline{V}$ directly—this system had $\overline{V} = 96.0$ cm^3 from a plot (using interpolated values of η), shown in Figure 5.7. As can be seen, the η_{rel} plot remained linear up to a concentration of about 0.5 mol dm^{-3} (about 0.01 mole fraction of DMF). This concentration exceeds the limits beyond which the Einstein relation could reasonably be expected to hold. The extent of the linearity of the plot, together with the feasible values obtained for the molar volume constitute good evidence for the existence of a DMF/water complex.

The formula of the complex was investigated. An estimation of the volumes of the possible complexes $DMF(H_2O)_2$ and $DMF(H_2O)_3$ using scale models (Section 5.3.4), gave 91 and 109 cm^3 mol^{-1} respectively. The volume obtained from the graphical application of equation 5.17 lies between these values. Accordingly, and in view of the imprecisions inherent in the volume estimations involving models, no firm conclusions can be drawn

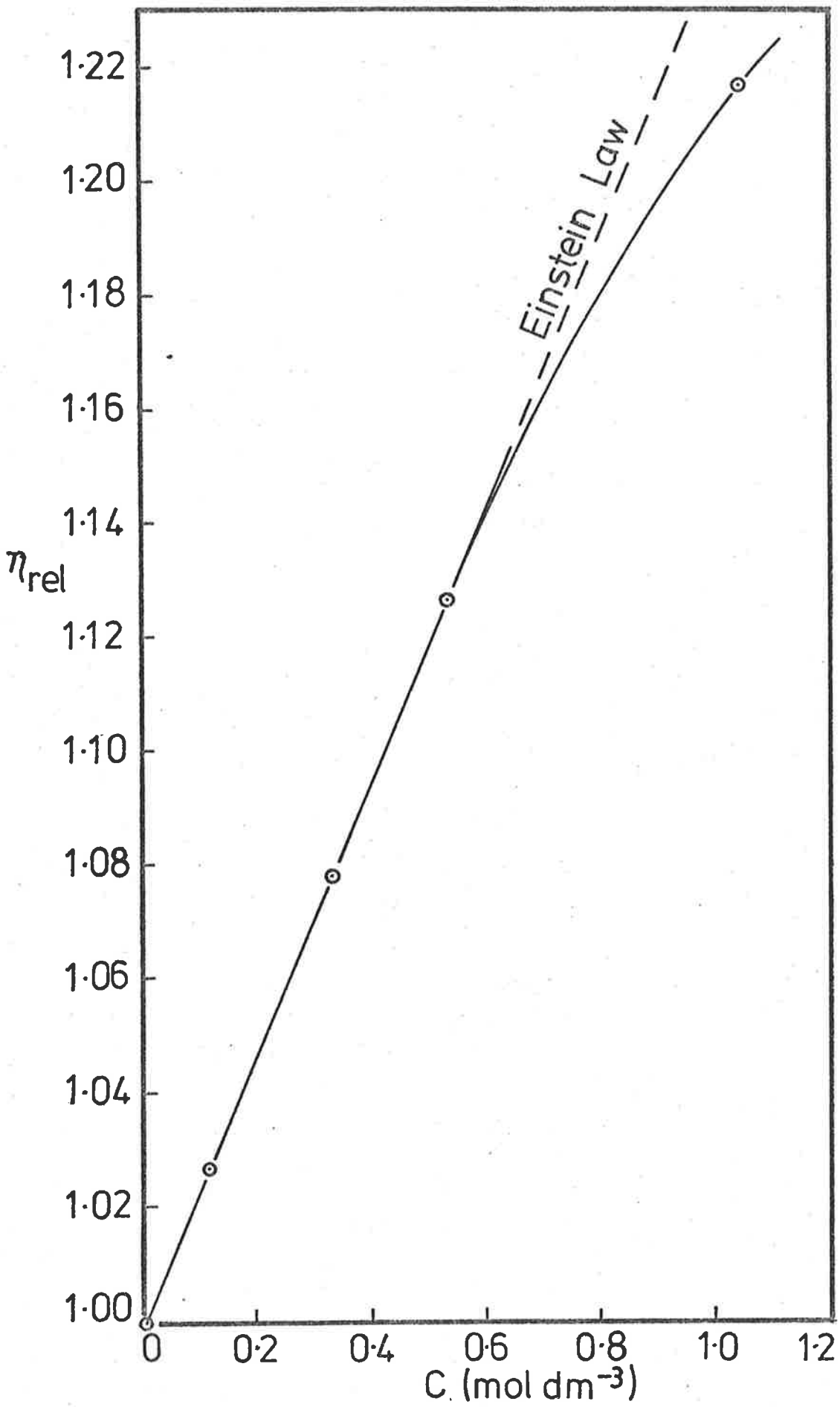

FIGURE 5.7 Relative viscosity of DMF/water mixtures at 25°C as a function of concentration of DMF.

from the results of this investigation. At least three possibilities exist–

* *The complex exists entirely as $DMF(H_2O)_2$.*

Molar volume estimates tend to support this possibility.

** *The complex exists only as $DMF(H_2O)_3$ leaving some DMF uncomplexed. (This means that the equilibrium constant for formation of complex is small).*

In this possibility, the molar volume of the molecules of the complex as obtained from the graph is a weighted average of the volumes of the $DMF(H_2O)_3$ complex and unhydrated DMF molecules. The proportion of free DMF molecules has been estimated at about 24% in this case.

*** *Both $DMF(H_2O)_2$ and $DMF(H_2O)_3$ form, all DMF being complexed.*

Here the molar volume of the complex obtained graphically is the weighted average of the molar volumes of the two possible complexes. Calculations indicate possible proportions as 72% $DMF(H_2O)_2$ and 28% $DMF(H_2O)_3$.

Whatever the formula of the complex, the evidence suggests that it tends to increase the viscosity of the solvent in water-rich compositions of the solvent. The dependence of viscosity upon free volume in DMF-rich compositions of solvent has already been discussed, the evidence here suggesting that water enhances the structure of the solvent. Combining the implications in the two regions of solvent composition it is clear a number of factors related to the solvent's structure must contribute to the magnitude of the equivalent conductance of an ion. These factors, including complexation and the bulk structure of liquid, appear to be related in a complicated, and as yet unknown way. The explanation of changes in equivalent conductance is made yet more difficult by the effects of ion-solvent interactions, as discussed in the following section.

5.5 The effect of chemical equilibrium between mixed solvent species and solute ions upon the value of the Walden Product

Hemmes[31] has illustrated mathematically how chemical equilibrium between solute ions and the molecules of a mixed solvent can lead to a highly complex variation of the Walden Product with changing solvent composition. In the simplest case, the ion M forms the solvated species MA_n in pure solvent A, where n is constant. When solvent B is added to the mixture its molecules enter into chemical equilibrium with MA_n.

$$MA_n + B \rightleftharpoons MA_{n-1}B + A$$

Assuming the Walden product, $k_i = \lambda_i^0 \eta$ for each of the above ions to be constant, Hemmes obtained the relation

$$\bar{\lambda}^0\eta = \frac{k_M + (k_{MB} K - k_M) x_B}{1 + (K-1) x_B} \tag{5.18}$$

where k_M, k_{MB} are the Walden products of MA_n and $MA_{n-1}B$ respectively, x_B is the mole fraction of B and K is the equilibrium constant in mole fraction units. $\bar{\lambda}^0$ is the apparent limiting ionic conductance of M. This equation predicts that $\bar{\lambda}^0\eta$ will vary with x_B despite the fact that both species obey the Walden Rule; only for the special case $k_M = k_{MB}$ will $\bar{\lambda}^0\eta$ be independent of composition. The complexity of the expression for $\bar{\lambda}^0\eta$ increases if B is a bidentate ligand or if more than one molecule of B reacts to produce more than one product. In the latter case, Hemmes obtained

$$\bar{\lambda}^0\eta = \frac{k_M + (k_{MB} K_1 - k_M) x_B + k_{MB_2} K_1 K_2 x_B^2}{1 + (K_1 - 1)x_B + K_1 K_2 x_B^2} \tag{5.19}$$

where K_1, K_2 are equilibrium constants for the successive replacement of A molecules in MA_n by B molecules; k_{MB_2} is the Walden product for the ion $MA_{n-2}B_2$.

If the derivative with respect to x_B of the right side of equation 5.19 is set to zero, solutions for x_B are found to satisfy the equation

$$x_B = \frac{-Q \pm (Q^2 - 4RS)^{1/2}}{2R} \tag{5.20}$$

where Q, R, S are each functions of at least three of K_1, K_2, k_M, k_{MB} and k_{MB_2}. This means that $\bar{\lambda}^0\eta$ shows a maximum or minimum for any mole fraction of B which satisfies equation 5.20. Clearly if the other ion of the solute also takes part in reactions with the solvent, the Walden product $\Lambda^0\eta$ will be a highly complex function of composition. It is of interest to note that the Walden products for CsCl (this research) and KCl in DMF/water mixtures both exhibit a maximum and a minimum (Figure 5.8).

Hemmes' theory was put to the test using the available data for Cl^- in DMF/water mixtures (Table 5.1). Using the method of simultaneous equations, several values of K, k_M and k_{MB} were obtained for sets of three data points applied to equation 5.18. Since the results were inconsistent and anomalous (some negative K values), the more complex equation (5.19) was investigated. In this case computer programs were applied to the data to estimate the five 'constants' K_1, K_2, k_M, k_{MB} and k_{MB_2} by the method of least squares

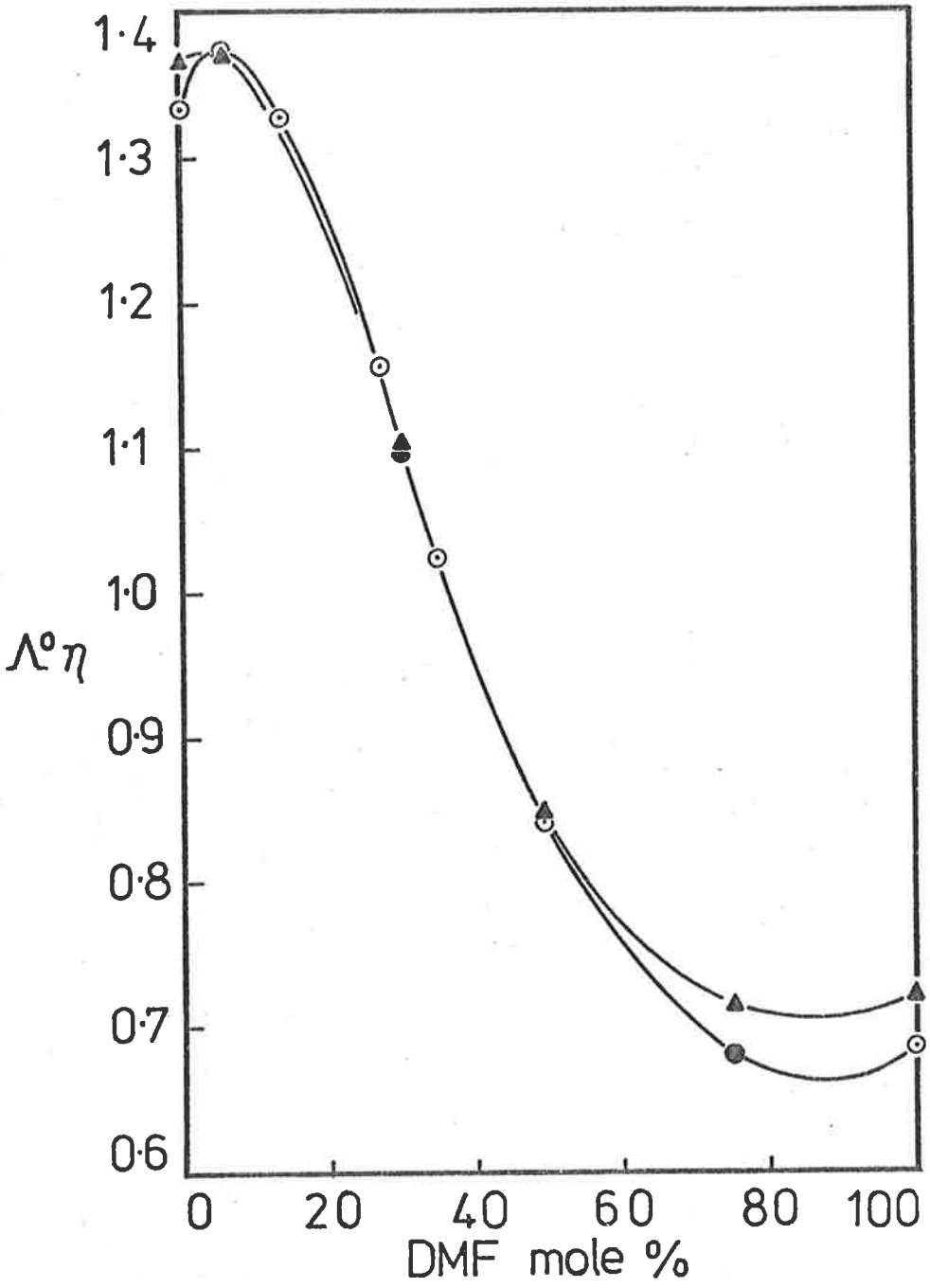

FIGURE 5.8 Walden Products of KCl and CsCl in DMF/water at 25°C

⊙ KCl, data of James

● KCl, this research

▲ CsCl

and also by the solution of simultaneous equations. Both methods gave similar but anomalous values for the equilibrium constants K_1 and K_2 (about -1 and -2 respectively). In consequence it must be concluded that Hemmes theory does not apply in this system. Evidently the Walden Products of the respective solvated species do not remain constant.

Hemmes' paper, and the material presented in section 5.4, provide good examples of the kind of complexities which workers in this field must expect to incorporate into an adequate model for ion-solvent interactions.

References

1. Stokes, G.G., *Trans. Camb. phil. Soc.*, **VIII**, 287, (1845).
2. Robinson, R.A. and Stokes, R.H., *Electrolyte Solutions*, Butterworths, London, Second Edition, Revised 1965, page 130.
3. Monica, M.D. and Senatore, L., *J. Phys. Chem.*, **74**, 205, (1970)
4. MacInnes, D.A., *The Principles of Electrochemistry*, Dover Publications Inc., New York, 1961, page 361.
5. D'Aprano, A. and Fuoss, R.M., *J. Soln. Chem.*, **4**, 175, (1975).
6. Reference 2, pages 123–124.
7. Reference 2, pages 307–310.
8. Fuoss, R.M., *Proc. Nat. Acad. Sci., U.S.A.*, **45**, 807, (1959).
9. Boyd, R.H., *J. Chem. Phys.*, **35**, 1281, (1961).
10. Boyd, R.H., *J. Chem. Phys.*, **39**, 2376, (1963).
11. Zwanzig, R., *J. Chem. Phys.*, **38**, 1603, (1963).
12. Zwanzig, R., *J. Chem. Phys.*, **52**, 3625, (1970).
13. Reference 2, page 11.
14. Dannhauser, W. and Johari, G.P., *Can. J. Chem.*, **46**, 3143, (1968).
15. Lind, J.E., Jr. and Fuoss, R.M., *J. Phys. Chem.*, **65**, 999, 1414, (1961).
16. ibid., *J. Phys. Chem.*, **66**, 1727, (1962).
17. Kunze, R.W. and Fuoss, R.M., *J. Phys. Chem.*, **67**, 911, (1963).
18. Justice, J-C. and Fuoss, R.M., *J. Phys. Chem.*, **67**, 1707, (1963).
19. Fabry, T.L. and Fuoss, R.M., *J. Phys. Chem.*, **68**, 971, (1964).
20. James, C.J., Ph.D. thesis, University of Adelaide, South Australia, 1972.
21. Atkinson, G. and Mori, Y., *J. Phys. Chem.*, **71**, 3523, (1967).
22. James, C.J. and Fuoss, R.M., *J. Soln. Chem.*, **4**, 91, (1975).
23. Ames, D.P. and Sears, P.G., *J. Phys. Chem.*, **59**, 16, (1955).
24. Prue, J.E. and Sherrington, P.J., *Trans. Faraday Soc.*, **57**, 1795, (1961).

25. Nakanishi, K., Kato, N. and Maruyama, M., *J. Phys. Chem.*, **71**, 814, (1967).

26. Samoilov, O. Ya, *Structure of Aqueous Electrolyte Solutions and the Hydration of Ions,* translated from the Russian by D.J.G. Ives, Consultants Bureau, New York, 1965.

27. Kavanau, J.L., *Water and Solute-Water Interactions,* Holden-Day Inc., San Francisco, London and Amsterdam, 1964, pages 8–10.

28. Assarsson, P. and Eirich, F.R., *J. Phys. Chem.*, **72**, 2710, (1968).

29. Weast, R.C., (ed.), *Handbook of Chemistry and Physics,* The Chemical Rubber Co., Cleveland, Ohio, 52nd Edition, 1971–1972, page D146.

30. Bernal, J.D. and Fowler, R.H. in Eisenberg, D. and Kauzmann, W., *The Structure and Properties of Water,* Oxford University Press, Oxford, 1969, page 185.

31. Hemmes, P., *J. Phys. Chem.*, **78**, 907, (1974).

APPENDICES

Appendix 1.1 CONDUCTIVITY PROGRAMS LOAOKA AND UNASS

These programs use procedures outlined in Chapter 3 to compute Λ^0, a and K_A (LOAOKA) or Λ^0 and a (UNASS) from input values of Λ and C. As many systems as desired may be processed in each computer run, but the last card of the final system must be followed by a blank card.

PROGRAM LOAOKA

1 *Sub-routines*
SUBG2, SUBQC and SUBENE

2 *Input data*

Card 1
FORMAT 102 – system identification – any combination of alphabetic or numeric characters up to 78 columns may be used.

Card 2
FORMAT 101 – the card is punched with the specific conductance of the solvent.

Card 3
FORMAT 104 – the symbols have the following meanings.

N	=	number of data points
D	=	solvent dielectric constant
ETA	=	solvent viscosity in poise
T	=	absolute temperature
QK	=	estimate of Λ^0
AR	=	estimate of ion size in Å
PKV	=	estimate of association constant

Cards 4 → N+4
FORMAT 106 – each card is punched with a value of C given at $C \times 10^4$, and its corresponding Λ value.

Card N+5
The last card of the final system being processed in the run is a blank. All preceding systems have N+4 cards.

3 *Output*
The principal output of LOAOKA is as follows:

Λ^0, its standard error $\sigma\Lambda^0$, a, σa, K_A, σK_A, σ (the standard error of the fit of the experimental Λ and C values to the Fuoss-Hsia equation) and $\delta\Lambda$ (the deviation between the experimental Λ and that computed from the F-H equation) for each Λ–C point.

Appendix 1.1 continued

PROGRAM UNASS

1 *Sub-routines*
SUBQC and SUBENE

2 *Input data*
Card 1, 2, 3 . . .N+3, N+4 correspond to cards 1, 3, 4 . . . N+4, N+5 used in LOAOKA. PKV in card 2 is ignored.

3 *Output*
Λ^0, $\sigma\Lambda^0$, a, σa, $\delta\Lambda$ and σ.

A listing of these programs is presented on the following pages.

```
      ----------------------------
      PROGRAM LOAOKA(INPUT,OUTPUT)
      ----------------------------

C.... PROGRAM ADAPTED FROM R.L.KAY≠S FUOSS HSIA  PROGRAM BY C.JAMES
C     MINOR MODIFICATIONS BY G.CHITTLEBOROUGH

C..... PROGRAM ITERATES FOR LAMDA 0 , A ZERO , $ ASSOCIATION CONST.
C.... PROGRAM TREATS  DATA FOR ASSOCIATED CASE ONLY*******************

      COMMON C(30),Q(30),G2(30),CG(30),F2(30),VF(30),FM(30),BCFM(30),
     1QC(30),QL(30),FMI(30),BCFMI(30),QCI(30),QCP(30),TDT(30),DQ(30),
     2DLQ(30),SQDL(30),SG(30),PKN(30),DQQ(30),WT(30),R(30),BARM(30),
     3DEN(30),QP(30),DK(30),
     4D,AA,QZ,FKAP,ALPHA,BETA,E1,E2,J


  100 PRINT 10
   10 FORMAT (1H1)

C     FIRST DATA CARD GIVES SYSTEM IDENTIFICATION
      READ 102
  102 FORMAT (78H
     1                          )

C    SECOND CARD GIVES KSP OF SOLVENT
      READ 101,SPK
 101  FORMAT(F10.2)

      READ104,N,D,ETA,T,QK,AR,PKV
```

```
      ------------------------
      PROGRAM LOAOKA CONTINUED
      ------------------------

  104 FORMAT(I5,F11.0,5F10.0)
      IF(N.EQ.0) GO TO 700

  210 PRINT 211
  211 FORMAT(1H0,*ASSOCIATED ELECTROLYTE*)
      PRINT124
  124 FORMAT(1H0)


      PRINT 102
      PRINT124
      PRINT 41,SPK
   41 FORMAT(14H  SOLVENT KSP=F5.2,3HE-6)
      PRINT112,D,ETA,QK,PKV,T,AR
  112 FORMAT(22H  DIELECTRIC CONSTANT=F8.2,11H VISCOSITY=F10.6,12H INITI
     1AL QZ=F8.3,/,22H INITIAL ASSOCN CONST=F8.3,13H TEMPERATURE=F8.2,12
     2H INITIAL AA=F8.3/)
   85 READ105,(C(J),Q(J),J=1,N)
  106 FORMAT (2F10.0)
      PRINT719
  719 FORMAT(1H0,* INPUT   DATA*)
      PRINT717
  717 FORMAT(1H 3X,7H10000 C,6X,1HQ,/)
      PRINT718,(C(J),Q(J),J=1,N)
  718 FORMAT(F11.4,F10.3)
      PRINT124
```

```
      ------------------------
      PROGRAM LOAOKA CONTINUED
      ------------------------

      QQ=280.195/D
C  BEGIN COMPUTATION HERE
  640 FLON=N
      DT=D*T
      SQRDT=SQRT(DT)
      ALPHA=820400./(SQRDT*DT)
      BETA=82.501/(ETA*SQRDT)
      E1=2.9422E12/(DT**3)
      E2=0.43329E8/((DT*DT)*ETA)
      TA=SQRT(6.0*E1)
      FKAP=50.294/SQRDT
  641 QZI=QK
      NX=0
      M1=0
      AA=AR
  650 NX=NX+1
      IF(PKV)652,649,651
  652 DO 653 J=1,N
      G2(J)=1.0
      CG(J)=C(J)*1.0E-4
  653 CONTINUE
      GO TO 610
  649 PKV=0.1
  651 DO 200 J=1,N
  200 CALL SUBG2 (TA,PKV,M1,SQRDT,QQ)
      IF(M1-10)610,610,196
```

```
      ------------------------
      PROGRAM LOAOKA CONTINUED
      ------------------------

  196 PRINT 197
  197 FORMAT(36HNO CONVERGENCE IN G1 AFTER 10 CYCLES)
      GO TO 100


  610 M=0
      M2=0
      QZ=QK
  504 AI=AA
      AP=1.005*AA
      M=M+1
      CYC=M
      IF(M-10) 520,513,513
  513 PRINT111
  111 FORMAT(1H0,*NO CONVERGENCE AFTER 10 CYCLES*)
      GO TO 100

  520 DO 33 J=1,N
      CALL SUBQC
      FMI(J)=FM(J)
      BCFMI(J)=BCFM(J)
      QCI(J)=QC(J)
      AA=AP
      CALL SUBQC
      QCP(J)=QC(J)
      TDT(J)=Q(J)+G2(J)*BCFMI(J)-G2(J)*FMI(J)*QZ
```

```
      ------------------------
      PROGRAM LOAOKA CONTINUED
      ------------------------

      DQ(J)=(200.0/AI)*(QCP(J)-QCI(J))
      AA=AI
      QZ=1.005*QZ
      CALL SUBQC
      QL(J)=QC(J)
      QZ=QZ/1.005
      DQQ(J)=(200.0/QZ)*(QL(J)-QCI(J))
      PKV=1.005*PKV
      CALL SUBS2 (TA,PKV,M1,SQRDT,QQ)
      IF(M1-10)32,32,196
   32 CALL SUBQC
      QP(J)=QC(J)
      PKV=PKV/1.005
   33 DK(J)=(200.0/PKV)*(QP(J)-QCI(J))
    3 SUM11=0.0
      SUM12=0.0
      SUM13=0.0
      SUM14=0.0
      SUM22=0.0
      SUM23=0.0
      SUM24=0.0
      SUM33=0.0
      SUM34=0.0
      DO 50 J=1,N
      SUM11=SUM11+DQQ(J)*DQQ(J)
      SUM12=SUM12+DQQ(J)*DQ(J)
```

```
      ------------------------
      PROGRAM LOAOKA CONTINUED
      ------------------------

      SUM13=SUM13+DQQ(J)*DK(J)
      SUM14=SUM14+DQQ(J)*TDT(J)
      SUM22=SUM22+DQ(J)*DQ(J)
      SUM23=SUM23+DQ(J)*DK(J)
      SUM24=SUM24+DQ(J)*TDT(J)
      SUM33=SUM33+DK(J)*DK(J)
   50 SUM34=SUM34+DK(J)*TDT(J)
      DET=SUM11*(SUM22*SUM33-SUM23*SUM23)-SUM12*(SUM12*SUM33-SJM13*SUM23
     1)+SUM13*(SUM12*SUM23-SUM13*SUM22)
      DETQ=SUM14*(SUM22*SUM33-SUM23*SUM23)-SUM12*(SUM24*SUM33-SUM23*SUM3
     14)+SUM13*(SUM23*SUM24-SUM22*SUM34)
      DETA=SUM11*(SUM24*SUM33-SUM23*SUM34)-SUM14*(SUM12*SUM33-SUM13*SUM2
     13)+SUM13*(SUM12*SUM34-SUM13*SUM24)
      DETK=SUM11*(SUM22*SUM34-SUM23*SUM24)-SUM12*(SUM12*SUM34-SUM13*SUM2
     14)+SUM14*(SUM12*SUM23-SUM13*SUM22)
      DQZ=DETQ/DET
      QZ=QZ+DQZ
      DLA=DETA/DET
      AA=AA+DLA
      DLK=DETK/DET
      PKV=PKV+DLK
      PRINT118,CYC,DLA,DQZ,DLK
  118 FORMAT(10H AT CYCLE F2.0,12H  DELTA AA =F7.4,12H  DELTA QZ =F7.4,1
     13H  DELTA PKV =F10.4)
      IF(PKV)320,320,321
  320 PKV=(PKV-DLK)/2.0
```

```
      ------------------------
      PROGRAM LOAOKA CONTINUED
      ------------------------

      PRINT119
  119 FORMAT(10X,23HPKV NEGATIVE  TRY PKV/2)
  321 DO 702 J=1,N
  702 CALL SUBG2 (TA,PKV,M1,SQRDT,QQ)
      IF(M1-10)703,703,196
  703 IF(AA)329,329,330
  329 AA=(AA-DLA)/2.0
      PRINT120
  120 FORMAT(20X,21HAA NEGATIVE  TRY AA/2)
      GO TO 504
  330 TSA=ABS (DLA/AA)
      IF(TSA-0.0001)331,331,332
  332 GO TO 504


  331 B=560.37/(D*AA)
      FBJ=EXP (B)/(B**3)
      PKCON=(2.523E-3)*(AA**3)*EXP(B)
      SMSQ = 0.
      SMDL=0.0
      DO 701 J=1,N
      CALL SUBQC
      DLQ(J)=QC(J)-Q(J)
      SMDL=SMDL+DLQ(J)
      SQDL (J) = DLQ(J)**2
```

```
      ------------------------
      PROGRAM LOAOKA CONTINUED
      ------------------------

  701 SMSQ = SMSQ + SQDL(J)
      REAL = N
      QUOT=SMSQ/(REAL-3.0)
      SIGMA = SQRT (QUOT)
      SG(NX)=SIGMA
      A11=ABS (SUM11)
      A12=ABS (SUM12)
      A13=ABS (SUM13)
      A22=ABS (SUM22)
      A23=ABS (SUM23)
      A33=ABS (SUM33)
      SGQ=SIGMA*SQRT ((A22*A33-A23*A23)/DET)
      SGA=SIGMA*SQRT ((A11*A33-A13*A13)/DET)
      SGK=SIGMA*SQRT ((A11*A22-A12*A12)/DET)
      S=ALPHA*QZ+BETA
      E=E1*QZ-E2
      PRINT124
  581 PRINT116,B,FBJ,PKCON
  116 FORMAT(11H BJERRUM-B=F10.3,10H WITH FBJ=F12.3,11H AND PKCON=F12.3)
      PRINT117,ALPHA,BETA,S,E1,E2,E
  117 FORMAT(8H  ALPHA=F7.4,5HBETA=F7.2,3H S=F7.2,4H E1=F6.3,4H E2=F6.2,
     13H E=F7.2)
      PRINT124
      PRINT126
  126 FORMAT(1H0,6X,*C*,12X,*CG*,11X,*GAMMA*,4X,*ACT SQU*,5X,*Q EXPT*,6X
     2,*Q CALC*,6X,*Q DASH*)
```

```
      ------------------------
      PROGRAM LOAOKA CONTINUED
      ------------------------

      PRINT127,(C(J),CG(J),G2(J),F2(J),Q(J),QC(J),DLQ(J),J=1,N)
  127 FORMAT(1X,F11.6,4X,F11.9,4X,F7.5,4X,F7.5,4X,F8.4,4X,F8.4,4X,F8.4)
      PRINT124
      PRINT114,QZ,SGQ,AA,SGA,PKV,SGK
  114 FORMAT(27H MINIMIZING VALUES ARE QZ =F10.3,4H PM F5.3,9H AND AA =F
     17.3,4H PM F5.3,/,/,17X,10H AND PKV =F10.3,4H PM F8.3)
      PRINT124
      PRINT123,SIGMA,SMDL
  123 FORMAT(25H     STANDARD DEVIATION =F6.3,18H WITH SUM-DELTAS =F6.3)
      PRINT124
      PRINT5000,QQ
 5000 FORMAT(1H0(*BJERRUM CRIT DIST=*,E14.7)
      PRINT124
      PRINT125
  125 FORMAT(55H**********************************************************)

      GO TO 100

  700 CONTINUE
      END
```

```
      ---------------------------
      PROGRAM UNASS(INPUT,OUTPUT)
      ---------------------------

C.... FUOSS HSIA EQUATION R.L. KAYS PROGRAM FOR THE NON ASSOCIATED CASE
      COMMON C(30),Q(30),G2(30),CG(30),F2(30),VF(30),FM(30),BCFM(30),
     1QC(30),QL(30),FMI(30),BCFMI(30),QCI(30),QCP(30),TDT(30),DQ(30),
     2DLQ(30),SQDL(30),SG(30),PKN(30),DQQ(30),WT(30),P(30),BARM(30),
     3DEN(30),QP(30),DK(30),
     4D,AA,QZ,FKAP,ALPHA,BETA,E1,E2,J
  100 PRINT10
   10 FORMAT(1H1)
      PRINT 213
  213 FORMAT(1H0,*NONASSOCIATED ELECTROLYTE*)
      READ 102
      PRINT 102
  102 FORMAT (78H
     1                          )
      PRINT124
  124 FORMAT(1H0)
      READ104,N,D,ETA,T,QK,AR,PKV
  104 FORMAT(I5,F11.0,5F10.0)
      IF(N.EQ.0) GO TO 700
      PKV=0.0
      PRINT719
  719 FORMAT(1H0,* INPUT   DATA*)
      PRINT124
      PRINT112,D,ETA,QK,PKV,T,AR
  112 FORMAT(22H  DIELECTRIC CONSTANT=F8.2,11H VISCOSITY=F10.6,12H INITI
     1AL QZ=F8.3,/,22H INITIAL ASSOCN CONST=F8.3,13H TEMPERATURE=F8.2,12
```

```
      ----------------------
      PROGRAM UNASS CONTINUED
      ----------------------

     2H INITIAL AA=F8.3/)
   85 READ106,(C(J),Q(J),J=1,N)
  106 FORMAT (2F10.0)
      PRINT717
  717 FORMAT(1H 3X,7H10000 C,6X,1HQ,/)
      PRINT718,(C(J),Q(J),J=1,N)
  718 FORMAT(F11.4,F10.3)
C
  640 FLON=N
      DT=D*T
      SQRDT=SQRT(DT)
      ALPHA=820400./(SQRDT*DT)
      BETA=82.501/(ETA*SQRDT)
      E1=2.9422E12/(DT**3)
      E2=0.43329E8/((DT*DT)*ETA)
      TA=SQRT(6.0*E1)
      FKAP=50.294/SQRDT
 1000 QZI=QK
      NX=0
      DO 1653 J=1,N
      G2(J)=1.0
 1653 CG(J)=C(J)*1.0E-4
      AA=AR
 1650 NX=NX+1
      M=0
      QZ=QK
```

```
      ------------------------
      PROGRAM UNASS CONTINUED
      ------------------------

 1504 AI=AA
      AP=1.005*AA
      M=M+1
      CYC=M
      IF(M-10)1520,1520,1513
 1513 PRINT111
  111 FORMAT(1H0,*NO CONVERGENCE AFTER TEN CYCLES*)
      GO TO 100
C
 1520 DO 1033 J=1,N
      CALL SUBQC
      FMI(J)=FM(J)
      BCFMI(J)=BCFM(J)
      QCI(J)=QC(J)
      AA=AP
      CALL SUBQC
      QCP(J)=QC(J)
      TDT(J)=Q(J)+G2(J)*BCFMI(J)-G2(J)*FMI(J)*QZ
      DQ(J)=(200.0/AI)*(QCP(J)-QCI(J))
      AA=AI
      QZ=1.005*QZ
      CALL SUBQC
      QL(J)=QC(J)
      QZ=QZ/1.005
 1033 DQQ(J)=(200.0/QZ)*(QL(J)-QCI(J))
 1003 SUM11=0.0
```

```
      ----------------------
      PROGRAM UNASS CONTINUED
      ----------------------

      SUM12=0.0
      SUM13=0.0
      SUM22=0.0
      SUM23=0.0
      DO 1050 J=1,N
      SUM11=SUM11+DQQ(J)*DQQ(J)
      SUM12=SUM12+DQQ(J)*DQ(J)
      SUM13=SUM13+DQQ(J)*TDT(J)
      SUM22=SUM22+DQ(J)*DQ(J)
 1050 SUM23=SUM23+DQ(J)*TDT(J)
      DET=SUM11*SUM22-SUM12*SUM12
      DETQ=SUM13*SUM22-SUM12*SUM23
      DETA=SUM11*SUM23-SUM12*SUM13
      DQZ=DETQ/DET
      QZ=QZ+DQZ
      DLA=DETA/DET
      AA=AA+DLA
      PRINT121,CYC,DLA,DQZ
  121 FORMAT(10H AT CYCLE F2.0,12H  DELTA AA =F7.4,12H  DELTA QZ =F7.4)
      IF(AA)1329,1329,1330
 1329 AA=(AA-DLA)/2.0
      PRINT120
  120 FORMAT(1H0,*     AA NEGITIVE TRY AA/2*)
      GO TO 1504
 1330 TSA=ABS(DLA/AA)
      IF(TSA-0.0001)1331,1331,1332
```

```
      ------------------------
      PROGRAM UNASS CONTINUED
      ------------------------

 1332 GO TO 1504
C
C
 1331 B=560.37/(D*AA)
      FBJ=EXP(B)/(B**3)
      PKCON=(2.523E-3)*(AA**3)*EXP(B)
      SMSQ=0.0
      SMDL=0.0
      DO 1701 J=1,N
      CALL SUBQC
      DLQ(J)=QC(J)-Q(J)
      SMDL=SMDL+DLQ(J)
      SQDL(J)=DLQ(J)**2
 1701 SMSQ=SMSQ+SQDL(J)
      REAL=N
      QUOT=SMSQ/(REAL-2.0)
      SIGMA=SQRT(QUOT)
      SG(NX)=SIGMA
      A11=ABS(SUM11)
      A22=ABS(SUM22)
      SGQ=SIGMA*SQRT(A11/DET)
      SGA=SIGMA*SQRT(A11/DET)
      S=ALPHA*QZ+BETA
      E=E1*QZ-E2
      PRINT124
      PRINT116,B,FBJ,PKCON
```

```
      ----------------------
      PROGRAM UNASS CONTINUED
      ----------------------

  116 FORMAT(11H BJERRUM-B=F10.6,10H WITH FBJ=F12.5,11H AND PKCON=F12.5)
      PRINT117,ALPHA,BETA,S,E1,E2,E
  117 FORMAT(7H ALPHA F9.5,5HBETA F9.5,3H S F9.4,4H E1 F9.4,4H E2 F9.4,
     13H E=F9.4)
      PRINT124
      PRINT129
  129 FORMAT(1H0,4X,*C*,6X,*EXP. LAMBDA*,6X,*LAMBDA CALC*,6X,*LAMBDA DAS
     1H*)
      PRINT130,(C(J),Q(J),QC(J),DLQ(J),J=1,N)
  130 FORMAT(1X,F10.4,4X,F10.4,4X,F10.4,4X,F10.4)
      PRINT128,QZ,SGQ,AA,SGA
  128 FORMAT(1H0,*MINIMIZING VALUES ARE QZ *,F10.3,2X,*PM*,F5.3,2X,*AND
     1A*,F7.3,2X,*PM*,F5.3)
      PRINT123,SIGMA,SMDL
  123 FORMAT(1H0,*STANDARD DEVIATION  *,F6.3,2X,*WITH SUM OF DELTAS  *,F
     16.3)
      PRINT125
  125 FORMAT(1H0(* CHOCKS AWAY CHAPS ALL OVER RED ROVER*)
C
C
      GO TO 100
  700 CONTINUE
      END
```

```
      ------------------------------------
      SUBROUTINE SUBG2 (TA,PKV,M1,SQRDT,QQ)
      ------------------------------------

C   SUBROUTINE TO COMPUTE GAMMA,GIVEN ASSOCN CONST
C..... FUOSS$ACCASCINA,ELECTROLYTIC CONDUCTANCE,INTERSCIENCE,1959 P.92-3

      COMMON C(30),Q(30),G2(30),CG(30),F2(30),VF(30),FM(30),BCFM(30),
     1QC(30),QL(30),FMI(30),BCFMI(30),QCI(30),QCP(30),TDT(30),DQ(30),
     2DLQ(30),SQDL(30),SG(30),PKV(30),DQQ(30),WT(30),R(30),BARM(30),    ),
     3DEN(30),QP(30),DK(30),
     4D,AA,QZ,FKAP,ALPHA,BETA,E1,E2,J

      CK=C(J)*1.0E-4
      TAU=TA*SQRT (CK)
      G1=1.0
      M1=0
  198 M1=M1+1
      IF(M1-10)203,203,199
  199 RETURN
  203 SRG=SQRT (G1)
      TOP=(4.20132E6)/(SQRDT**3)
      BOT=(50.294)/(SQRDT)
      SRC=SQRT(CK)

      F2(J)=(TOP*SRC*SRG)/(1.0+(BOT*AA*SRC*SRG))

      F2(J)=EXP(-2.0*F2(J))
      VAR=PKV*CK*F2(J)
      IF(VAR-0.03) 204,205,205
```

```
      ------------------------
      SUBROUTINE SUBG2 CONTINUED
      ------------------------

  204 G2(J)=1.0-VAR+2.0*(VAR**2)-5.0*(VAR**3)
      GO TO 206
  205 G2(J)=(SQRT (1.0+4.0*VAR)-1.0)/(2.0*VAR)
  206 TESTG=ABS (G1-G2(J))
      IF(TESTG-0.00005) 201,202,202
  202 G1=G2(J)
      GO TO 198
  201 CG(J)=CK*G2(J)
      RETURN
      END
```

```
      ----------------
      SUBROUTINE SUBQC
      ----------------

C     SUBROUTINE TO CALC. EQUIV. COND.

      COMMON C(30),Q(30),G2(30),CG(30),F2(30),VF(30),FM(30),BCFM(30),
     1QC(30),QL(30),FMI(30),BCFMI(30),QCI(30),QCP(30),TDT(30),DQ(30),
     2DLQ(30),SQDL(30),SG(30),PKN(30),DQQ(30),WT(30),R(30),BARM(30),
     3DEN(30),QP(30),DK(30),
     4D,AA,QZ,FKAP,ALPHA,BETA,E1,E2,J

      B=560.37/(D*AA)
      CR=CG(J)
      SQRC=SQRT (CR)
      Y=FKAP*AA*SQRC
      SVF=0.000473*CR*(AA**3)
      VF(J)=1.0+SVF
      W=0.7071
      X=Y
      CALL SUBENE(X,ENE)
      TZ=ENE
      P1=1.0+X+0.5*X*X
      P2=1.0+W*X+0.25*X*X
      P3=1.0+W*X+0.1667*X*X
      P4=2.0*P2*(1.0+X)*(1.0+X)
      P5=2.0*P3*P4
      P6=0.4576/(P4*P3)
      X=(1.0+W)*Y
      CALL SUBENE(X,ENE)
```

```
--------------------------
SUBROUTINE SUBOC CONTINUED
--------------------------

 T1=ENE
 X=(2.0+W)*Y
 CALL SUBENE(X,ENE)
 T2=ENE
 X=X/2.7071
 TR1=(7.0*T2+P1*T1-4.0*P1*P2*TZ)/(4.0*P4)
 XSQ=X*X
 PM2=-9.0/4.0+9.0*W/2.0+(-7.0/12.0+7.0*W/3.0)*X+(1.0/24.0+7.0*W/12.
10)*XSQ
 BF23=PM2/P5
 AL8=8.0*BF23+2.0/P4+P6
 TOP=1.0+(9.0*W/8.0+0.5)*X+(W+1.0/24.0)*XSQ
 BOT=P2*P3*(1.0+X)
 RATIO=TOP/BOT
 BM1=4.0*RATIO
 BM2= (4.0*(1.0+0.75*X))/(P3*(1.0+X))
 ALGV=(16.0+6.0*W+(7.0+10.0*W)*X+(3.0+4.0*W)*XSQ)/(48.0*P2*(1.0+X)*
1(1.0+X))
 TF2=-8.0*ALGV-4.0*TR1+4.0/(3.0*B*P2*(1.0+X))
 TF1=-4.0*TR1-AL8+BM1/B+BM2/(B*B)-2.0/(B**3)
 FNEG=-ALPHA*SQRC+E1*CR*TF1-E2*CR*TF2/QZ
 FM(J)=(1.0+FNEG)/VF(J)
 BCFM(J)=BETA*SQRC*FM(J)/(1.0+Y)
 QC(J)=(G2(J))*(QZ*FM(J)-BCFM(J))
 RETURN
 END
```

```
      ------------------------
      SUBROUTINE SUBENE(X,ENE)
      ------------------------

C   SUBROUTINE FOR CALCN OF NEG.EXPONENTIAL INTEGRALS

C..... FUOSS$ACCASCINA,ELECTROLYTIC CONDUCTANCE,INTERSCIENCE,1959
C.....                  PAGES 150 TO 153
      CON=-ALOG(X)-0.57722
      FN= 0.0
      FAC = 1.0
      TOT =0.0
      QNP = -1.0
   30 FN=FN+1.0
      FAC = FAC*FN
      QNP = -1.0*X*QNP
      FNTH = QNP/(FN*FAC)
      TOT=TOT+FNTH
      TRM=ABS ((1.0E4)*FNTH)
      ABT=ABS (TOT)
      IF (ABT-TRM) 30,30,40
   40 ENG=CON+TOT
C*************************************************************************
C..... WHEN USED WITH PROGRAM PITTSV2 THE CARD IMMEDIATELY  BELOW
      ENE=ENG*EXP (X)
C..... MUST BE REMOVED FROM THIS ROUTINE
C*************************************************************************
      RETURN
      END
```

Appendix 2.1 Viscosity and Density of DMF/water mixtures at 25°C

DMF mole %	*Density g cm^{-3}*	*Viscosity cP*
0.0	0.99704_4	0.890_3
2.361	0.99622_3	1.098_7
5.804	0.99637_1	1.401_5
6.005	0.99639_2	1.419_9
10.068	0.99690_6	1.764_9
13.493	0.99700_6	2.014_7
14.094	0.99698_4	2.057_1
18.698	0.99630_0	2.313_8
26.042	0.99340_1	2.500_6
26.935	0.99291_9	2.501_7
35.056	0.98770_4	2.393_8
49.629	0.97632_0	1.873_8
61.949	0.96681_6	–
64.670	0.96478_7	1.372_6
83.450	0.95289_6	–
100.00	0.94389_0	0.801_2

Appendix 3.1 The concentration dependence of Λ for KCl, CsCl and KNCS in DMF/water mixtures at 25°C

$C \times 10^4$	Λ	$\delta\Lambda \times 10^3$
KCl in 0.30 mole fraction DMF		
48.046	41.744	2
62.077	41.383	-4
75.412	41.070	2
88.406	40.806	-3
105.051	40.486	5
120.557	40.229	3
KCl in 0.75 mole fraction DMF		
12.132	55.791	-0.4
22.501	54.355	-1
31.774	53.341	1
40.520	52.522	2
46.400	52.028	0.5
54.264	51.417	0.7
61.262	50.919	-3
161.897	45.939	0
CsCl in pure water, Run 1		
11.280	150.473	9
25.235	148.964	11
42.067	147.652	0
73.017	145.892	0
101.654	144.633	2
CsCl in pure water, Run 2		
16.344	149.770	7
33.278	148.208	-10
44.822	147.373	-1
59.654	146.471	2
70.406	145.899	1
81.735	145.349	1
99.563	144.572	0
CsCl in 0.09 mole fraction DMF		
23.377	79.280	2
44.325	78.338	-3
69.158	77.503	-4
91.325	76.881	8
107.429	76.498	-1
121.554	76.184	-3

Appendix 3.1 continued

$C \times 10^4$	Λ	$\delta\Lambda \times 10^3$
CsCl in 0.30 mole fraction DMF, Run 1		
13.246	42.825	4
33.706	41.854	-9
58.923	41.005	3
81.979	40.398	8
105.554	39.892	-6
CsCl in 0.30 mole fraction DMF, Run 2		
12.662	42.803	9
23.522	42.248	-15
43.106	41.464	5
79.942	40.422	5
106.116	39.845	-3
CsCl in 0.5 mole fraction DMF		
9.928	43.666	6
22.842	42.569	-9
40.112	41.495	-4
54.098	40.790	2
70.819	40.065	8
94.664	39.192	0
116.241	38.501	-3
CsCl in 0.75 mole fraction DMF		
13.862	57.484	-2
23.289	55.942	1
32.698	54.694	3
43.157	53.519	1
55.192	52.351	-1
70.035	51.105	-3
85.783	49.950	-1
101.493	48.929	2
KNCS in pure water		
11.450	136.926	13
29.115	135.224	-4
39.571	134.498	-8
49.212	133.925	-9
60.005	133.360	-1
73.753	132.725	2
87.472	132.163	1
100.478	131.681	6

Appendix 3.1 continued

$C \times 10^4$	Λ	$\delta\Lambda \times 10^3$
KNCS in 0.50 mole fraction DMF, Run 1		
11.272	46.420	-3
26.291	45.535	5
40.442	44.975	-1
57.440	44.446	0
73.995	44.027	-1
86.591	43.748	-1
99.098	43.498	-1
114.755	43.212	2
KNCS in 0.5 mole fraction DMF, Run 2		
11.765	46.370	1
27.311	45.490	-4
41.642	44.924	2
53.742	44.546	0
80.660	43.869	1
105.631	43.370	0
118.236	43.149	-1
KNCS in 0.75 mole fraction DMF		
13.041	63.137	2
27.565	61.661	-3
42.115	60.615	-1
59.446	59.643	0
72.127	59.045	2
86.225	58.461	1
98.599	58.002	-2

Appendix 4.1 Cationic Transport Numbers of KNCS in DMF/water solvents at 25°C

C mol dm^{-3}	*Solvent correction*	*Tube section*	*Ave. Current mA*	*Time sec*	t_+
In 0.75 mole fraction DMF					
0.009989	1.0001	1	0.1996_6	4364.8	0.3897_5
		2	0.1962_5	4421.4	0.3911_0
		3	0.1942_6	4365.7	0.3915_2
0.010754	1.0017	1	0.2016_4	4650.6	0.3905_7
0.021790	1.0009	1	0.2994_3	6354.4	0.3897_0
		2	0.2967_4	6403.8	0.3898_7
		3	0.2952_7	6274.4	0.3912_7
0.031484	1.0004	1	0.4010_9	6857.4	0.3892_9
		2	0.3986_3	6900.2	0.3889_3
		3	0.3982_2	6725.3	0.3908_4
0.039318	1.0002	2	0.4931_9	6961.1	0.3890_4
		3	0.4933_0	6799.5	0.3896_2
In 0.50 mole fraction DMF					
0.019741	1.0041	1	0.3062_1	4695.4	0.4687_3
		2	0.3046_0	4716.2	0.4687_3
		3	0.3031_0	4631.3	0.4693_5
0.039156	1.0025	1	0.4447_9	6411.5	0.4679_9
		2	0.4431_2	6434.7	0.4676_7
		3	0.4422_5	6295.2	0.4686_4